



HAL
open science

Structural Change, Land Use and Urban Expansion

Nicolas Coeurdacier, Florian Oswald, Marc Teignier

► **To cite this version:**

Nicolas Coeurdacier, Florian Oswald, Marc Teignier. Structural Change, Land Use and Urban Expansion. 2021. hal-03812819

HAL Id: hal-03812819

<https://sciencespo.hal.science/hal-03812819>

Preprint submitted on 13 Oct 2022

HAL is a multi-disciplinary open access archive for the deposit and dissemination of scientific research documents, whether they are published or not. The documents may come from teaching and research institutions in France or abroad, or from public or private research centers.

L'archive ouverte pluridisciplinaire **HAL**, est destinée au dépôt et à la diffusion de documents scientifiques de niveau recherche, publiés ou non, émanant des établissements d'enseignement et de recherche français ou étrangers, des laboratoires publics ou privés.



Distributed under a Creative Commons Attribution - NonCommercial - NoDerivatives 4.0 International License

STRUCTURAL CHANGE, LAND USE AND URBAN EXPANSION

Nicolas Cœurdacier, Florian Oswald, and Marc Teignier

SCIENCES PO ECONOMICS DISCUSSION PAPER

No. 2021-14

Structural Change, Land Use and Urban Expansion

Nicolas Coeurdacier
SciencesPo Paris, CEPR

Florian Oswald
SciencesPo Paris

Marc Teignier
Serra Húnter Fellow,
University of Barcelona

December 3, 2021*

Abstract

We develop a multi-sector spatial equilibrium model with endogenous land use: land is used either for agriculture or housing. Urban land, densely populated due to commuting frictions, expands out of agricultural land. With rising productivity, the reallocation of workers away from agriculture frees up land for cities to expand, limiting the increase in land values despite higher income and increasing urban population. Due to the reallocation of land use, the area of cities expands at a fast rate and urban density persistently declines, as in the data over a long period. As structural change slows down, cities sprawl less and land values start increasing at a faster rate, as in the last decades. Quantitative predictions of the joint evolution of density and land values across time and space are confronted with historical data assembled for France over 180 years.

Keywords: Structural Change, Land Use, Productivity Growth, Urban Density.

JEL-codes: O41, R14, O11

*We would like to thank Zsófia Bárány, Pierre-Philippe Combes, Emeric Henry, Thomas Chaney and our colleagues as well as numerous seminar and conference participants for comments and insights. We thank Alberto Nasi and Carla Guerra Tomazini for research assistance. We gratefully acknowledge funding under the Banque de France-SciencesPo Partnership. Marc Teignier acknowledges financial support from Spanish Ministry of Economy and Competitiveness, Grant PID2019-106543RA-I00, as well as from the Barcelona Economic Analysis Team.

1 Introduction

Since the early years of the industrial revolution, the population massively migrated from rural areas towards cities. This widespread phenomenon of urbanization went together with the reallocation of workers away from the agricultural sector towards manufacturing and service sectors—a phenomenon of structural change. How do cities grow when these well-known phenomena occur? Cities can become denser for a given area—growth at the intensive margin. They can also become larger in surface to accommodate more workers—via growth at the extensive margin. Over a long period, cities have been growing essentially in area, at such a fast speed that their average density has been falling. In other words, over time, cities expanded faster in area than in population. We precisely document this stylized fact for France since 1870 but it is also documented on a global scale in [Angel et al. \(2010\)](#). In France, the population of the main cities has been multiplied by almost 4 since 1870, while their area increased by a factor 30: the average urban density has thus been divided by a large factor of about 8. This paper shows that this persistent decline in density, despite the process of urbanization, is well explained by the most conventional theories of structural change with non-homothetic (Stone-Geary) preferences and augmented with endogenous land use—whereby land can be used for agriculture or urban housing.

A crucial insight of our theory is to consider that the value of agricultural land at the urban fringe determines the opportunity cost of expanding the area of cities for housing purposes. With low agricultural productivity, agricultural goods and farmland are expensive. High agricultural land values make cities initially small in area and very dense as households cannot afford large homes—a manifestation of the ‘food problem’ ([Schultz \(1953\)](#)). With structural change driven by rising (agricultural) productivity, workers move away from rural areas towards cities, freeing up agricultural land. As the value of land at the urban fringe falls and households free up resources to buy larger homes, cities expand in area at a fast rate. Together with the reallocation of workers across sectors, reallocation of land use occurs—from agricultural use to urban use. We document that for France, since 1840, about 15% of French land formerly used for agriculture is no longer used for this purpose. As long as the transitory process of reallocation away from agriculture continues, cities grow faster in area than population and average urban density keeps falling with urban expansion. Thus, our theory provides a novel mechanism explaining the sprawl and the suburbanization of cities. This complements the traditional urban view that cities have sprawled following improvements in the commuting technologies that have allowed households to live further away from their workplace.

Our framework also provides novel predictions regarding the historical evolution of land values. When productivity is low and agricultural goods are in high demand for subsistence needs, the value of farmland is high relative to income. With economic development, structural change frees up farmland for urban expansion and puts downward pressure on its price. The value of agricultural land as share of income falls and, over time, the value of urban land constitutes the largest fraction of aggregate land values. These predictions are in line with the data as shown in [Piketty and Zucman](#)

(2014). Moreover, despite rising housing demand, the fast expansion of cities at the extensive margin due to structural change initially limits the increase in urban land rents and housing prices. When the reallocation of workers out of agriculture slows down, so does the reallocation of land use at the fringe of cities. If workers' productivity increases further, the value of land must adjust to prevent further expansion of cities with rising housing demand. Land values start to increase at a faster rate. Our theory thus predicts flat land and housing values for decades before shooting up as the process of structural change ends. This prediction resembles very much the data for France and most advanced economies as best illustrated in Knoll et al. (2017): real housing prices being flat for decades since the nineteenth century before increasing at a fast rate in the recent decades—a *hockey-stick* pattern of housing prices and land values. Therefore, our theory provides novel insights on the joint evolution of the density of cities and land values along the process of economic development. It also helps understanding how the structure of cities, e.g. their urban extent and density evolves with the process of structural transformation. It sheds new light on the origins of urban sprawl in the process of economic development—a central matter in the artificialization of soils and their environmental impact (IPCC (2018)).

The contribution of our paper is threefold. First, we document new stylized facts on land use and urban expansion for France since the mid-nineteenth century. In particular, using historical maps and satellite data for the more recent period, we document the historical decline of the density of French cities. Between 1870 and 1950, the average density was divided by about 3 and again by about 2.5 until 1975—the thirty years post-World War II being characterized in France by a faster structural change and *rural exodus* (Mendras (1970), Bairoch (1989), Toutain (1993)). Together with the slowdown of structural change in the more recent decades, average urban density did not fall much since. These facts, together with the historical evolution of urban and agricultural land values in France, motivate our theory.

The second contribution is to develop a spatial general equilibrium model of structural change with endogenous land use—agricultural or residential land use. The production side features three sectors: rural, urban and housing. The rural (resp. urban) sector produces agricultural (resp. non-agricultural) tradable goods, the production of the rural good being more land intensive. The housing sector produces location-specific housing units using the urban good and land in the process. Land is in fixed supply and land use rivalrous: land is either used for agriculture or for housing. Following the traditional monocentric model after Alonso et al. (1964), Muth (1969), and Mills (1967), urban land use (cities) emerges endogenously due to commuting costs for workers to produce urban goods: urban land is thus more densely populated than rural land and the urban fringe corresponds to the longest commute of a worker producing urban goods. Importantly, the rental price of land at the fringe of the city must be equalized across potential usages—the marginal productivity of land in the rural sector (agriculture) determining the opportunity cost of expanding further urban land. The last important components of our theory are the drivers of structural change. Structural change is driven by the combination of non-homothetic preferences on the demand side, particularly a subsistence consumption for the rural good, and increasing (agricultural)

productivity on the supply side. This generates transitory dynamics with rising productivity in agriculture that are at the heart of our story: in the old times, due to low agricultural productivity, land is scarce with high values of farmland with respect to income. Moreover, households devote a large fraction of their resources to feed themselves and cannot afford large homes. Few urban workers are concentrated on a very small area and urban land is very densely populated. Later on, with agricultural development, farmland is getting less valuable. This frees up rural land for cities to expand, accommodating rising demand for housing of more numerous urban workers. The city sprawls and average urban density falls through two channels: the fall in the rental price of farmland at the urban fringe and the increasing share of spending towards housing. Note that the decline in urban density occurs even without improvements in the commuting technology—the usual source of sprawling in urban economics. At the latest stages of the transition, in more recent times, the reallocation of workers and land use slows down. Urban expansion slows, urban density declines less and land prices increase at faster rate. As a side-product, we also show how commuting frictions together with location-specific land values generate a wedge between the workers marginal productivities in the rural and urban sector, an ‘agricultural productivity gap’ (Gollin et al. (2014)).

The other natural candidate to account for urban sprawl over time is the development of faster urban commutes, which made urban households live further away from work. Building upon LeRoy and Sonstelie (1983) and DeSalvo and Huq (1996), we incorporate into our theory a commuting mode choice model, which allows for an endogenous decision of individuals of how to commute, based on their opportunity cost of time and location. More specifically, as the opportunity cost of time in the city increases with rising urban productivity, workers optimally choose faster commuting modes and live further away from the center: the city expands at the expense of rural land.¹ Thus, although the mechanisms are entirely different, both urban *and* rural productivity growth lead to sprawling and suburbanization together with a decline in average urban density. However, the implications for density across urban locations are different. Increasing urban productivity and faster commutes lead to a reallocation of urban workers away from the center towards the city fringe. As a consequence, central density falls more than average urban density since suburban density increases. To the contrary, increasing agricultural productivity and structural change lead to the addition of lower and lower density settlements at the fringe of cities: suburban density falls more than the average urban density. While central density did fall since the mid-nineteenth century, historical data for Paris shows that it fell less than the average urban density. This suggests that both channels—the structural change and the commuting speed channels—have been playing a role in driving the density decline.

Regarding the price of land, we also show that agricultural productivity growth and structural change are crucial to understand their evolution. If land reallocation away from agriculture towards urban use was only driven by urban productivity growth and faster commutes, rural land would be

¹In our theory, commuting costs (as a share of income) falls endogenously as individuals choose faster commuting modes when urban income increases. Results are qualitatively the same if one assumes an exogenous fall in commuting costs.

getting scarcer and more valuable: the value of farmland and agricultural rents (i.e. rental income) would increase, as a share of income. Agricultural land rents would also become relatively more important than urban ones – predictions that are widely counterfactual to the evidence in [Piketty and Zucman \(2014\)](#). Quite differently, structural change driven by increasing rural productivity frees up farmland, lowering its value relative to income and reducing the importance of agricultural land rents to the profit of urban ones. These predictions are much more in line with the data.

In a third contribution, we develop a quantitative version of our spatial equilibrium model applied to the French context since 1840. Using data from various historical sources, we measure sectoral factors of production and productivities over long period and calibrate our model to fit the process of structural change in France. In order to account for the use of faster commutes over time, we make use of a tractable parametrization of commuting costs and calibrate the elasticities of commuting speed to urban income and commuting distance using individual commuting data. We show that the quantitative predictions of the model match relatively well the joint evolution of population density and land values over time and across space. We also disentangle the relative importance of falling commuting costs relative to our novel mechanisms based on structural change in explaining the persistent decline in urban density—emphasizing further the quantitative importance of improvements in agricultural productivity for the expansion of cities.

Related literature. The paper relates to several strands of literature in macroeconomics and spatial economics. From a macro perspective, it relates to the literature linking productivity changes and land values, starting with [Ricardo \(1817\)](#). This traditional view would imply that a fixed factor such as land should continuously rise in value with economic development (see, among others, [Nichols \(1970\)](#) and [Grossman and Steger \(2017\)](#) for a recent contribution). However, such a prediction would not fit well the measurement of housing prices and land values over a long period as in [Piketty and Zucman \(2014\)](#) and [Knoll et al. \(2017\)](#) (see also [Davis and Heathcote \(2007\)](#) for related U.S. evidence). An alternative view developed in [Miles and Sefton \(2020\)](#) argues that the rise in land and housing prices can be mitigated by improvements in commuting technologies, which allow cities to expand outwards. Our approach, in the tradition of the theory of structural change, also argues that land used to be scarce and valuable with low productivity in agriculture but rising productivity alleviates pressure on land—putting downward pressure on its value. In a sense, our theory reconciles these different views in a unified framework. From a theoretical perspective, we contribute to the literature on structural change, surveyed in [Herrendorf et al. \(2014\)](#), by considering a spatial dimension—adding an endogenous use of land and a housing sector—in the most conventional multi-sector model with non-homothetic preferences ([Kongsamut et al. \(2001\)](#), [Gollin et al. \(2007\)](#), [Herrendorf et al. \(2013\)](#), [Boppart \(2014\)](#), [Comin et al. \(2021\)](#), [Alder et al. \(2021\)](#)). Structural change and urbanization are known to be tightly linked ([Lewis \(1954\)](#)). [Gollin et al. \(2016\)](#) shows that not only economic development but also natural resources rents lead to urbanization. However, the literature has rarely investigated the spatial dimension of structural change, largely abstracting from spatial frictions. [Michaels et al. \(2012\)](#) and [Eckert et al. \(2018\)](#) are notable exceptions. The crucial difference to those is the ability of our framework to replicate the evolution

of population density within locations—putting emphasis on the internal structure and density of cities—, while their focus is more on the distribution of population and the sectoral specialization across regions. We also emphasize the implications for land values across time and space, largely absent in these studies. Adding a spatial dimension to a multi-sector model of structural change also generates endogenously an ‘agricultural productivity gap’ (Gollin et al. (2014)) due to the mere presence of commuting frictions and location-specific housing. This provides a complementary explanation to urban-rural wage gaps, different from migration costs or selection of migrants towards cities (Restuccia et al. (2008), Lagakos and Waugh (2013), Young (2013)).

Our paper also contributes to the literature in spatial economics on urban expansion surveyed in Duranton and Puga (2014, 2015). An important feature of our framework is the existence of preferential residential locations within cities, shaping the population density across space, due to the presence of commuting frictions (Alonso et al. (1964); Muth (1969); Mills (1967)). We expand this literature by bringing the endogenous sectoral allocation of factors and the general equilibrium structure at the heart of the macro literature. Importantly, contrary to the bare bone urban monocentric model, land is in fixed supply and the price of land at the boundary of the city becomes an endogenous object itself affected by the process of structural change. The most related work to our approach developed in Brueckner (1990) shows how location-specific land values pin down rural-urban migrations and the extent of urbanization in a spatial equilibrium (see also Brueckner and Lall (2015) for a survey). However, without the drivers of structural change and endogenous land values at the urban fringe as in our framework, this approach stays relatively silent regarding the long-run dynamics of urbanization and land values. In this latter dimension, our work relates to the literature measuring and explaining land values across space (see Glaeser et al. (2005), Albouy (2016), Albouy et al. (2018) and Combes et al. (2018) for recent contributions). In particular, we show that the dispersion of land values across space and the scarcity of land in some locations depend very much on the extent of economic development and structural change. Our approach also provides an alternative mechanism generating a large sprawling of cities together with economic development. More specifically, it explains, why, over time, most cities expand faster in area than in population as documented on a global scale by Angel et al. (2010). In the French context, we also relate to the historical measurement of urban land use in Combes et al. (2021). Our story is complementary to the usual explanations based on the improvement of commuting technologies and/or the relocation of economic activity within cities (see references in Glaeser and Kahn (2004) and Heblich et al. (2018), Redding (2021) for recent contributions). Lastly, our paper contributes to the literature on quantitative spatial economics surveyed in Redding and Rossi-Hansberg (2017) (see also Ahlfeldt et al. (2015)) by emphasizing the extensive margin of cities.

The paper is organized as follows. Section 2 provides motivating empirical evidence on land use, land values, urban expansion and population density across space over long period in France. Section 3 provides a baseline spatial general equilibrium model of land use and structural change which enlightens the main mechanisms. Section 4 develops a quantitative version calibrated to French historical data. Section 5 concludes.

2 Historical Evidence from France

2.1 Land use and Employment in Agriculture

Data. Using various sources described in Appendix A, we assemble aggregate data on employment shares in agriculture and agricultural land use since 1840. Historical data on land use in agriculture are available roughly every 30 years (or less) until the 1980s and then at higher frequency. They are largely extracted from secondary sources based on the Agricultural Census (Recensement Agricole), and cross-checked with various alternative historical sources (Toutain (1993) among others). Post-1950, data are from the Ministry of Agriculture.

Employment. As all countries going through structural transformation, France exhibits a large reallocation of labor away from agriculture over the period, from about 60% employed in agriculture in 1840 to about 2.5% today (Figure 1, dashed line).² The process of structural change accelerated significantly over the period 1945-1975: in 1945, 36% of the working population are still in agriculture and this number falls below 10% in 1975. In this sense, France is a bit peculiar relative to the other advanced economies: it is still a very agrarian economy right after World War II—much more than the U.K. or the U.S. This measurement is described in detail in Appendix A.2.

Land use. Although measurement is sometimes difficult for the very early periods, one can confidently argue that, in the aggregate, the share of French land used for agriculture significantly fell since 1840 (Figure 1, solid line).³ Our preferred estimates are that about two thirds of French land was used for agriculture in 1840. In 2015, this number is down to 52%. In other words, about 15% of French land use has been reallocated away from agriculture. While this might not seem like a very large number, this is very large from the perspective of urban expansion. 15% of the French territory is actually more than the total amount of land with artificial use in France nowadays (about 9% of total land today).⁴ While this is difficult to assess over such a long period, the novel usage of the land formerly used in agriculture, it is likely that a significant fraction of this land has been artificialized—allowing cities to expand. More precise data on land use over the period 1982-2015 show that the surface of artificialized soils increased by about 2 millions of hectares (3.7% of the French territory), about 70% of the quantity of the land no longer used for agriculture over the same period.⁵ The measurement of cities area (presented below) provides further compelling evidence that a significant fraction of agricultural land was reallocated towards urban land use. We present details in Appendix A.1.

²Estimates of rural population are also available for the same time-period (see Appendix A.2). Rural population follows a similar path with, as expected, higher levels as many people in rural areas do not work directly in agriculture. One needs to be cautious though when using data on rural vs. urban population as the (ad-hoc) definition by official statistics varies over the period.

³The main issue is the definition of agricultural land (in particular, the allocation of grazing fields) which is not entirely consistent across years before World War II. See Appendix A.1 for details.

⁴Since 1982, data on land use beyond agricultural land use are available on a regular basis from the Enquetes Teruti and Teruti-Lucas.

⁵The rest of agricultural land is to a large extent converted into forests and woods (Enquetes Teruti and Teruti-Lucas). Their surface, including groves and hedges, increased by almost 1 million of hectares between 1982 and 2015.

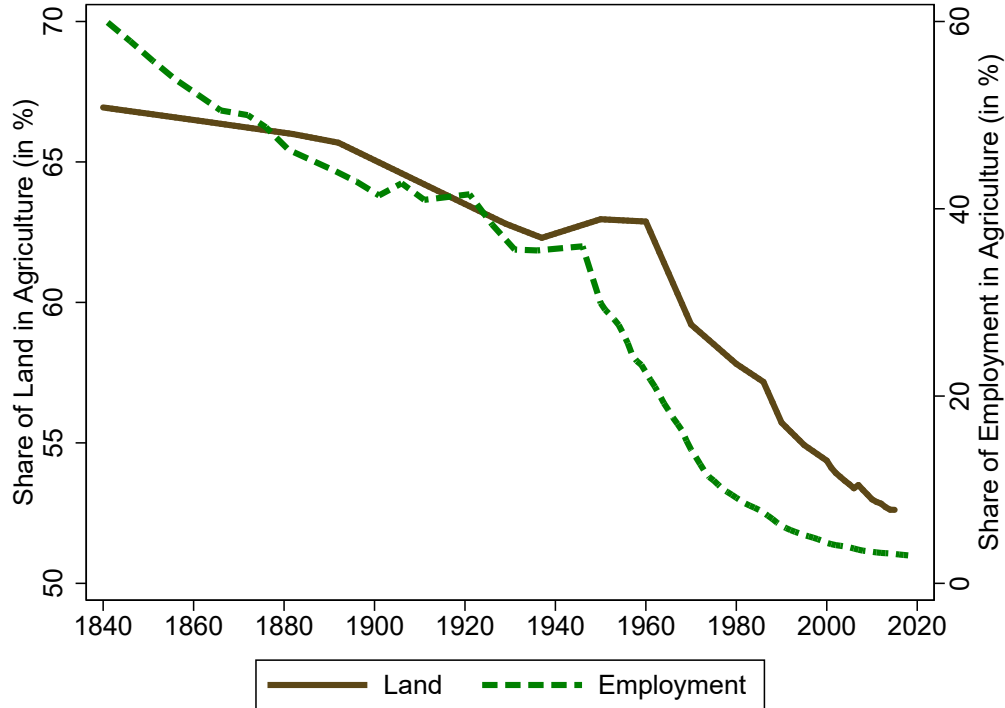


Figure 1: Land use and labor reallocation in France (1840-2015).

Notes: The solid line shows the share of French land used for agriculture (left-axis). The dashed line shows the share of workers in the agricultural sector (right-axis). *Source:* See Appendix A.1.

2.2 Urban Expansion

Data. We use maps, aerial photographs and satellite data to measure the area of the main French cities at different dates: 1866 (military maps, e.g. carte d’Etat Major), 1950 (maps and/or photographs), and every ten to fifteen years after 1975 using satellite data from the Global Human Settlement Layer (GHSL) project.⁶ One caveat of our area measurement is that we cannot have any measurement between 1866 and 1950. Data and procedure for the measurement of urban extent across French cities are detailed in Appendix A.7. Measurement of the urban extent using maps in 1866 and 1950 is performed for the 100 largest cities in population in the initial period. For a given city, the urban extent ends when the land is not continuously built. For the satellite data, it is delimited by grid cells where the fraction built is below 30% and a requirement that cells are connected.⁷ By way of example, Figures 26 and 27 in Appendix A.7.1 show the area measurement for a medium-size French city, Reims, in 1866 and 1950 using maps. Figure 35 shows the same city of Reims in 2016 viewed from the sky, with an area of about 57 km²—about 20 times larger than its 1866 counterpart. This last figure also clearly shows how the city is surrounded by agricultural

⁶We double-check the quality of photo/map measurement in the most recent period relative to satellite data measurement (see Appendix A.7.5). The cross-sectional correlation between both measures is very high. We also cross check our measures with Angel et al. (2010) for Paris and find very similar results.

⁷Measurement is not very sensitive to alternative thresholds (see Appendix A.7.6). Figures 31 and 32 in the same Appendix illustrate how GHSL data are used to delineate the urban boundaries of Marseille and Bordeaux.

land—a crucial element for our story where urban land expands out of farmland. This feature is not specific to Reims. Recent satellite observations from the Corine Land Cover project – further detailed in Appendix A.8 – show that our sample of cities are surrounded mainly by agricultural land: apart from their coastal part and water bodies, two thirds of land use in the near surroundings of cities is agricultural.⁸

Using Census data, we relate the measured land area used by cities to the corresponding population. Data for the first available Census in 1876 are used for the initial period of study. Census data defines population at the municipality level (‘commune’) and an urban area can incorporate more than one municipality. In 1870, this is not a major concern as the main ‘commune’ of the city is the whole city population. In later periods, one needs to group municipalities (‘communes’) into an urban area. Post 1975, GHSL data combines satellite images with Census data on population. This directly provides the population of every grid cells of our measured urban area, circumventing the issue. However, for the 1950 period, the different municipalities that are part of our measured areas must be selected. This is done on a case by case basis, looking at the map of each of the 100 largest urban areas. This way, we make sure that the overall population of the area incorporates all the corresponding municipalities’ population. The procedure is detailed in Appendix A.7.2.⁹

The area and population of French cities. Not surprisingly, more populated cities are larger in area at a given date. However, in the cross-section, the urban area increases strictly less than one for one with urban population: more populated cities are denser on average.¹⁰ This stands in contrast with their evolution in the time-series. Over time, cities have been increasing much faster in area than in population. Let us give some order of magnitude and describe the average evolution over time for the most populated 100 French cities in 1876. Figure 2 shows the evolution of the total area and population of these 100 cities over the period considered—both variables being normalized to 1 to show the increase in size. Since 1870, the area of cities has been multiplied by a factor close to 30 on average. This is very large. Between 1870 and 1950, the area of cities was roughly multiply by a factor 6. Between 1950 and today, the area of cities was multiplied again by a factor 5 on average—the fastest rate of increase being observed over the period 1950-1975. For comparison, the population of these largest cities has been multiplied by a factor close to 4 since 1870.¹¹ As urban area increased at a much faster rate than urban population, the average urban density significantly declined over the period.

The density of French cities. Using the population and the area of cities at the different dates, one can measure the evolution of urban densities across the different cities over 150 years. While

⁸The rest is made of forest/moors and discontinuous urban land (e.g. leisure/transport infrastructure, industrial/commercial sites, ...)—both categories in roughly equal proportions. See details in Appendix A.8.

⁹For most cities in 1950, only very few ‘communes’ are agglomerated into one city. Only the largest cities, and particularly Paris, are the results of the agglomeration of many different ‘communes’.

¹⁰In the cross-section, at a given date, a 10% increase in the population of a city corresponds to approximately a 8.5% increase in its area and this elasticity varies fairly little across the different time periods.

¹¹French population was multiplied by a bit less than 2 over the entire period. Due to the reallocation of people way from rural areas towards cities, we get roughly a factor 4 over the period.

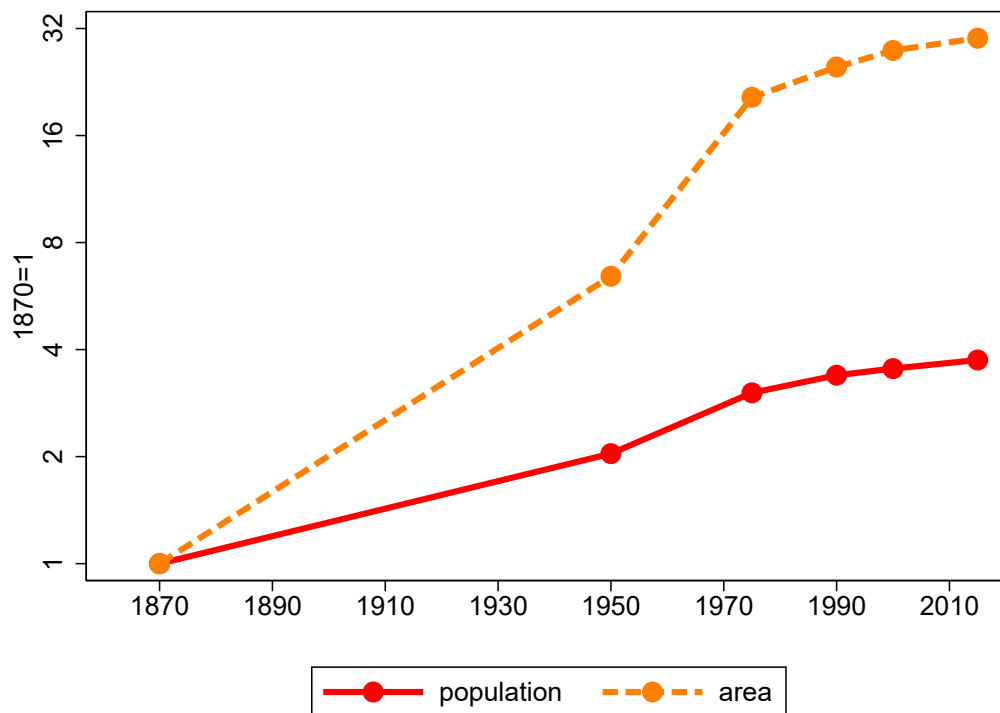


Figure 2: Urban area and population of the 100 largest cities in France (1870-2015).

Notes: The dashed line shows the total urban area of the 100 cities relative to the initial period (sum of all the urban areas) . The bottom solid line shows the total population relative to the initial period in the same cities. Both area and population are normalized to unity in the initial period. *Source:* See Appendix A.7.

in the cross-section larger cities are denser, the density of French cities declined over time—area expanding at a faster rate than population. This is shown in Figure 3 for the population-weighted average of density across the 100 largest French cities. The average urban density fell massively over the period: density has been divided by a factor of roughly 8. Urban density fell at the fastest rate over the period 1950-1975 and barely falls thereafter. Thus, urban density fell the most over the period when people massively left rural areas and the employment share in agriculture also fell the most. The later slowdown of the decline in density coincides with the slowdown in the rate of structural transformation.¹²

Ideally, one would like to explore how density evolved in different locations of a city (within-city variations). This would provide information on whether density fell in the central locations or in the outskirts of the city. Unfortunately, for most cities we are not able to differentiate the central density to the suburban one as most cities expand the area of their main historical ‘commune’, particularly so over the period 1870-1950. Thus, we cannot measure the historical population in different parts of a city. However, it can be done for Paris which is divided into several districts. Figure 4 shows the evolution of the density of Central Paris relative to the average urban density of the metropolitan area: the central density of Paris did fall over time but significantly less than

¹²The historical decline in urban density is observed across all cities although the magnitude differs across cities. See Appendix A.7.4 for further insights on the evolution of urban density across different cities.

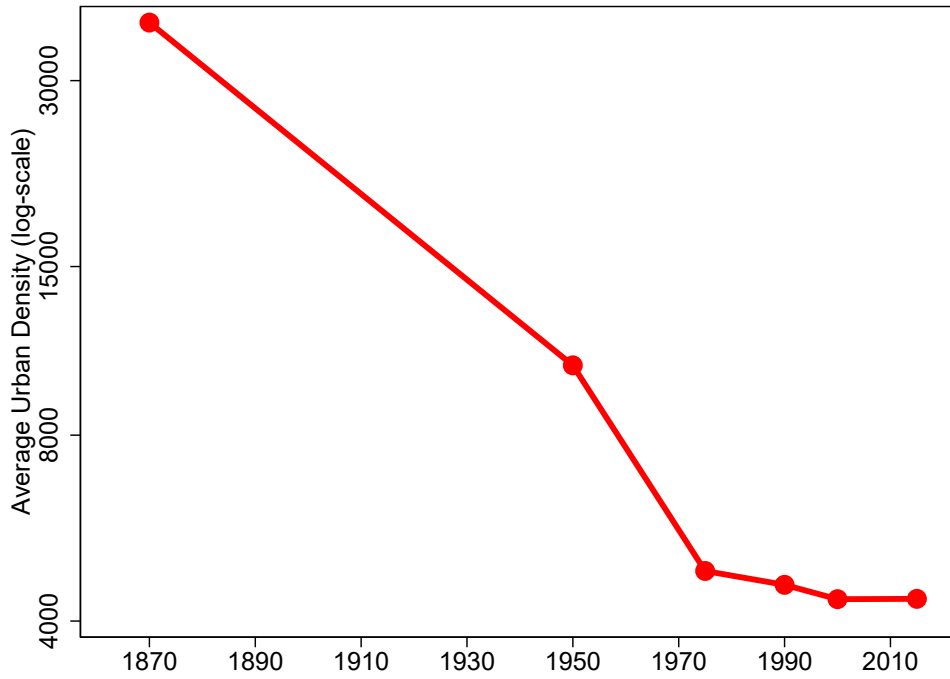


Figure 3: The historical decline in urban density.

Notes: The solid line shows the urban density averaged across the top 100 French cities (weighted average with 1975 population weights). *Source:* Etat major, IGN, GHSL and Census. See Appendix A.7 for details.

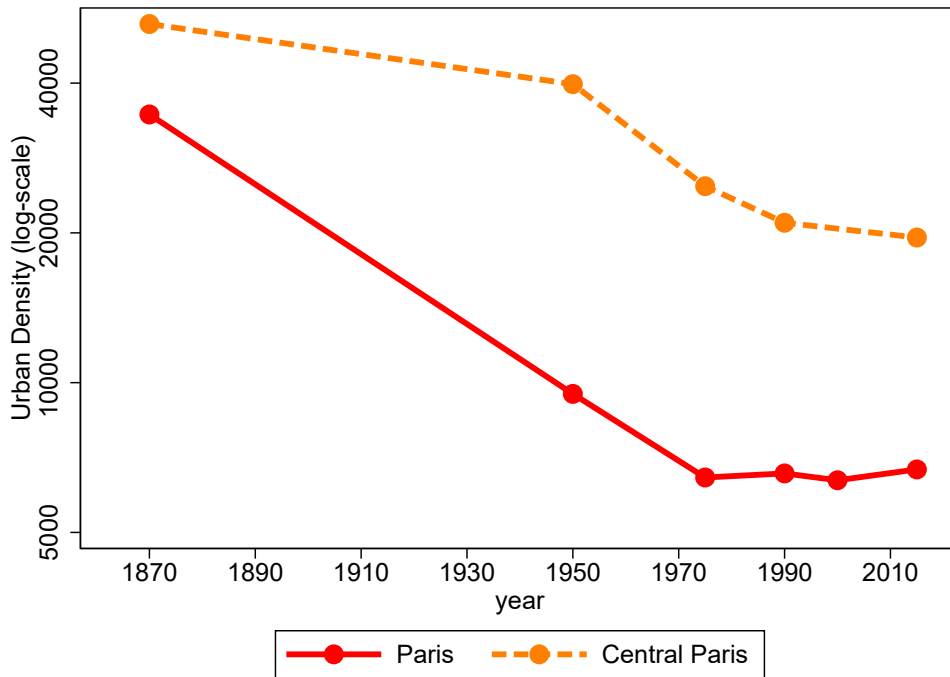


Figure 4: The historical decline in urban and central density in Paris.

Notes: The solid line shows the average urban density in Paris; the dashed line shows the density in Central Paris (districts 1 to 6). *Source:* Etat major, IGN, GHSL and Census.

the average density of the city. This suggests that the decline in average urban density is not only due to a reallocation of urban residents away from dense centers but also due to the addition of less and less dense suburban areas at the city fringe over time.

2.3 Land values

Data. Data on land and housing values (over income) for France over a long period can be found in [Piketty and Zucman \(2014\)](#).¹³ Historical data for the real housing price index for France are provided in [Knoll et al. \(2017\)](#).

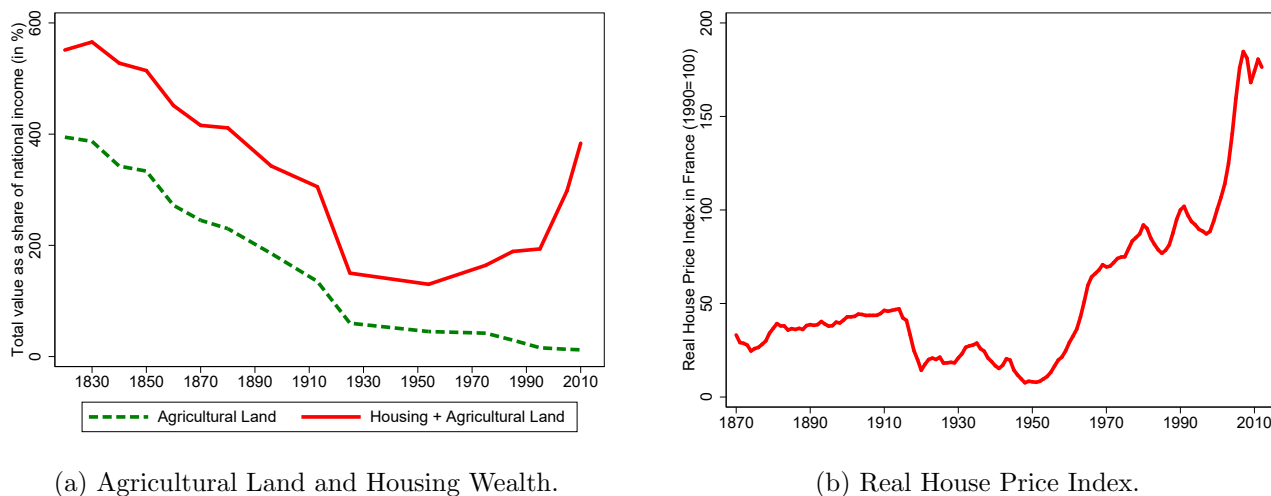


Figure 5: Land and Housing Values in France.

Notes: The left plot shows agricultural wealth as a share of French national income in % (dashed) and the sum of agricultural and housing wealth as a share of national income in % (solid). The right plot shows the French housing price index deflated by the CPI. Data are from [Piketty and Zucman \(2014\)](#) (panel 5a) and [Knoll et al. \(2017\)](#) (panel 5b).

Historical evolution. Figure 5a describes the evolution of the aggregate value of French land over income since 1820. The fall in the value of housing and land wealth (as a share of income) in the pre-World War II period is essentially driven by a declining value of farmland. While farmland was expensive relative to income in the nineteenth century, it is today relatively cheap. This is confirmed by data on average farmland prices: since 1850, the average value of an agricultural field (per unit of land) as a share of per capita income has been divided by a factor of 15 in France. This fact is at the heart of our story: structural change puts downward pressure on farmland values—allowing cities to expand at a fast rate. As a consequence, there is an important reallocation of land values across usage, from agricultural land towards housing (or urban) land. While the value of agricultural land accounted for more than 70% of housing and land wealth in 1820, it accounts for only 3% in 2010. Lastly, despite the falling value of farmland as share of income, the total value of housing and land wealth (as share of income) grows at an increasing rate after 1950.

¹³Using various data sources, we also computed a measure of farmland prices per unit of land. Our estimates are consistent with [Piketty and Zucman \(2014\)](#).

This steep increase, arguably driven by the increasing value of urban land where most of the population is concentrated, echoes the findings of Knoll et al. (2017).¹⁴ They show that for developed countries, including France, housing prices have been quite stable until the 1950s before rising at an increasing pace—a *hockey-stick* shape of housing prices as shown in Figure 5b.

To sum-up, our historical data shows a set of salient facts over the last 180 years: beyond the well-known reallocation of labor away from agriculture, land has been reallocated away from agricultural use. Migrations away from the rural areas were accompanied with urban expansion both in area and population. However, given that urban area grew at a significantly faster pace than urban population, the average urban density massively declined over the period, particularly so in the decades following World War II in France. Together with this process of structural change, the value of farmland as a share of income shrank a lot to the benefits of non-agricultural (urban) land.

These stylized facts motivate our subsequent theoretical analysis where we introduce a spatial dimension together with endogenous land use to the most standard theory of structural change with non-homothetic preferences.

3 A Baseline Model

3.1 Production

We consider an economy producing an urban good (u) and a rural good (r). The urban good is thought as a composite of manufacturing goods and services, while the rural good is thought as an agricultural good. The urban good is also used in the production of housing services. Goods and factor markets are perfectly competitive. Both goods are perfectly tradable.

Factor Endowments. The economy is endowed with land and a continuum of workers, both in fixed supply. Land area is denoted S . Land can be used to produce the rural good or for residential purposes. Each worker is endowed with one unit of labor and we denote by L the total population of workers.

Production and Factor Payments. The production of the urban good only uses labor as input. One unit of labor produces θ_u units of the urban good. Perfect competition insures that the urban wage is

$$w_u = \theta_u, \tag{1}$$

in terms of units of the urban good, which is used as numeraire.¹⁵ Aggregate production of the urban good is

$$Y_u = \theta_u L_u,$$

¹⁴Bonnet et al. (2019) show that this increase in the price of housing is largely driven by the price of land and not by the capital and structure component.

¹⁵For now, we consider the urban productivity θ_u (and thus the urban wage) as exogenous. We consider agglomeration forces in Section 4.

where L_u denotes the number of workers working in the urban sector.

The production of the rural good uses labor and land according to the following constant returns to scale technology

$$Y_r = \theta_r (L_r)^\alpha (S_r)^{1-\alpha},$$

where L_r denotes the number of workers working in the rural (agricultural) sector, S_r the amount of land used for production and θ_r a Hicks-neutral productivity parameter. $0 < \alpha < 1$ is the intensity of labor use in production, $1 - \alpha > 0$ ensures that land is used more intensively to produce the rural good.¹⁶

Define p the relative price of the rural good in terms of the numeraire urban good. Rural workers and land are paid their marginal productivities,

$$w_r = \alpha p \theta_r \left(\frac{S_r}{L_r} \right)^{1-\alpha}, \quad (2)$$

$$\rho_r = (1 - \alpha) p \theta_r \left(\frac{L_r}{S_r} \right)^\alpha, \quad (3)$$

where w_r is the rural wage and ρ_r the rental price of land anywhere in the rural sector.

Remark. The important technology assumption is that the rural sector uses a fixed factor, land, for production, which implies (stronger) decreasing returns to scale to labor in this sector compared to the urban sector. The fact that the urban sector does not use land is not crucial as long as this sector is less land intensive than the rural one.

3.2 Spatial Structure and Commuting Costs

Spatial structure. Total available land S is devoted to either housing or rural goods production. The production of the urban good takes place in the city, while the production of the rural good, being more land intensive, takes place in the rural area. For now, we assume that production of the urban good takes place in only one location $\ell = 0$. An extension with multiple locations (multiple cities) is provided in Appendix B.2.

One can think of $\ell = 0$ as the Central Business District (CBD) in a standard urban model, where space is given by the interval $[0, S]$. Workers' residence ℓ can lie anywhere in this interval, however, they face spatial frictions $\tau(\ell)$ when commuting to work in the urban sector. A worker residing in location ℓ and working in the urban sector earns wage *net of spatial frictions* equal to $w(\ell) = w_u - \tau(\ell)$, with $\tau(0) = 0$ and $\partial\tau(\ell)/\partial\ell \geq 0$. The commuting cost $\tau(\ell)$ incorporates all spatial frictions which lower disposable income available for consumption when living further away from the location of production. It includes time-costs of commuting and the effective spending on transportation.¹⁷

¹⁶The model is extended in Appendix B.1.1 to explore a more general CES production function for the rural good.

¹⁷It could also incorporate an income reduction if it is harder to find a job when living further away from the location of production.

The commuting cost is partly endogenous in our framework, because urban households adjust their mode of commuting depending on their income and their location, as described in details below.

Since spatial frictions increase with ℓ , urban workers locate as close as possible to $\ell = 0$. If one denotes $\ell = \phi < S$ the furthest away location of an urban worker, ϕ is endogenous in our framework and represents the fringe of the city. Workers residing in locations beyond ϕ produce the rural good, which does not involve spatial frictions, as rural workers do not commute.

Remarks. The spatial structure calls for a number of important remarks. First, if it were possible for all workers to locate at $\ell = 0$, there would be no spatial frictions. Second, one should note that for $\ell \leq \phi$, land will be used for residential purposes to host urban workers. As a consequence, land available for rural production would also be maximized if all workers could locate at $\ell = 0$. This case could correspond to an entirely ‘vertical’ city, where land use and spatial frictions are irrelevant. We view this extreme case as a standard two-sector model of structural transformation. Last, the spatial frictions $\tau(\ell)$ do not involve traffic congestion in the baseline—the reason why a more compact city (lower ϕ) always saves on commuting costs in our baseline economy. We allow for congestion and agglomeration effects in Appendix C.4.

Commuting costs. We provide a micro-foundation for the commuting costs, $\tau(\ell)$, where urban workers choose a commuting mode m depending on their location ℓ and opportunity cost of time (wage rate w_u). This modelling approach helps mapping commuting costs into observables from commuting data but results do not depend qualitatively on the micro-foundation as long as commuting costs are increasing in the opportunity cost of time and commuting distance.

Commuting costs in location ℓ , $\tau(\ell)$, are the sum of spending on commuting using transport mode m , $f(m)$, and time-costs proportional to $w_u \cdot t(\ell)$, where $t(\ell)$ denotes the time spent on daily commutes of an individual located in ℓ , such that

$$\tau(\ell) = f(m) + \zeta w_u \cdot t(\ell), \quad (4)$$

whereby $0 < \zeta \leq 1$ represents the valuation of commuting time in terms of foregone wages. Transportation modes m available are optimally chosen. They are continuously ordered by their speed, as in DeSalvo and Huq (1996), such that m denotes both the mode and the speed of commute. Faster commutes are more expensive and $f(m)$ is increasing in m . For tractability, we use the following functional form, $f(m) = \frac{c_\tau}{\eta_m} m^{\eta_m}$, with $\eta_m > 0$ and c_τ a cost parameter measuring the efficiency of the commuting technology. With speed m , the commuting time (both ways) is equal to $\frac{2\ell}{m}$. This yields the following expression for the commuting costs,

$$\tau(\ell) = \frac{c_\tau}{\eta_m} m^{\eta_m} + 2\zeta w_u \left(\frac{\ell}{m} \right). \quad (5)$$

This expression for commuting costs facilitates parametrization and preserves some tractability,

while elucidating the main mechanisms.¹⁸ We turn to the optimal choice of transportation mode.

Optimal mode of transportation. At any given moment in time, prevailing technology offers different transportation modes ordered by their respective speed m . An individual in location ℓ chooses the mode of transportation corresponding to speed m in order to minimize the commuting costs $\tau(\ell)$. By equalizing the marginal cost of a higher speed m to its marginal benefits in terms foregone wage, the optimal chosen mode/speed satisfies,

$$m = \left(\frac{2\zeta w_u}{c_\tau} \right)^{1-\xi} \cdot \ell^{1-\xi}, \quad (6)$$

where $\xi \equiv \frac{\eta_m}{1+\eta_m} \in (0, 1]$. Individuals living further away choose faster commuting modes. The speed of commuting also increases with the wage rate as a higher wage increases the opportunity cost of time. Using Equations 5-6, we get that equilibrium commuting costs satisfy,

$$\tau(\ell) = a \cdot (w_u \ell)^\xi, \quad (7)$$

where $a \equiv \left(\frac{1+\eta_m}{\eta_m} \right) c_\tau^{\frac{1}{1+\eta_m}} (2\zeta)^{\frac{\eta_m}{1+\eta_m}} > 0$. Commuting costs increase with the wage rate (the opportunity cost of time) and the commuting distance with constant elasticities.¹⁹ Since individuals optimally choose the commuting speed, the elasticity ξ of commuting costs to the wage rate is strictly smaller than unity. This is important as it implies that, for a given residential location, the share of resources devoted to commuting falls with rising urban productivity and wages. In equilibrium, this makes individuals willing to live further away in order to enjoy larger homes. This is the channel through which rising urban productivity leads to faster commutes and suburbanization. Our derivation of commuting costs also enlightens the calibration as the elasticity of commuting costs to commuting distance (resp. income) is directly tied to the elasticity of commuting speed to commuting distance (resp. income), which have data counterparts (Equation (6)).

3.3 Preferences and Consumption

Preferences. Preferences over urban and rural goods are non-homothetic as in [Kongsamut et al. \(2001\)](#) and [Herrendorf et al. \(2013\)](#) among others. Consider a worker living in a location ℓ . Denote $c_r(\ell)$ the consumption of rural (agricultural) goods, $c_u(\ell)$ the consumption of urban goods (used a

¹⁸The cost $f(m)$ has several possible interpretations. At a more macro level, it can represent the fixed cost of installing public transportation, where a faster mode is more expensive (a train line versus the horse drawn omnibus). At a more individual level, it represents the cost of buying an individual mean of transportation—a bike being cheaper than an automobile. However, this reduced-form approach sets aside the possibility that the implemented commuting technologies and the effective speed of commuting depends in a more sophisticated way on the equilibrium allocation in the city (e.g. traffic congestion or the construction of transportation infrastructures may depend on the whole spatial allocation of urban residents). The extension in Appendix B.1.2 uses a more general function for the spending on commuting f , also increasing in the commuting distance ℓ and urban wages w_u : $f = f(m, \ell, w_u)$. Longer commutes are more expensive and higher urban labor costs also increase commuting costs.

¹⁹Commuting costs also falls with improvements in the commuting technology (lower a). a is alike a relative price of commuting: if technology improves relatively faster in the commuting sector, the relative price a of commuting (in terms of urban goods) falls. Our baseline simulations will hold a fixed focusing on urban productivity as the main driver of faster commutes — decreasing commuting costs as a share of income.

a numeraire) and $h(\ell)$ the consumption of housing. The composite consumption good is

$$C(\ell) = (c_r(\ell) - \underline{c})^{\nu(1-\gamma)} (c_u(\ell) + \underline{s})^{(1-\nu)(1-\gamma)} h(\ell)^\gamma \quad (8)$$

where \underline{c} denotes the minimum consumption level for the rural good, and where \underline{s} stands for the initial endowment of the urban good. Preference parameters ν and γ belong to $(0, 1)$. Workers derive utility only from consumption. The utility of a household in location ℓ is equivalent to $C(\ell)$.

Budget constraint. The household earns a wage income net of spatial frictions $w(\ell)$ in location ℓ . Given the spatial structure, $w(\ell) = w_u - \tau(\ell)$ for $\ell \leq \phi$ and $w(\ell) = w_r$ for $\ell > \phi$. The households also earns land rents, r . Land rents are redistributed lump-sum equally across workers and are thus assumed to be independent of location. The budget constraint of a worker in location ℓ satisfies

$$pc_r(\ell) + c_u(\ell) + q(\ell)h(\ell) = w(\ell) + r, \quad (9)$$

with $q(\ell)$ the rental price per unit of housing (henceforth the housing price) in location ℓ .

Expenditures. Maximizing utility (Equation (8)) subject to the budget constraint (Equation (9)), expenditures on each yields

$$pc_r(\ell) = (1 - \gamma)\nu(w(\ell) + r + \underline{s} - p\underline{c}) + p\underline{c} \quad (10)$$

$$c_u(\ell) = (1 - \gamma)(1 - \nu)(w(\ell) + r + \underline{s} - p\underline{c}) - \underline{s} \quad (11)$$

$$q(\ell)h(\ell) = \gamma(w(\ell) + r + \underline{s} - p\underline{c}). \quad (12)$$

Due to the presence of subsistence needs ($\underline{c} > 0$), individuals reallocate consumption away from the rural good with rising income, increasing the consumption share of the urban good and housing. The reallocation of demand towards the urban good is stronger when $\underline{s} > 0$.

3.4 Equilibrium Sorting

Mobility equations. We consider an equilibrium, where ex-ante identical workers sort across locations. Since the rural and the urban good are perfectly tradable, urban workers, which would all prefer locations closer to $\ell = 0$, compete for these locations. Adjustment of housing prices through the price of land makes sure that households remain indifferent across different locations. Using Equations (10)-(12), this implies the following mobility Equation, where consumption is equalized to \bar{C} across locations ℓ ,

$$\bar{C} = C(\ell) = \kappa \frac{w(\ell) + r + \underline{s} - p\underline{c}}{q(\ell)^\gamma}, \quad (13)$$

with κ constant across locations, equal to $((1 - \gamma)\nu)^{(1-\gamma)\nu} ((1 - \gamma)(1 - \nu))^{(1-\gamma)(1-\nu)} \gamma^\gamma / p^{\nu(1-\gamma)}$.

The mobility Equation (13) implies that $\left(\frac{w(\ell) + r + \underline{s} - p\underline{c}}{q(\ell)^\gamma}\right)$ is constant across locations. This holds within urban locations ($\ell \leq \phi$), within (identical) rural locations as well as when comparing an

urban and rural worker. Since workers in the rural sector do not face spatial frictions and live in ex-post identical locations, $\ell \geq \phi$, the price of housing must be the same across these locations. We denote by q_r the price of housing in the rural sector, where $q_r = q(\ell \geq \phi)$. A worker in the rural sector is paid his marginal productivity w_r , receives land rents r and faces the same housing price $q_r = q(\phi)$ than an urban worker at the fringe. Therefore we have

$$w(\phi) = w_r = w_u - \tau(\phi). \quad (14)$$

In other words, the urban worker at the urban fringe must have the same wage net of commuting frictions than a rural worker. Equation (14) is essential to understand the spatial allocation of workers: higher spatial frictions at the fringe ϕ reduce incentives of rural households to move to the city. Equation (14) also shows how the spatial structure matters to understand the urban-rural wage gap.

Housing Rental Price Gradient. Within city locations ($\ell \leq \phi$), the housing price adjusts such that workers are indifferent across locations. Using Equations (13) and (14), we get

$$q(\ell) = q_r \left(\frac{w(\ell) + r + \underline{s} - p\underline{c}}{w(\phi) + r + \underline{s} - p\underline{c}} \right)^{1/\gamma} = q_r \left(\frac{w(\ell) + r + \underline{s} - p\underline{c}}{w_r + r + \underline{s} - p\underline{c}} \right)^{1/\gamma}. \quad (15)$$

Within the city, $q(\ell)$ is falling with ℓ to compensate workers who live in worse locations. For ℓ above ϕ , the housing price is constant across locations and equal to q_r . A crucial difference compared to the standard urban model is that the price at the fringe q_r is endogenously determined in our general equilibrium model.

3.5 Housing Market Equilibrium

Housing Demand. Using Equation (15), the demand for housing space per worker in each location $h(\ell)$ is increasing with ℓ for $\ell \leq \phi$,

$$h(\ell) = \gamma \left(\frac{w(\ell) + r + \underline{s} - p\underline{c}}{q(\ell)} \right) = \left(\frac{\gamma}{q_r} \right) (w(\phi) + r + \underline{s} - p\underline{c})^{1/\gamma} (w(\ell) + r + \underline{s} - p\underline{c})^{1-1/\gamma}. \quad (16)$$

Facing higher housing prices, household closer to the CBD demand less housing space. Importantly, a lower fringe price q_r and lower spending for subsistence $p\underline{c}$ increase the demand for housing space in the city. For locations in the rural area, housing demand per rural worker is constant equal to $h(\ell \geq \phi) = \gamma \left(\frac{w_r + r + \underline{s} - p\underline{c}}{q_r} \right)$.

Housing Supply. The supply of housing (floorspace) is provided by land developers, which can use more or less intensively the land for residential purposes. In each location ℓ , developers supply housing space $H(\ell)$ per unit of land with a convex cost, $\frac{H(\ell)^{1+1/\epsilon}}{1+1/\epsilon}$ with $\epsilon > 0$, paid in units of the

numeraire.²⁰ Profits per unit of land of the developers are

$$\pi(\ell) = q(\ell)H(\ell) - \frac{H(\ell)^{1+1/\epsilon}}{1 + 1/\epsilon} - \rho(\ell),$$

where $\rho(\ell)$ is the rental price of a unit of land in location ℓ (henceforth the land price). Similarly to the housing price $q(\ell)$ above, for locations beyond the fringe ϕ , the land price is constant, hence $\rho_r = \rho(\ell \geq \phi)$.

Maximizing profits gives the following supply of housing $H(\ell)$ in a given location ℓ ,

$$H(\ell) = q(\ell)^\epsilon, \tag{17}$$

where the parameter ϵ is the price elasticity of housing supply. More convex costs to build intensively on a given plot of land reduces the supply response of housing to prices.²¹

Lastly, free entry imply zero profits of land developers. This pins down land prices in a given location,

$$\rho(\ell) = \frac{q(\ell)H(\ell)}{1 + \epsilon} = \frac{q(\ell)^{1+\epsilon}}{1 + \epsilon}. \tag{18}$$

Equation (18), together with Equation (15), implies that land prices are higher in locations closer to the city center, more so if land developers can build more intensively (higher ϵ).

Arbitrage across land use implies that the land price in the urban sector, $\rho(\ell)$, must in equilibrium be above the marginal productivity of land for production of the rural good (Equation (3)), where the condition holds with equality in the rural part of the economy, for $\ell \geq \phi$,

$$\rho_r = \frac{q_r^{1+\epsilon}}{1 + \epsilon} = (1 - \alpha)p\theta_r \left(\frac{L_r}{S_r} \right)^\alpha. \tag{19}$$

Importantly, this equation shows that a fall in the relative price of rural goods and/or a reallocation of workers away from the rural sector lowers the price of urban land at the city fringe.

Housing Market Clearing. Consider first locations within the city, $\ell \leq \phi$. Market clearing for housing in each location implies $H(\ell) = D(\ell)h(\ell)$, where $D(\ell)$ denotes the density (number of urban workers) in location ℓ . Within the city, the density $D(\ell)$ follows from Equations (16) and (17), hence

$$D(\ell) = \frac{H(\ell)}{h(\ell)} = \frac{q(\ell)^{1+\epsilon}}{\gamma(w(\ell) + r + \underline{s} - p\underline{c})}. \tag{20}$$

²⁰The urban good is used as an intermediary input for the production of housing space. $1/\epsilon > 0$ is a cost parameter measuring the convexity of the cost function. In extension B.1.3, we use a more general cost function. The parameter $\epsilon = \epsilon(\ell)$ can depend on the location.

²¹Some equivalent formulation holds for a Cobb-Douglas production function of housing (see Combes et al. (2018)).

Density for $\ell \leq \phi$ can be rewritten using Equation (15) and Equation (18) as

$$D(\ell) = \rho_r \frac{1+\epsilon}{\gamma} (w(\phi) + r + \underline{s} - p\underline{c})^{-\frac{1+\epsilon}{\gamma}} (w(\ell) + r + \underline{s} - p\underline{c})^{\frac{1+\epsilon}{\gamma}-1}. \quad (21)$$

Importantly, a lower rural land price ρ_r at the urban fringe lowers density across all urban locations. Integrating density defined in Equation (21) across urban locations gives the total urban population,

$$L_u = \int_0^\phi D(\ell) d\ell = \rho_r \int_0^\phi \frac{1+\epsilon}{\gamma} (w(\phi) + r + \underline{s} - p\underline{c})^{-\frac{1+\epsilon}{\gamma}} (w(\ell) + r + \underline{s} - p\underline{c})^{\frac{1+\epsilon}{\gamma}-1} d\ell. \quad (22)$$

Equation (22) pins down the city size ϕ . It says that if more workers are willing to move in the urban sector, the city will have to be bigger in area to host them— ϕ is increasing with L_u . One should also notice that the city's area increases if the price of land ρ_r at the fringe is lower, if subsistence needs $p\underline{c}$ are lower, if housing supply conditions are tighter (low ϵ), and if commuting frictions $\tau(\ell)$ are lower.

In the rural area, $\ell \geq \phi$, market clearing for residential housing imposes

$$L_r \gamma (w_r + r + \underline{s} - p\underline{c}) = S_{hr} (q_r)^{1+\epsilon} = S_{hr} (1+\epsilon) \rho_r,$$

where S_{hr} is the amount of land demanded in the rural area for residential purposes. This leads to the following demand of land for residential purposes in the rural area,

$$S_{hr} = \frac{L_r \gamma (w_r + r + \underline{s} - p\underline{c})}{(1+\epsilon) \rho_r}. \quad (23)$$

Land and labor market clearing. Land is used for residential or productive purposes. With total land available in fixed supply S , the land market clearing condition is

$$S_r + S_{hr} + \phi = S$$

Using Equation (23), this is equivalent to

$$S_r = S - \phi - \frac{L_r \gamma (w_r + r + \underline{s} - p\underline{c})}{(1+\epsilon) \rho_r}. \quad (24)$$

The labor market clearing is such that the total population L is located either in the city or in the rural area,

$$L_u + L_r = L. \quad (25)$$

Land rents. Aggregate land rents, rL , include the land rents generated both in the city and in the rural area,

$$rL = \int_0^\phi \rho(\ell) d\ell + \rho_r \times (S - \phi), \quad (26)$$

where it is useful to notice that the rental income in the city exceeds the rental income of farmland for the same area due to spatial frictions.

3.6 Goods markets equilibrium

A last step consists in clearing the goods market for rural and urban goods to pin down the allocation of labor across sectors for a given equilibrium city size ϕ .

Aggregate per capita income. Let us introduce y as the aggregate per capita income in the economy net of spatial frictions that is spent on both goods,

$$y = r + \frac{L_r}{L}w_r + \frac{1}{L} \int_0^\phi w(\ell)D(\ell)d\ell.$$

Goods market clearing conditions. Aggregating Equations (10)-(11) across locations, we get that aggregate per capita consumption of rural good and urban good satisfy

$$\begin{aligned} pc_r &= \nu(1 - \gamma)(y + \underline{s} - p\underline{c}) + p\underline{c} \\ c_u &= (1 - \nu)(1 - \gamma)(y + \underline{s} - p\underline{c}) - \underline{s} \end{aligned}$$

The rural good is only used for consumption. This gives the following market clearing condition for the rural good,

$$\nu(1 - \gamma)y + \nu(1 - \gamma)(\underline{s} - p\underline{c}) + p\underline{c} = py_r, \quad (27)$$

where $y_r = \frac{Y_r}{L}$ denotes the production per worker of the rural good.

The urban good market clearing is more involved as urban goods are either consumed, used as intermediary inputs to build residential housing (in all locations) or used to pay for commuting costs. The sum of these three uses equals the supply of the urban good, expressed per capita,

$$c_u + \frac{1}{L} \int_0^\phi \tau(\ell)D(\ell)d\ell + \frac{1}{L} \frac{\epsilon}{1 + \epsilon} \int_0^S q(\ell)H(\ell)d\ell = y_u, \quad (28)$$

where $y_u = \frac{Y_u}{L}$ denotes the production per worker of the urban good.

3.7 Equilibrium allocation

For a given set of exogenous parameters, technological parameters $(\theta_u, \theta_r, \alpha)$, commuting cost parameters (a, ξ) and resulting spatial frictions $\tau(\ell)$ at each location $\ell \in \mathcal{L}$, housing supply conditions ϵ , and preference parameters, $(\nu, \gamma, \underline{c}, \underline{s})$, the equilibrium is defined as follows:

Definition 1. *An equilibrium is a sectoral labor allocation (L_u, L_r) , a city fringe (ϕ) and rural land used for production (S_r) , sectoral wages (w_u, w_r) , a rental price of farmland (ρ_r) , a relative price of rural goods (p) and land rents (r) , such that:*

- *Factors are paid the marginal productivity, Equations (1)-(3).*
- *Workers are indifferent in their location decisions, Equation (14).*
- *The demand for urban residential land (or the city fringe ϕ) satisfies Equation (22).*
- *Land and labor markets clear, Equations (24) and (25).*
- *Land rents satisfy Equation (26).*
- *Rural and urban goods markets clear, Equations (27) and (28).*

The main intuition for the equilibrium allocation goes as follows: if the urban sector hosts more workers, the area of the city has to be larger (ϕ tends to increase with L_u). However, if the city is larger in area, the worker in the further away urban location commutes more, making the urban sector less attractive for workers: a higher ϕ reduces the incentives of workers to move from the rural to the urban sector (L_u tends to decrease with an increasing ϕ). Given technology, the combination of these two forces pins down the allocation of workers across sectors together with the land used for urban residential housing.

However, the equilibrium cannot be described analytically. Thus, we use numerical illustrations to explain the main mechanisms through which increasing productivity, in the rural and urban sectors, change the population, area and density of cities in our framework. The numerical simulations are not aiming at being a measurement tool but at elucidating the main channels at play to understand urban expansion when economies go through the process of structural change. A quantitative evaluation in the context of France is provided in Section 4.

3.8 Numerical illustrations

Parameter values. We consider an economy as described above endowed with land and labor, both normalized to 1. While the exercise is not quantitative, we nevertheless set parameters values in a reasonable range with respect to the data. The share of land in rural production is set to 25% ($\alpha = 0.75$). We set the constant elasticity of housing supply ϵ to 4 in the range of empirical estimates. Preferences towards the different goods are set to roughly match the employment share in agriculture and the housing spending share in the recent period in France— $\nu = 2.5\%$ and $\gamma = 30\%$. At each date t , the productivity is assumed to be the same in both sectors, $\theta_{u,t} = \theta_{r,t}$, and the initial productivity is normalized to unity. Both sectors are growing at the same constant rate of productivity growth of 1.25% per annum. Most importantly, together with rising productivity, structural change emerges due to the presence of subsistence needs for rural goods, $\underline{c} = 2/3$. As we focus on subsistence needs, we set \underline{s} to zero. With such preferences, the share of employment in the rural sector is about 60% at start. For comparison, we explore at a later stage the model dynamics when structural change is driven by increasing demand for urban goods rather than subsistence needs ($\underline{s} \gg \underline{c}$). The values for the commuting costs parameters are set such that the urban area

remains small relative to land used in agriculture, $a = 2$.²² The parameter determining the elasticity of commuting costs to urban income and commuting distance, ξ , is set to 2/3 to generate an increase in the average urban commuting speed comparable to the data (see Miles and Sefton (2020)).²³

Baseline. Figure 6 summarizes the model dynamics following rising productivity in both sectors—starting at an initial period labeled 1840 for illustration purposes. The top panel shows the evolution of employment, spending shares and relative prices. As well known in the literature, due to low initial (rural) productivity, the share of workers needed to produce rural goods is high at start to satisfy subsistence needs. The demand for rural goods for subsistence makes them initially relatively expensive and households spend a disproportionate share of income on rural goods. With rising (rural) productivity solving the ‘food problem’, workers move away from the rural to the urban sector, the relative price of rural goods falls, as well as the spending share towards rural goods.

The bottom panel of Figure 6 shows outcomes that are more specific to our theory with endogenous land use: urban area (compared to urban population), urban densities (average, central and fringe) and land rents (as a share of income). Along the process of structural change, urban area grows faster than urban population, leading to a fall in the average urban density (plots (d) and (e) of Figure 6). This is the outcome of two different forces. On one hand, this is the natural consequence of *rural* productivity growth solving the ‘food problem’: higher rural productivity frees up farmland for cities to expand, lowering farmland rents relative to income. Moreover, as workers spend less on rural goods, they can afford larger homes and spend relatively more on housing. The city expands outwards at a fast rate. As land at the city fringe is getting cheaper (relative to income), the city expands by adding a less and less dense suburban fringe over time, contributing to the fall in average urban density (plot (e) of Figure 6).

On the other hand, rising *urban* productivity leads to a reallocation of workers away from the dense center towards the fringe—contributing further to the fall in average urban density. With a rising urban income, workers move towards the suburbs to enjoy larger homes despite a rising opportunity cost of commuting time. This is so because they optimally choose faster commuting modes when moving towards the suburbs. Thus, although the mechanisms are entirely different, both rural and urban productivity growth contribute to urban sprawl and falling urban density in this experiment.

Regarding land rents, the reallocation of workers away from agriculture and the fall in the relative price of rural goods exerts downward pressure of the price of farmland. Thus, land rents are reallocated away from the rural part towards the urban part (plot (f) of Figure 6)).

To sum up, beyond the well-known predictions regarding employment shares across sectors, our theory is able to qualitatively reproduce the salient facts described in Section 2 for France regarding the expansion of the urban area, the evolution of urban density and land values.

²²In our formulation of the commuting costs, a is a transformation of the different commuting costs parameters but one can always set the commuting efficiency c_r to target a given a (see Equation 7).

²³In Miles and Sefton (2020), the average speed of commuting in England has been multiplied by almost 5 since 1840—in line with our baseline experiment described below. Parisian data detailed in Appendix A.9 shows a similar increase.

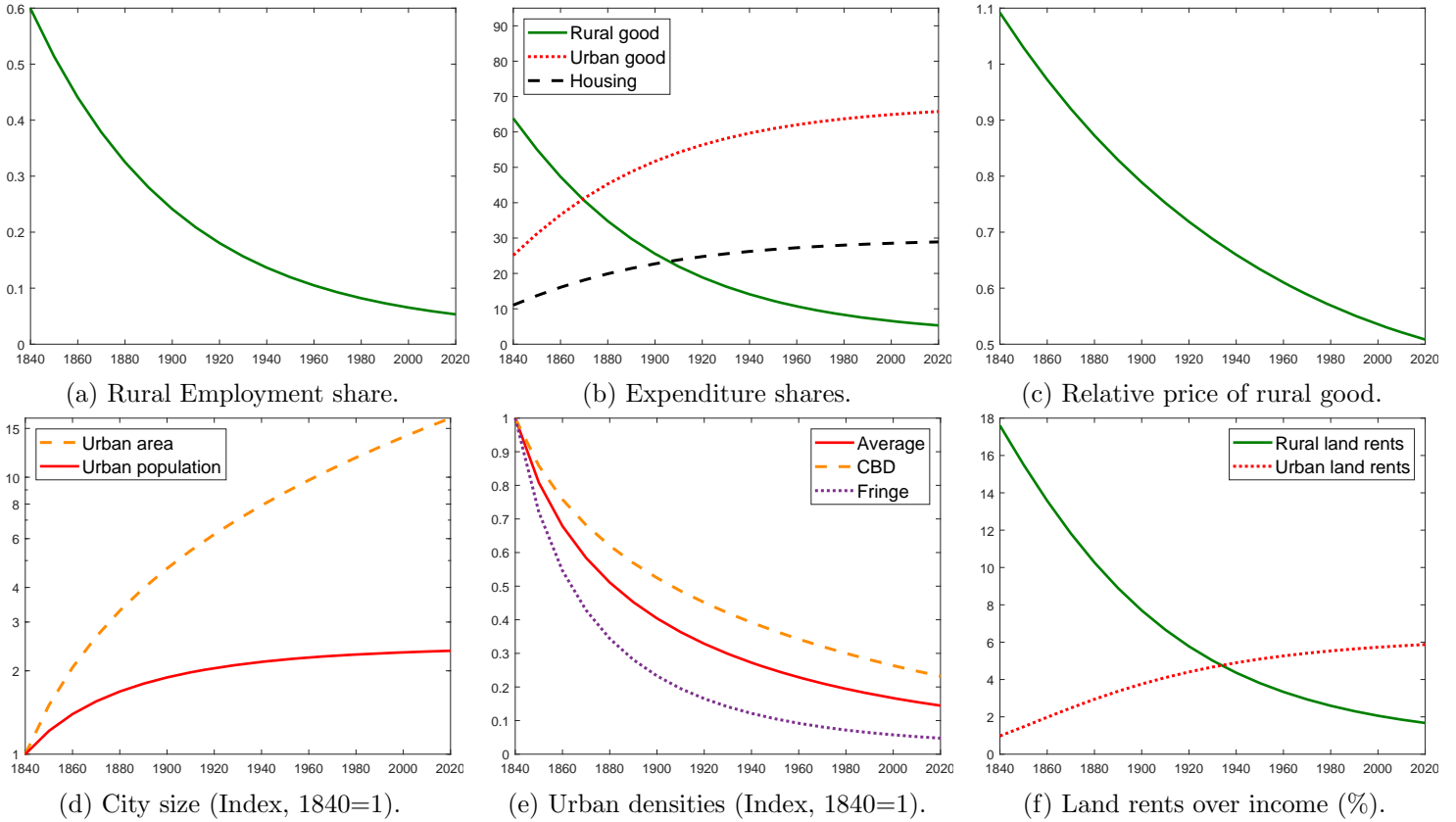


Figure 6: Baseline numerical illustration.

Notes: Simulation with 1.25% constant productivity growth in both sectors, $\underline{c} > 0$, and $\underline{s} = 0$.

Rural versus urban productivity growth. To disentangle further the mechanisms at play, it is useful to investigate the model’s implications when only rural or urban productivity growth occurs. Figure 7 shows selected model’s outcomes with only rural productivity growth— θ_r growing at 1.25% per year, while θ_u is set to unity throughout. The qualitative implications are similar to the baseline illustration. Workers move away from the rural sector, the rural good and farmland are getting less expensive and urban density falls despite rising urban population. However, the city sprawls less: without urban productivity growth, there is less reallocation away from central locations towards the fringe. Average urban density mostly falls due to the addition of lower density habitat at the urban fringe where land gets cheaper—central density falling significantly less.

Figure 8 shows model’s outcomes with only urban productivity growth— θ_u growing at 1.25% per year, while θ_r is set to unity throughout (resp. a high value for comparison). Here, the qualitative implications are more widely different from the baseline illustration. Urban productivity growth leads to urban expansion in area but not in population: many rural workers are required to satisfy subsistence needs and feed the population (plot (a) of Figure 8).²⁴ The city expands in area as higher urban productivity reallocates urban workers away from the center towards the urban

²⁴Urban population might even very slightly fall as more workers are required to produced subsistence needs with less land available for agriculture.

fringe. As the demand for land at the fringe rises, so does the price: farmland is getting more expensive. This, in turn, increases suburban density, mitigating the overall fall in urban density. As a consequence, central density is falling more than the average one (plot (b) of Figure 8). With only urban productivity growth, rural land rents (as a share of income) do not fall and there is no reallocation of land values towards the urban areas (plot (c) of Figure 8). Thus, rising urban productivity and faster urban commutes are not sufficient to account for the evolution of urban densities and land rents across space.

Lastly, it is important to note that the reallocation of urban residents away from the center towards the suburbs is significantly stronger at a higher level of rural productivity. In other words, the interaction between rural and urban productivity matters for the area expansion of cities (plot (a) of Figure 8). If rural productivity is low, people spend most of their resources on rural necessity goods, limiting their ability to expand their housing space when urban productivity increases. As a consequence, rising urban productivity reallocate significantly less people towards the suburbs and cities stay dense despite higher urban wages. To the opposite, when rural productivity is high enough, rising urban productivity expands the urban area much more as urban residents afford larger housing space. In this sense, beyond the direct effect of rural productivity on urban expansion, rural productivity is also crucial as it provides the necessary incentive for people to relocate towards the city fringe and use faster commutes when urban productivity increases.

To sum up, our numerical illustrations show how, in the presence of subsistence needs, agricultural productivity growth not only matters for urbanization and the reallocation of workers away from the rural sector, but it is also essential to replicate the large historical decline in urban density, the fall in farmland prices (relative to income) and the reallocation of land rents towards urban areas.

Labor push versus labor pull. In the baseline illustration, the driver of structural change is rural productivity growth combined with subsistence needs for rural goods—a model where rising productivity frees up resources for the urban sector to expand (‘rural labor push’). An alternative view on structural change would emphasize a rising demand for (luxury) urban goods as income rises (‘urban labor pull’). In our set-up, this would correspond to a high \underline{s} relative to \underline{c} . For comparison, we simulate the economy with a value for \underline{s} twice as big as \underline{c} ($\underline{s} = 2\underline{c} = 1.2$), such that, keeping all other parameters to their baseline values, the initial share of employment in the rural sector remains close to 60%. Under such preferences, Figure 9 shows the model dynamics following rising productivity in both sectors. While such a calibration can generate employment shares broadly in line with the evidence, it cannot generate the observed fall in urban density. As income increases, the spending share on housing falls as the income elasticity of housing demand is low: workers are willing to reduce their housing size to consume more of the urban good. Thus, the city does not expand much in area to host more numerous urban workers and urban density does not fall. Urban density tends to increase due to the reallocation of workers towards the urban center (plot (b) of Figure 9): as they shrink their housing size, urban workers relocate away from the suburbs towards

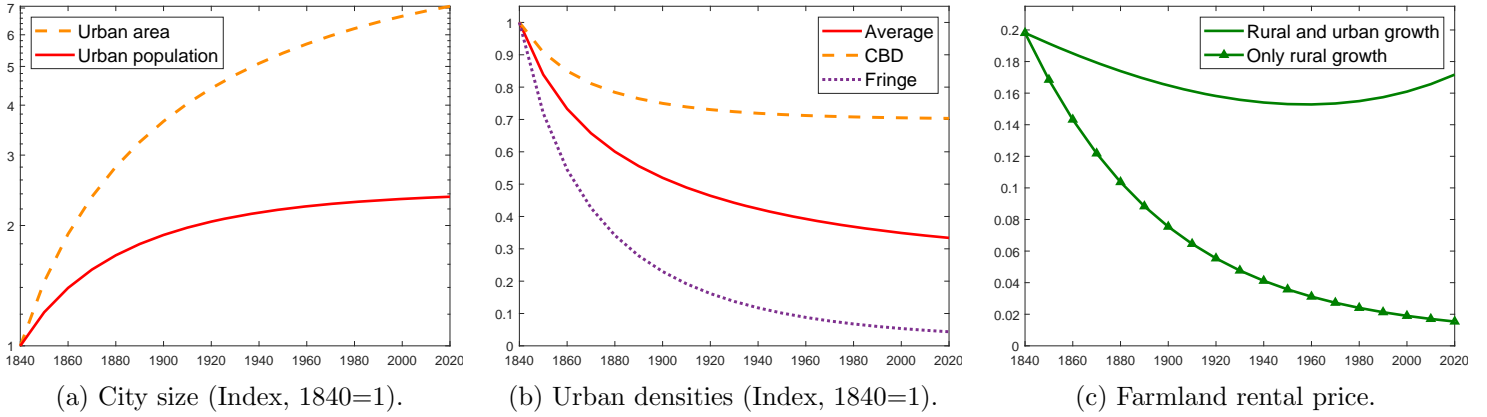


Figure 7: Numerical illustration with only rural growth.

Notes: Simulation with 1.25% constant rural productivity growth and constant urban productivity; $\underline{c} > 0$ and $\underline{s} = 0$.

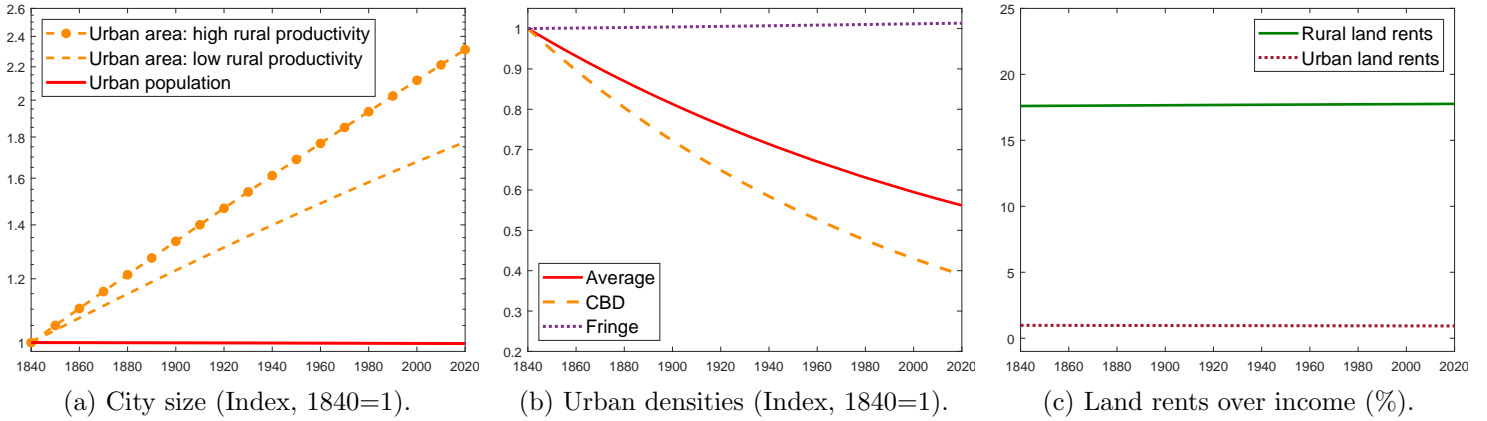


Figure 8: Numerical illustration with only urban growth.

Notes: Simulation with 1.25% constant urban productivity growth and constant rural productivity; $\underline{c} > 0$ and $\underline{s} = 0$. The line with circles corresponds to the simulation with rural productivity being equal to the last period value, while the others correspond to the simulation with rural productivity being equal to the initial period value.

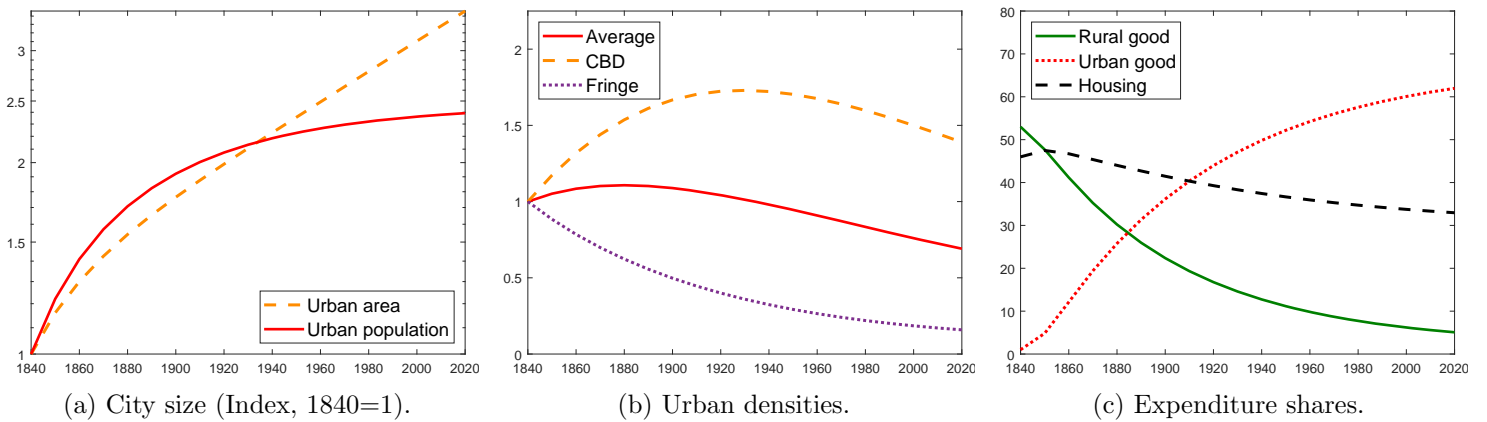


Figure 9: Numerical illustration with $\underline{s} > \underline{c} > 0$.

Notes: Simulation with 1.25% constant productivity growth in both sectors. The preference parameters are such that $\underline{s} = 2\underline{c} > 0$, while keeping the initial rural employment share close to 60%.

central locations, increasing central density—the opposite of the data.²⁵ A high enough subsistence need is thus important for urban density to decline as it leads to an increase in the housing spending share following structural change. Note also that the evolution of the spending share on housing is informative regarding the relative magnitude of \underline{c} and \underline{s} (plot (b) of Figure 6 and plot (c) of Figure 9). An increasing share of housing spending, as in the data (see the calibration description in Section 4), points towards a calibration where \underline{c} is significantly larger than \underline{s} .

4 Quantitative Model

We develop a quantitative version of the model to account for the process of structural change and urban expansion in France. The quantitative model is calibrated in 10-year steps using French historical data since 1840. Data are described in detail in Appendix A. We implement first a single city economy without agglomeration/congestion forces. One can interpret the following quantitative simulations as aggregate outcomes for the ‘average’ French city.

We present in this section results from an extended model which is better suited to match the data. We describe the extensions in detail in Appendix B. First, we consider a surface instead of a line segment as given land endowment. The city is circular with endogenous radius ϕ and area $\pi\phi^2$. Second, we allow for a more flexible parametrization of the commuting costs and of the construction costs faced by land developers. The latter are such that the housing supply elasticities depend on the location within the city (as in Baum-Snow and Han (2019)). Lastly, we consider a dynamic version of the model where households maximize their lifetime utility with borrowing and lending in a risk-free asset, which is in net-zero supply. Given a discount factor β , this pins down the path of the equilibrium real interest rate in our simulations and allows the computation of land values beyond rents. The relevant model for the current section is thus the one defined in Appendix B.1.4.

4.1 Calibration

The technology parameters are calibrated externally and the remaining parameters are set to match some outcomes observed in the data. While some parameters are jointly determined to minimize the distance between the model’s outcomes and a set of specified moments in the data, we provide, for sake of space, the main intuitions behind the identification of the model’s parameters. Details of the joint estimation of parameters $\{\nu, \gamma, \underline{c}, \underline{s}, a\}$ and the minimization procedure are provided in Appendix B.2.4. The parameter values for the baseline simulation of the quantitative model are summarized in Table 1.

²⁵Suburban (fringe) density does fall in this experiment (plot (b) of Figure 9). The same mechanisms as in our baseline illustration also play a role: farmland is getting cheaper at the city fringe due to structural change.

Parameter	Description	Value
S	Total Space	1.0
L_0	Total Population in 1840	1.0
θ_0	Initial Productivity in 1840	1.0
α	Labor Weight in Rural Production	0.75
σ	Land-Labor Elasticity of Substitution	1.0
ν	Preference Weight for Rural Consumption Good	0.03
γ	Utility Weight of Housing	0.3
\underline{c}	Rural Consumption Good Subsistence Level	0.74
\underline{s}	Initial Urban Good Endowment	0.21
β	Discount Factor	0.94
ξ_l	Elasticity of commuting cost wrt location	0.55
ξ_w	Elasticity of commuting cost wrt urban wage	0.75
a	Commuting Costs Base Parameter	2.25
ϵ_r	Housing Supply Elasticity in rural area	5.0
$\epsilon(0)$	Housing Supply Elasticity at city center	2.0

Table 1: Parameter values

Technology. The share of land used in agriculture is set to 25%, $\alpha = 0.75$ as in [Boppart et al. \(2019\)](#). [Boppart et al. \(2019\)](#) provide an estimate very close to unity for the elasticity of substitution between land and labor in agriculture. Thus, as in our baseline model, rural production in the quantitative model is Cobb-Douglas but we perform sensitivity with respect to this elasticity of substitution in [Appendix C.3](#).

The path for productivity in both sectors, θ_r and θ_u , is calibrated to match its data counterpart using French sectoral data on production, employment and agricultural land use since 1840.²⁶ The estimated path for θ_r and θ_u (displayed in [Figure 10](#)) is in line with the evolution of the standards of living in France over the period. Such a path for productivity is consistent with the conventional view that the nineteenth century is characterized by faster productivity growth in non-agricultural sectors, manufacturing in particular, while agricultural productivity grew significantly faster post-World War II. More specifically, starting the agricultural crisis in the late nineteenth century, technological progress in the French agriculture was particularly slow and delayed relative to other countries, before catching up at a fast rate post World War II ([Bairoch \(1989\)](#)). See [Appendices A.4](#) and [B.2.1](#) for details on estimation and smoothing of the θ_r, θ_u data for use in the model.

Demographics. Population, L_t , is normalized to unity in the first period and set at each date to match the increase of the French population since 1840 according to Census data. Over the period considered, the French population roughly doubled and the increase in the labor force is of the same magnitude. Going forward, we use the projections for the French population by INSEE until 2040 and set a constant growth rate of 0.4% thereafter.

²⁶1840 is the first date of observation for agricultural land use necessary to compute the path of rural productivity. Due to the normalization of price indices, θ_r and θ_u are set equal to unity in this initial period. The yearly path of θ_s in the data is smoothed to remove business cycles fluctuations.

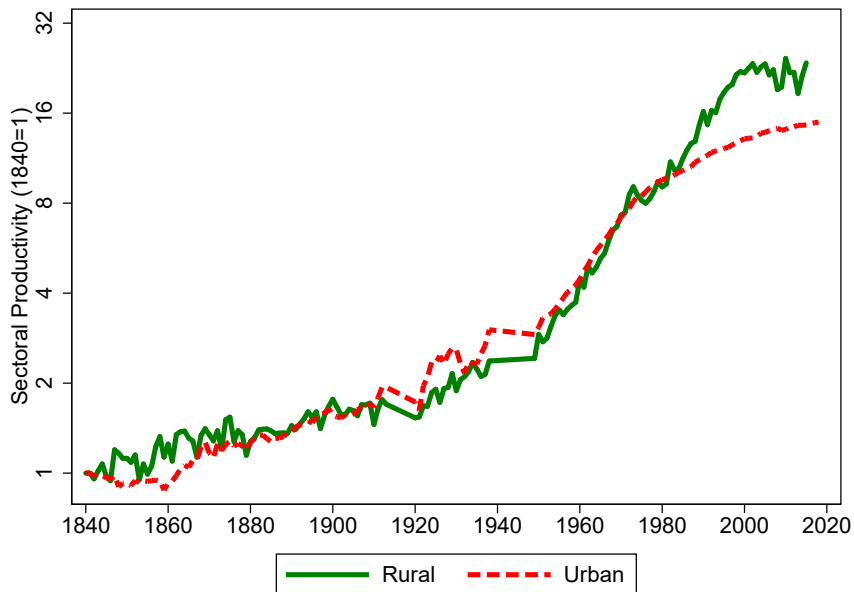


Figure 10: Estimated Productivity Series, Rural (θ_r) and Urban (θ_u), 1840=1 (1840-2019). Estimation details in Appendix A.4.

Preferences. Given technology, demographics, and the commuting costs elasticities, the preference parameters $\{\nu, \gamma, \underline{c}, \underline{s}\}$ are jointly set such that the agricultural employment share and the housing spending share are in line with the data. More precisely, the subsistence needs in agriculture parameter, \underline{c} , determines the initial agricultural employment share in 1840, while the preferences parameter towards the rural good, ν , determines the long-run employment of share in agriculture. Similarly, the endowment of urban good, \underline{s} , determines the housing spending share for the year 1900 (23.7% with a 5-year average around 1900)—our initial period of observation regarding consumption expenditures, while the preference parameter towards housing services, γ , determines the housing spending share in recent years (31.4% in 2015).

The last preference parameter, the discount factor β , is irrelevant for the equilibrium allocation but pins down the rate of interest and thus matters for the value of land at each date. It is set externally to 0.94 such that the value of agricultural land over income matches the data in 1840.

Housing supply conditions. Existing estimates of the housing supply elasticities, ϵ , typically vary between 2 and 5, depending on the location as well as on the estimation technique (see, among others, Albouy et al. (2018), Combes et al. (2017) and Baum-Snow and Han (2019)).²⁷ Baum-Snow and Han (2019) provides evidence of the *within-city* variation of the housing supply elasticities, ranging from about 2.5 at the CBD to about 5 at the fringe of cities. For the purpose of the quantitative analysis, we extend the baseline theory by allowing location-specific housing supply elasticities, $\epsilon(\ell)$ with $\partial\epsilon(\ell)/\partial\ell \geq 0$ (see Appendix B.1.3 for details). This is meant to capture that

²⁷With Cobb-Douglas production of housing using land and structure, there is a mapping between the elasticity ϵ and the land share in housing production. Typical estimates of the land share varies between 0.2 and 0.3, corresponding to elasticities between 2 and 4.

it might be more costly for developers to build closer to the center than in the suburbs or the rural part of the economy. Following [Baum-Snow and Han \(2019\)](#), we set an elasticity of 2 at the CBD and 5 at the fringe and the rural area, and we report sensitivity to this value in [Appendix C.1](#).²⁸ For comparison purposes, we also perform sensitivity analysis with a constant elasticity of housing supply, $\epsilon = 3$, with results displayed in [Appendix C.2](#).

Commuting costs. For the purpose of our quantitative analysis, we expand the commuting choice model by introducing a more general spending cost on commuting f , which still depends on the mode choice m but also on the commuting distance ℓ and the labor costs w_u (see [Appendix B.1.2](#) for details). Intuitively, beyond its speed, the pecuniary cost of a commuting mode depends on the distance traveled (e.g. cost of gasoline/energy) as well as the overall level of wages (e.g. wage of the bus driver). Under some parametric assumptions, commuting costs under an optimal mode choice are of the following form (comparable to [Equation \(7\)](#)),

$$\tau(\ell) = a \cdot w_u^{\xi_w} \cdot \ell^{\xi_\ell},$$

where the elasticities of commuting costs to income, ξ_w , and to distance, ξ_ℓ , are both positive and below unity. The parameter a is inversely related to the efficiency of the commuting technology. We use individual level commuting data detailed in [Appendix A.9](#) to calibrate the elasticities ξ_w and ξ_ℓ . In the model, the elasticity of speed to commuting distance is equal to $1 - \xi_\ell$. We find in [Appendix A.9.1](#) that this elasticity is precisely estimated within a narrow range around 0.45—depending on the sample used and the controls.²⁹ Thus, ξ_ℓ is set externally to 0.55.

The elasticity of commuting costs to income ξ_w is tied to the evolution of urban speed when average income increases. More precisely, $(1 - \xi_w)$ is the elasticity of speed to wage income at a given commuting distance. Using the individual commuting data detailed in [Appendix A.9.2](#), one can estimate the percentage change in speed over 30 years for a given commuting distance. Over the period 1984-2013, this increase is 11% for an increase in measured urban productivity of 44%—yielding an estimate for $\xi_w = 1 - \frac{11}{44}$. Thus, ξ_w is set externally to 0.75.

The remaining parameter a is estimated to make the urban area, $\pi\phi^2$, represent 18% of rural land in the recent period—the measured artificial land is 18% of the land used for agriculture in 2015. Results are not very sensitive to a as long as $\pi\phi^2$ is a relatively small fraction of the available land.

4.2 Results

We present model’s predictions over the period 1840-2020 under the baseline calibration with only one representative city. Data counterparts, when available, are described in [Appendix A](#).

Structural change. [Figure 11](#) shows that our model is able to account for the patterns of structural

²⁸We assume that the elasticities $\epsilon(\ell)$ evolve linearly from the central value to the fringe value. Results are barely affected when performing sensitivity analysis with respect to the functional form of $\epsilon(\ell)$.

²⁹Commuting data also shows that the relationship between speed and commuting distance is very close to log-linear as in the model. See same [Appendix](#).

change observed in the data. Rising rural productivity reallocates labor away from the rural sector and makes rural necessity goods less valuable. The relative price of rural goods falls as productivity increases. Our model fits the data on the historical evolution of the relative price remarkably well, despite not being targeted (Figure 11b). Moreover, rising income leads to a reallocation of spending away from rural goods towards the urban good and housing services: the spending share on the rural good gradually falls, the share spent on the urban good continuously increases, and so does the spending share on housing services, although at a slower speed (Figure 11c). Overall, the spending share patterns are broadly in line with the data if one abstracts from fluctuations in the interwar period (see Figure 25 in Appendix A.5).

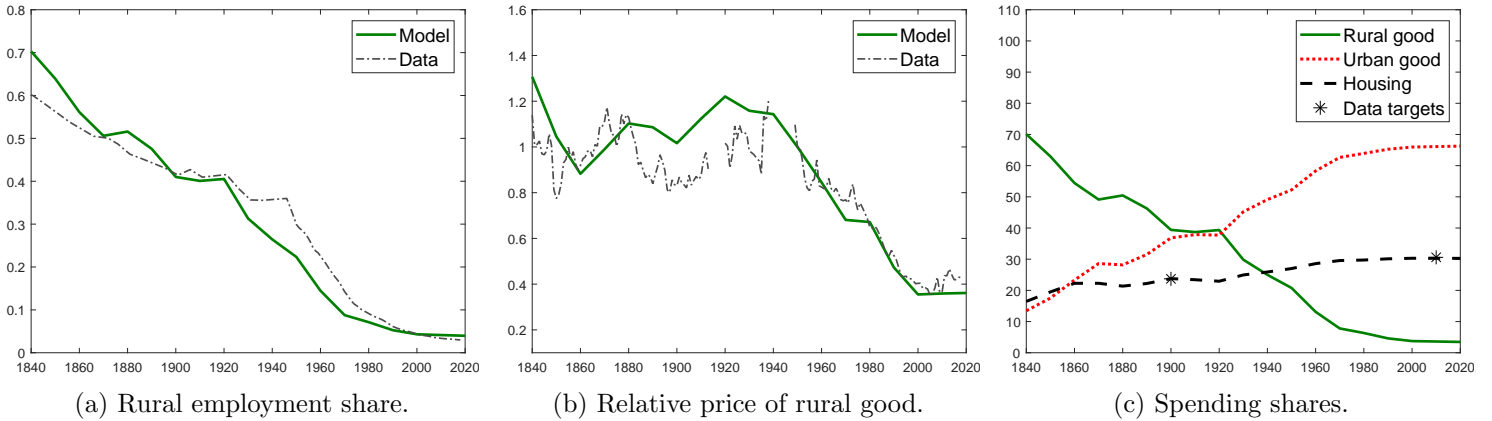


Figure 11: Structural change.

Notes: Outcomes of the baseline simulation of the quantitative model where parameters are set to the values of Table 1. Corresponding data for the employment share, the relative price of rural goods and spending shares are described in appendices A.2, A.3 and A.5. The relative price is normalized to 1 in 1950.

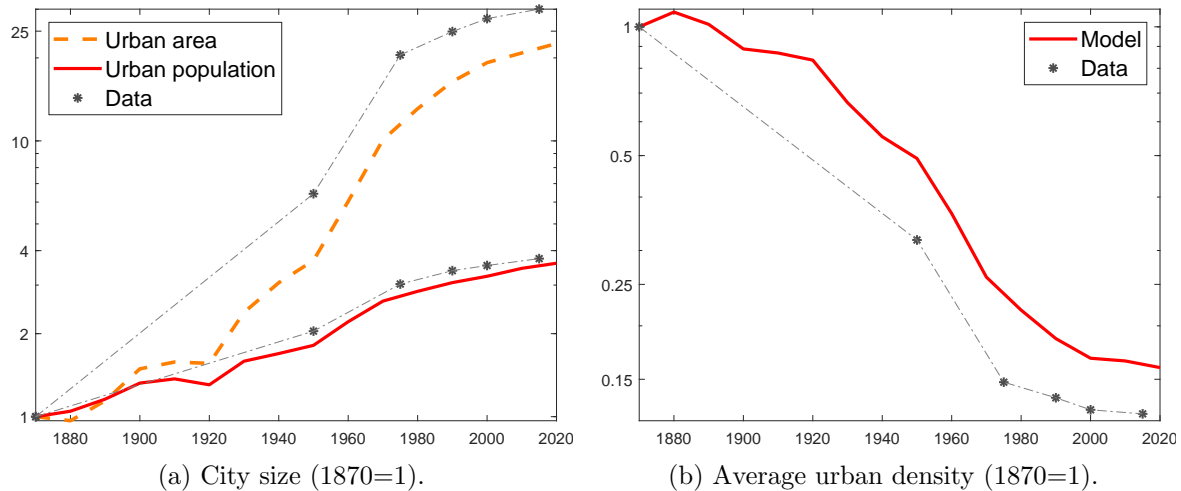


Figure 12: Urban expansion.

Notes: Outcomes of the baseline simulation of the quantitative model where parameters are set to the values of Table 1. Plots start in 1870 for comparison with data. Corresponding data for urban population, area and average density are described in Appendix A.7. Data and model outcomes are normalized to 1 in 1870 and shown on a log-scale.

Urban expansion. Figure 12 shows the model’s outcomes regarding the evolution of city size (area

versus population) and the average urban density. For comparison with data on urban expansion, the plots start in 1870—normalizing the 1870-value to unity. In line with the data, cities expand much faster in area than in population (Figure 12a). While our model does not account for the full observed expansion of the urban area, it explains a very large fraction. As a consequence, the model predicts a large fall in average urban density—density is divided by more than 6 since 1870, slightly less than in the data (Figure 12b). As structural change slows down, so does the fall in urban density.

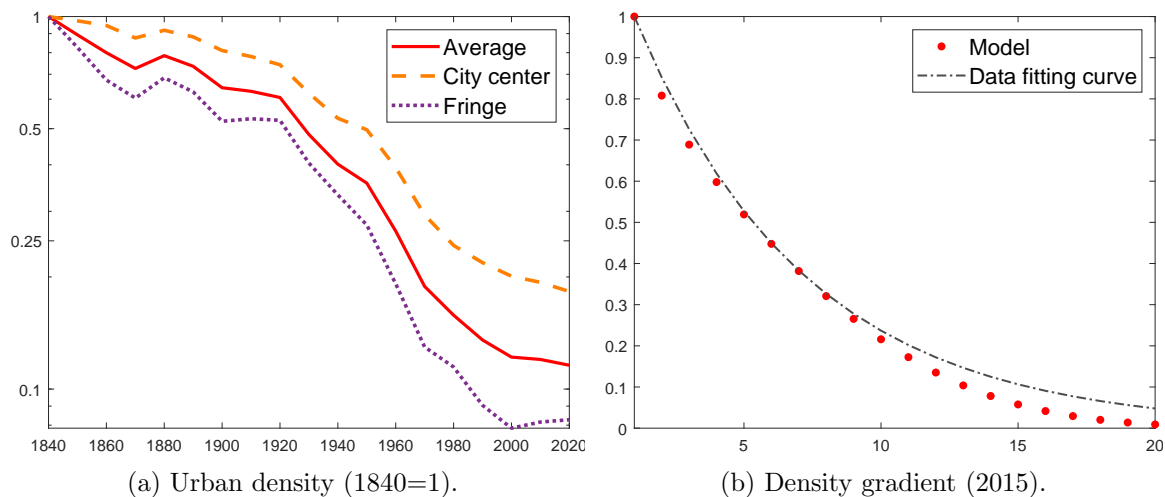


Figure 13: Density across space.

Notes: Outcomes of the baseline simulation of the quantitative model where parameters are set to the values of Table 1. Density in different urban locations (left plot) is normalized to 1 in 1840 for readability. Density of the city center is computed on a circle ending at 15% of the initial city radius in 1840. The right panel shows the model implied urban density at 20 equal-sized bins of distance from the center in 2015, where we normalized by the most central bin. For comparison, we also plot an exponential decay model whose coefficient we estimate from data as described in appendix A.7.4.

Density across space. Figure 13 shows the model’s predictions for density in different locations. Figure 13a depicts the evolution of the central density and the density at the fringe of the city (relative to the average), where densities are normalized to 1 in 1840 for readability.³⁰ The fall in average density is driven both by a fall in central density and a fall in density at the urban fringe. Central density falls because households find it worth to use faster commuting modes and to move towards the suburbs as their income rises. The fall in density at the suburban fringe is the natural consequence of structural change: the reallocation of workers away from agriculture combined with less valuable agricultural goods puts downward pressure on the price of farmland. Households can afford larger homes in the suburban parts of the city. The latter mechanism, more specific to our theory, is crucial to generate a fall in average density that is larger than the fall in the central one—in line with the Parisian data discussed in Section 2. Our model predicts that the overall fall in the central density is about 60% of the fall in the average density—in the ballpark of the estimates for Paris. Lastly, one can measure the density gradient by distance deciles within the

³⁰The fringe of the city center is at 15% of the radius of the city in 1840.

urban area, both in the data and in the model in the recent period. The model’s predictions are shown in Figure 13b. The shape of the curve is very close to an exponential (fitted curve) as in the data, and the value of the coefficient of the fitting curve is 0.16 as in the data (see Appendix A.7.4). Thus, our quantitative model provides a reasonable fit of the data regarding the density of urban settlements across time and space.

Commuting speed and the ‘agricultural productivity gap’. Our model with endogenous commuting costs generates predictions regarding the evolution of commuting speed across time. Moreover, the marginal urban worker, which has the longest commute, needs to be compensated relative to the rural worker. Our model thus predicts an endogenous urban-rural wage gap, which depends on the city fringe (ϕ) and the endogenous commuting costs in this furthest away location. These predictions are shown in Figure 14. Over time, our model generates almost a five-fold rise in the average commuting speed (Figure 14a). We collected historical data on the use of different commuting modes for Paris to provide an estimate of the evolution of the average commuting speed in the Parisian urban area (see Appendix A.9 for details). The overall increase in average speed since 1840 predicted by the model is of a similar magnitude than in the Parisian data.³¹ Beyond the overall increase, the predictions over the whole period line up relatively well with the evolution of commuting speed in the Parisian area. The increase by a factor of about 2 until 1930 reflects the more intensive usage of public transport and their increase in speed over this period (from the initial horse-drawn omnibus to the metro). The later increase, more specifically post-World War II, reflects the increasing car usage. Overall, the model provides predictions regarding the evolution of the average urban speed that are of reasonable magnitude.

Following Gollin et al. (2014), Figure 14b shows the ‘agricultural productivity gap’—a monotonic transformation of commuting costs at the fringe of the city proportional to the urban-rural wage gap, w_u/w_r . We compute the raw ‘agricultural productivity gap’ as,

$$\text{Raw-APG} = \frac{L_r/L_u}{VA_r/VA_u},$$

where VA_i denotes the value added in sector i . The value predicted by the model for the recent period, around 1.5, is in line with the values computed by Gollin et al. (2014) for France—lying in between their Raw-APG and Adjusted-APG. Computing the Raw-APG for the entire sample period directly from historical national accounts data, we find that our model falls short of the entire gap, especially for the initial years, but explains a large fraction since 1960.³² Our quantitative model suggests that spatial frictions combined with location-specific housing can generate urban-rural wage gaps of a significant economic magnitude. It also provides insights on the persistence of fairly large gaps even in developed countries, where labor misallocation is arguably less relevant.

³¹Miles and Sefton (2020) find a very similar increase in speed for the U.K.. Such historical data are not available for the rest of France but recent data indicates that this is likely to be a slight lower bound of the overall increase since car use is more limited in the Parisian urban area than elsewhere.

³²Using wage data, Sicsic (1992) provides estimates of the urban-rural wage gap in France over the period 1852-1911. Like in the U.K., he finds a significant increase of the gap over the period, in line with our predictions.

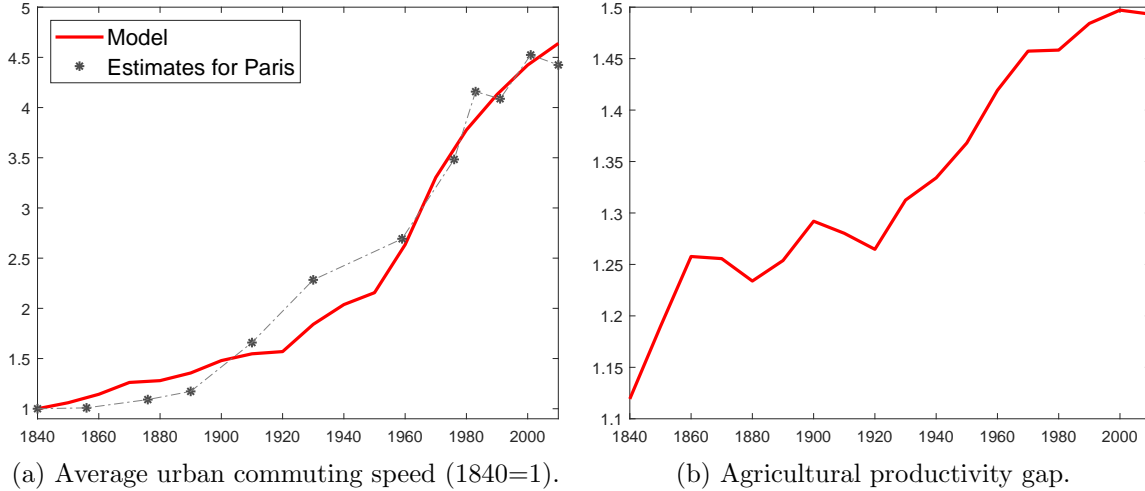


Figure 14: Commuting speed and the ‘agricultural productivity gap’.

Notes: Outcomes of the baseline simulation of the quantitative model where parameters are set to the values of Table 1. The average urban commuting speed (left plot) is the density-weighted average of speeds across urban locations (see Appendix B.1.6 for definition, normalization to 1 in 1840). Estimates for Paris are detailed in Appendix A.9.3. The agricultural productivity gap (right plot) is defined as $\frac{L_r/L_u}{V_{Ar}/V_{Au}}$.

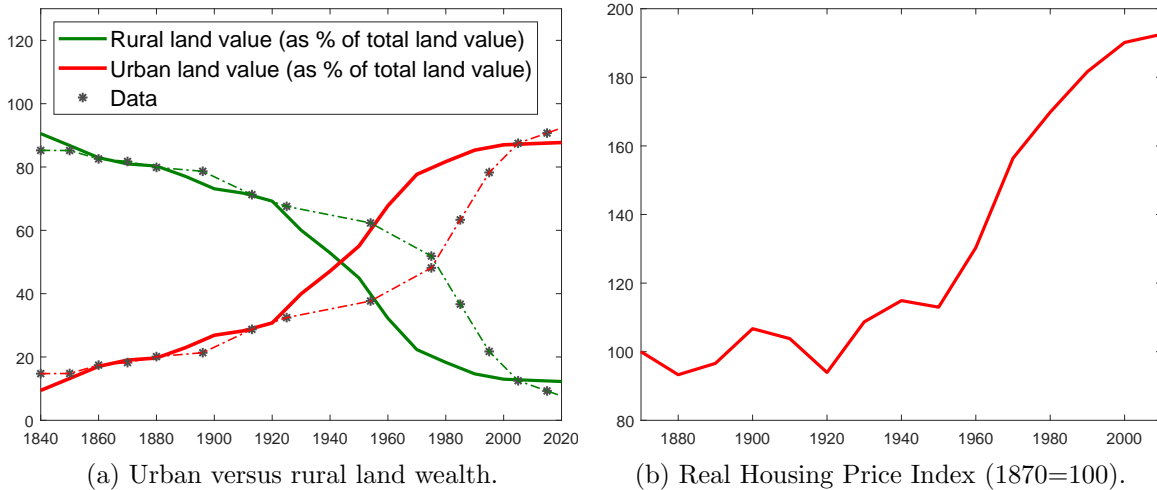


Figure 15: Land values and housing price.

Notes: Outcomes of the baseline simulation of the quantitative model where parameters are set to the values of Table 1. Land and housing values are computed as the discounted sum of future land rents in each location. Corresponding data (dashed) are based on Piketty and Zucman (2014) and described in more detail in Appendix A.6. The real housing price index averages the purchasing housing prices across locations (deflated using a model implied GDP-deflator). Details on the computation are provided in Appendix B.1.5.

Land values and housing prices. Figure 15 shows the model’s predictions for land values and housing prices. Figure 15a shows the reallocation of land value across rural and urban use. Due to structural change, the value of rural land relative to urban land fell dramatically. In the model, while the value of agricultural land constituted more than 80% of the total land value, it is less than 10% nowadays. This is broadly in line with data from Piketty and Zucman (2014) even though our model partly misses the timing of the reallocation around the time of World War II—arguably due

to war destructions.³³ Importantly, the value of urban land (per unit of land) increased faster in the recent decades. This mirrors the evolution of the housing price index since 1870 (Figure 15b), whose shape reminds of the hockey-stick shown in Figure 5b. The model generates about half of the increase in housing prices described in Knoll et al. (2017) post-World War II. Quantitatively, the model misses the very steep increase starting the late 1990s, most likely due to factors outside the model such as the large decline in interest rates and/or a tightening of land use restrictions.

4.3 Sensitivity analysis

In order to shed further light on the mechanisms at play and discuss the sensitivity of our results to the different elements of the model, we perform alternative experiments. More specifically, these experiments aim at showing how structural change and the use of faster commutes interact in driving the urban expansion. We also discuss the robustness of our findings to the production side in the rural and housing sector.

The role of rural productivity growth. To emphasize further the crucial role of technological progress in agriculture and structural change for our results, it is useful to perform sensitivity analysis with a lower rural productivity growth. We perform simulations with a stagnating (resp. slowly growing) rural productivity, where the growth rate of θ_r is 2% (resp. 20%) of the baseline at each date. Results of these simulations are shown in Figure 16 for some variables of interest together with the baseline simulation for comparison. With low improvements of the rural technology, the urban density falls significantly less and might even increase if rural productivity stays sufficiently low (Figure 16a). The growth of population and urban productivity puts pressure on land in the rural area to feed an increasing and richer population. This increases the relative price of rural goods and the price of farmland at the urban fringe (Figure 16c)—preventing the city to expand.³⁴ Furthermore, facing higher price of rural goods, households reduce their housing spending share to feed themselves, reducing the demand for urban land. These forces tend to make the city much denser than our baseline—more so at the urban fringe due to rising farmland values (Figure 16b). Thus, urban density might increase despite the reallocation of urban workers towards the less dense part of the city as they commute faster due to rising urban productivity. It is worth emphasizing that population growth, by putting pressure on land, makes improvements in agricultural productivity even more crucial to generate a sizable expansion in urban area.

This simulation does not say that improvements in commuting technologies do not matter for the expansion in area of cities. However, it makes clear that they matter only when combined with rural productivity growth and structural change. The next experiment provides further insights on the quantitative role of commuting costs for our results.

³³To compute the urban land value in the data, we multiply the housing wealth by the share of land in housing, whose average is 0.32 in the data for the period 1979-2019. More details are provided in Appendix A.6.

³⁴In the simulation with stagnating rural productivity, the city even shrinks in size. Workers move away from cities despite urban productivity growth as more rural workers are needed to feed the increasing population.

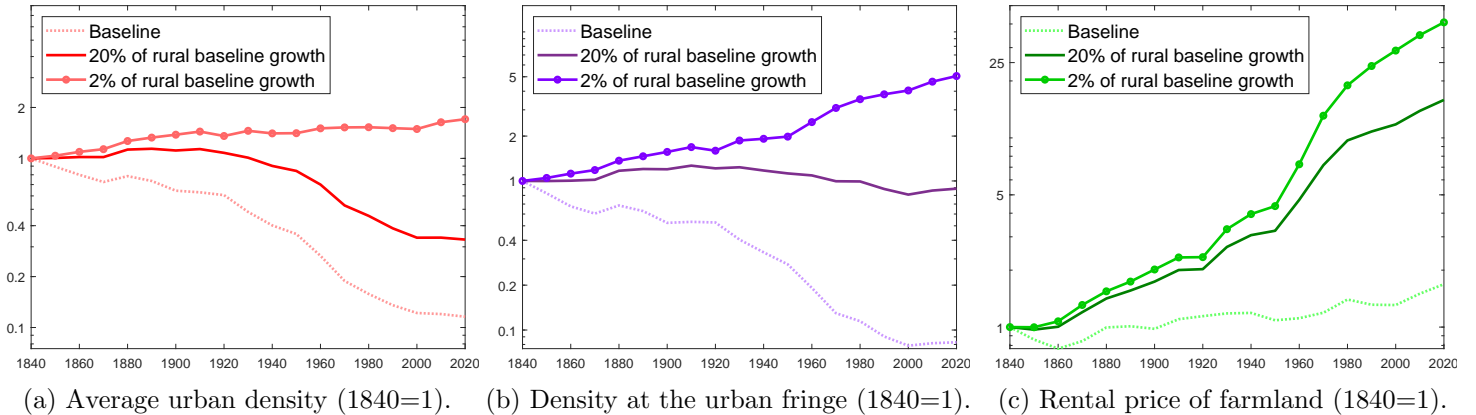


Figure 16: Sensitivity to rural productivity growth.

Notes: Productivity growth in the rural sector is set to 2% of the baseline rural productivity growth (solid line), resp. 20% of the baseline (solid line with circles). All other parameters are kept to their baseline value of Table 1. Simulation for the baseline rural productivity growth is shown in dotted for comparison.

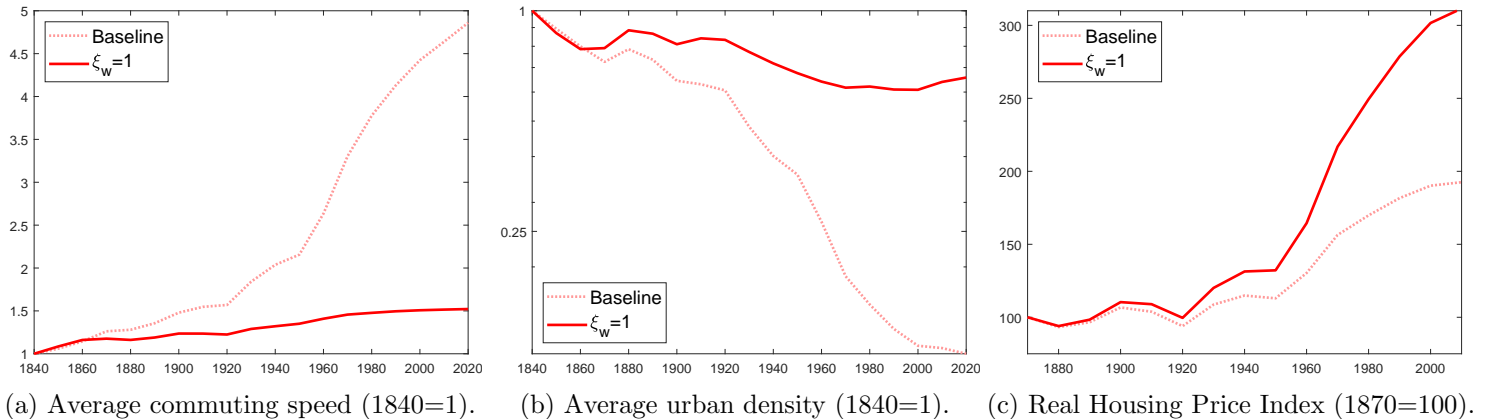


Figure 17: Sensitivity to the elasticity of commuting costs to income.

Notes: The elasticity of commuting cost to income, ξ_w , is set to 1. All other parameters are kept to their baseline value of Table 1. Simulation for the baseline calibration shown in dotted for comparison.

The elasticity of commuting costs to income. To shed further light on the quantitative importance of falling commuting costs and rising commuting speed, we set the elasticity of commuting costs to income, ξ_w , to unity, $\tau(\ell) = a.w_u.\ell^{\xi_\ell}$. With such a calibration, the fraction of wages devoted to commuting in given location does not fall with rising urban productivity, contrary to our baseline. This is so because the speed of commuting does not increase with a rising opportunity cost of time (urban wage).³⁵ When compared to our baseline, this illustrates the quantitative role of the use of faster commutes when urban productivity increases. Figure 17 shows the results in this alternative calibration together with our baseline for comparison purposes. Figure 17a makes clear that increasing the elasticity of commuting costs to income limits the increase in the average commuting speed over the period.³⁶ As the cost of faster commutes increases more than in our

³⁵In this knife-edge calibration, workers do not switch to faster modes at a given location when facing an increase in their wage: the increase in the operating cost of faster commutes offsets the benefits due to a rising opportunity cost of time.

³⁶The average speed still increases slightly as, due to structural change, workers locate in suburban locations where

baseline, urban workers do not relocate away from central locations towards the suburban part of the city. This severely limits the expansion in area of the city relative to the baseline and the average urban density falls significantly less (Figure 17b).

Thus, when combined with rural productivity growth, the use of faster commutes and the corresponding decline in commuting costs (as a share of the urban wage) is quantitatively important to account for the overall decline in urban density—particularly so in central locations. In this alternative simulation, as the urban area expands much less but urban population grows essentially as much due to structural change, urban land values and housing prices increase much more than in our baseline (Figure 17c). This mirrors the role of improvements in commuting modes to limit the increase in urban land values emphasized in [Heblich et al. \(2018\)](#) and [Miles and Sefton \(2020\)](#).³⁷

The elasticity of substitution between land and labor in the rural sector. Our baseline simulation assumes a unitary elasticity of substitution between land and labor, $\sigma = 1$. Values used in the literature typically range between 0 and 1 ([Bustos et al. \(2016\)](#) and [Leukhina and Turnovsky \(2016\)](#)). We perform sensitivity analysis with a lower value of 0.25. We also show results for a high value of 4 to enlighten further the quantitative importance of the adjustment of land values at the fringe of the city for our results.³⁸ Results are displayed in Appendix C.3 for variables of interest (Figure 52). With a lower elasticity of substitution, the rental price of farmland falls more (increases less) following structural change as land and labor are more complement in the rural sector. As the opportunity cost of expanding the city is lower, the urban area increases more and the average urban density falls more. This is driven by a larger fall of density in the cheaper suburban parts. With $\sigma = 0.25$, the model matches the expansion in area and the corresponding decline in average density observed in French cities since 1870. To the opposite, if land and labor are more substitutes ($\sigma = 4$), the reallocation of workers away from agriculture puts less downward pressure on the value of farmland, limiting the expansion of the urban area and the decline in density, which falls short of the data. These experiments further illustrate the importance of the farmland price adjustment at the urban fringe to understand the reallocation of land use.

The housing supply elasticity. Our baseline simulation features location-specific housing supply elasticities with a lower elasticity at the city center relative to the fringe. As sensitivity analysis, we set the elasticity to 3 in all locations, in the mid-range of empirical estimates.³⁹ Results regarding the time evolution of the aggregate variables of interest—employment, relative price of rural goods, urban area, average urban density and land values—are barely affected. The most noticeable difference is that a constant housing supply elasticity generates a city center much denser relative to the suburban part. Compared to our baseline simulation, a more elastic housing supply at the center leads to a larger provision of housing in these locations. As a consequence, the gradient of

they are willing to use faster commuting modes.

³⁷Higher urban housing prices generate an agricultural productivity gap about twice as large as in our baseline simulation in the recent period. Equivalently, the urban resident at the fringe faces much higher commuting costs.

³⁸A higher σ limits the fall of farmland values at the fringe of cities when workers move towards the urban sector.

³⁹This corresponds to a land share in housing of 25%, slightly lower than the average in the data over the period 1979-2019.

population density is significantly steeper than in the data (Figure 51 in Appendix C.2).

4.4 Extensions

Agglomeration and congestion. We introduce urban agglomeration forces by assuming that the urban productivity increases externally with urban employment, $\theta_u(L_u) = \theta_u \cdot L_u^\lambda$. We set $\lambda = 0.05$, in the range of empirical estimates for France (Combes et al. (2010)). Other parameters are left identical to the baseline calibration for comparison, adjusting the initial value of θ_u to have the same initial urban productivity. For variables of interest, results in presence of agglomeration forces are displayed in Figure 18 together with the baseline simulation. While the city expands slightly more in area, there is barely no effect of agglomeration forces on urban population. The faster increase in the urban wage due to agglomeration forces increases urban housing demand and reduces urban commuting costs (as a share of income). This relocates urban households towards the suburbs where they can enjoy larger homes and the city sprawls more. However, a higher urban income makes also rural goods more valuable increasing rural workers' wage almost one for one. General equilibrium forces thus prevent workers' reallocation towards cities. They also make rural land more valuable—mitigating the area expansion of the city. As a consequence, despite higher incomes driven by urban expansion, the economy with agglomeration forces behave quantitatively similarly to our baseline.

We also consider additional urban congestion costs by assuming that commuting costs are increasing with urban population, $a(L_u) = a \cdot L_u^\mu$. This summarizes the potential channels through which larger cities might involve longer and slower commutes for a given commuting distance. We set $\mu = 0.05$ and we re-scale the constant a to have the same initial value for the commuting costs, leaving other parameters to their baseline values. The evolution of the variables of interest is shown on the same Figure 18 for comparison. Congestion forces move the equilibrium in the opposite direction of agglomeration forces. They reduce the expansion in area and the extent of suburbanization. By increasing commuting costs, they also increase urban housing prices. However, via general equilibrium forces, they also make rural goods and rural land less valuable—severely mitigating the direct effect of congestion costs on urban expansion.

Commuting distance and residential location. Guided by the structure of French cities, our baseline results hinge on the assumption of a monocentric model where urban individuals commute to the city center to work. While endogeneizing firms location across space is beyond the scope of the paper, one can still partly relax the monocentric assumption by assuming that commuting distance, $d(\ell)$, does not map one for one with residential distance ℓ from the central location. Using data available for the recent period to investigate the link between commuting distance and residential location (see Appendix A.9.2 for details), we find that households residing further away do commute longer distances on average. However, commuting distance increases less than one for one with the distance of residence from the city center. Data also show that individuals residing very close to

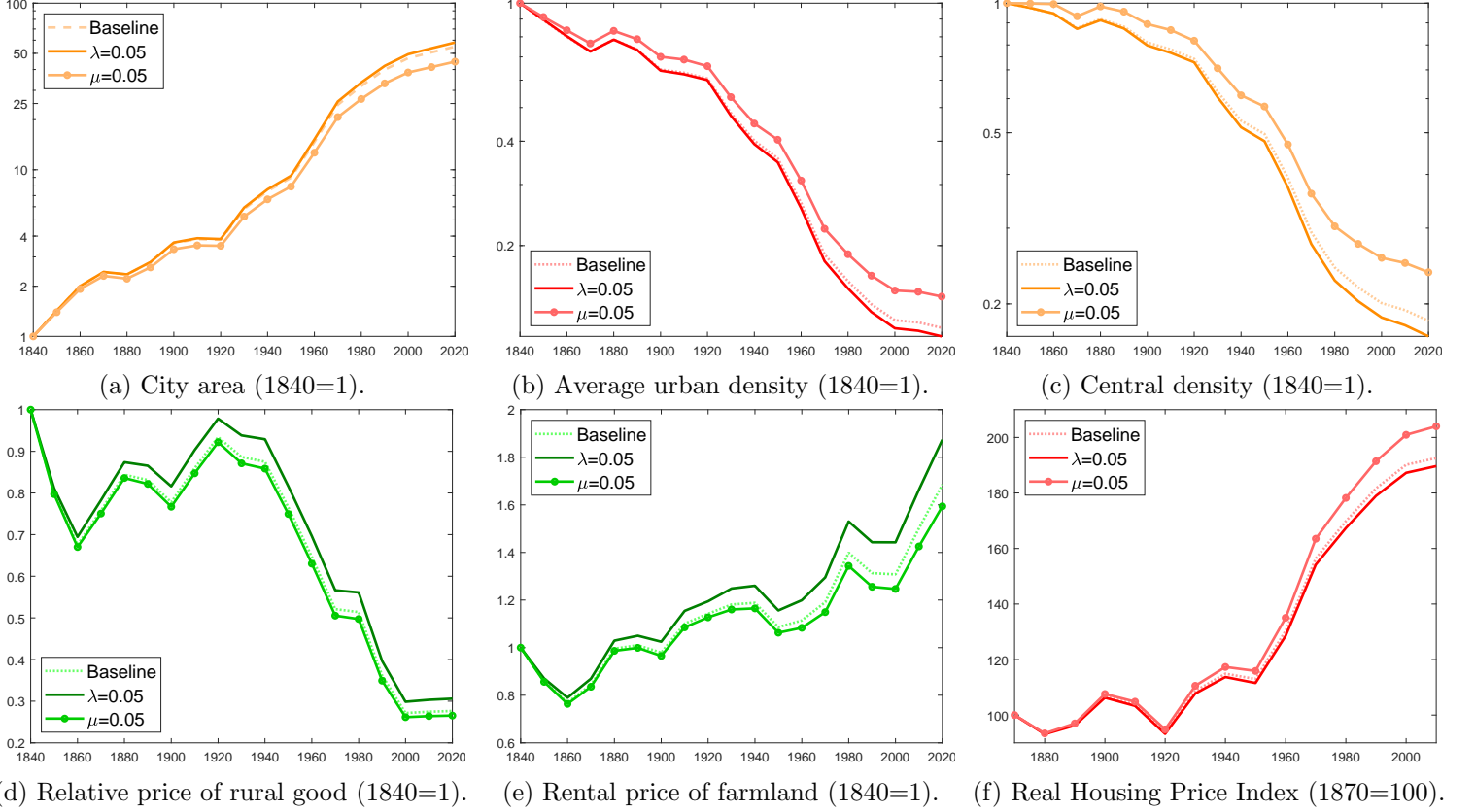


Figure 18: Agglomeration and congestion forces.

Notes: The solid line represents outcomes in presence of agglomeration forces, with parameter $\lambda = 0.05$. The solid line with dots represents outcomes in presence of congestion forces, with parameter $\mu = 0.05$. Other parameters set to their baseline value of Table 1 up to a normalization of the initial urban productivity. For comparison, outcomes of the baseline simulation are shown with a dotted line.

the center commute longer distances than the distance of their home from the central location.⁴⁰ Based on these observations, we model commuting distance $d(\ell)$ in a reduced-form way as follows,

$$d(\ell) = d_0(\phi) + d_1(\phi) \cdot \ell, \quad (29)$$

with $d_0(\phi)$ being a positive and increasing function of ϕ satisfying $\lim_{\phi \rightarrow 0} d_0(\phi) = 0$, and $d_1(\phi)$ being a decreasing function belonging to $(0, 1)$ with $\lim_{\phi \rightarrow 0} d_1(\phi) = 1$. d_0 represents the (minimum) commuting distance traveled by an individual living in the center, while d_1 is the slope between commuting distance and residential distance from the center. This specification fits recent data well. It also makes sure that at the limit of $\phi \rightarrow 0$, the city is monocentric as all the jobs must be centrally located. It is important to note that commuting costs are now defined as,⁴¹

$$\tau(\ell) = a \cdot w_u^{\xi_w} \cdot (d(\ell))^{\xi_\ell}.$$

⁴⁰Data also show that commuting distance increases less with the distance of residence from the center in larger cities—pointing towards a larger dispersion of employment away from the center in larger cities. See Appendix A.9.2.

⁴¹This remains consistent with our calibrated value of ξ_ℓ estimated using commuting distance. The elasticity of speed $m(\ell)$ to commuting distance $d(\ell)$ being $1 - \xi_\ell$.

As detailed in Appendix C.5, we make the following parametric assumptions guided by the data: $d_0(\phi) = d_0 \cdot \phi$, with d_0 calibrated to 5% and $d_1(\phi) = \frac{1}{1+d_1 \cdot \phi}$, with d_1 calibrated to 2. For the sake of space, details and results of this extension are relegated to Appendix C.5. We find that our results are not much affected (Figure 55). Quantitatively, the city expands more in area in the last decades under this specification of the commuting distance, bringing the model closer to the data. As a consequence of this larger sprawling, the average urban density falls more. This is driven by a larger fall of central density, the most noticeable difference relative to our baseline monocentric model. With urban expansion, residents in central locations end up commuting larger distances—implicitly due to the reallocation of jobs away from the center—, this makes central locations less attractive relative to suburban ones.

Multiple cities. We extend our quantitative model with a single region/city to allow for K different regions. The spatial structure in each region k is identical to the one-city version.⁴² Regions are heterogeneous only in their urban productivity—with $\theta_{u,k}$ the urban productivity in region/city k . Workers are freely mobile within and across regions and labor markets clear globally. Urban and rural goods are freely traded within and across regions and goods markets clear globally. For quantitative evaluation, we consider 20 regions, corresponding to the 20 largest French cities in 1870. Each region is endowed with the same land area as our baseline and aggregate population preserves the baseline endowment of land per head.⁴³ City-specific urban productivities, $\theta_{u,k}$, are set to match the distribution of population of the different cities over the period 1870-2015, while keeping aggregate urban productivity equal to its baseline value estimated from French historical national accounts. Other parameters are set to their baseline values of Table 1. Details of this extension together with the numerical solution method are provided in Appendix C.6.

For aggregate variables of interest (aggregate sectoral employment, aggregate land use, relative price of rural goods/farmland, ...), the model with multiple regions behaves quantitatively very similarly to the baseline with only one city. Intuitively, the one-city model describes well the dynamics of aggregate variables for a representative ‘average’ city. Thus, we focus on the dispersion of city size and density, which are novel outcomes relative to our baseline. Detailed outcomes of the model are relegated to Appendix C.6. Beyond the targeted distribution of population across cities, the model does a fairly good job at reproducing the distribution of urban area and average urban density across time and space. Figure 19 plots the log of average urban density in a given city against its data counterpart for the dates where it is observed in the data (1870, 1950, 1975, 1990 and 2015).⁴⁴ The model predicts that, over time, for a given city, urban density falls as urban population increases—in line with the predictions of our one-city model. In the cross-section, more populated cities are

⁴²Each region k is made of urban and rural land, with only one (potential) city per region. For each region, the city center is centrally located within each region and regions are assumed large enough in area such that cities do not expand in neighboring regions.

⁴³This makes sure that, with homogeneous urban productivity, the version with multiple regions behaves like the one-city model in each region.

⁴⁴Figure 56 in Appendix C.6 does the same for urban population (targeted) and area (non-targeted). The model-implied outcomes are defined up to a constant of normalization defining the unit of measurement. In Figure 19 they are normalized such that the average across all observations matches the data counterpart.

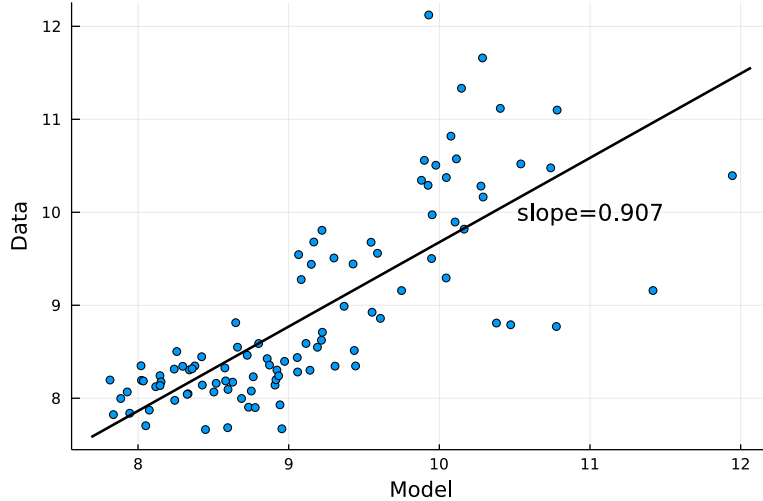


Figure 19: Average Urban Density in Model vs Data

Notes: This plot shows the combined cross sections of urban density (in log) in the 20 largest cities for the years 1870, 1950, 1975, 1990 and 2015 in model vs data. The model outcomes have been normalized such that the average value of density is equal to the one found in the data. See Appendix C.6 for details.

however denser as they feature higher housing prices. At a given date, the reallocation of workers towards a more productive city does not imply the general equilibrium effects on rural (good and farmland) relative prices at the heart of the time series evolution of urban density when cities grow in size. Importantly, both predictions, over time and in the cross-section, are qualitatively in line with the data discussed in Section 2. Quantitatively, the model does notably better in the time-series than in the cross-section. At a given date, more populated cities are significantly denser in the model than they are in the data (relative to less populated ones).

As last sensitivity analysis, we consider the model with multiple-cities where, in each city, residential location does not map one for one into commuting distance. Using the same parametric assumptions, Equation (29) applies for each city k of fringe ϕ_k . Results and details are relegated to Appendix C.6. The fit between model and data improves slightly under this specification for commuting distance. In line with the data shown in Appendix A.9, commuting distances in the center (resp. at the fringe) are larger (resp. lower) in larger cities in this specification relative to the monocentric model. This, in turn, increases the area of more populated cities in the cross-section at a given date, reducing their average density and bringing the model closer to the data. More populated cities in the model are still noticeably denser than in the data but less so compared to the monocentric model.

5 Conclusion

This paper develops a spatial general equilibrium model of structural change with endogenous land use and studies its implications for urbanization. We document a persistent fall of urban density in French cities since 1870 and show that the theoretical and quantitative predictions of the model are

broadly consistent with the data. The quantitative version of our theory calibrated to French data explains (at least) three fourths of the urban area expansion and of the decline in average urban density, about half of the rise in housing prices, and most of the land value reallocation from rural to urban since the mid-nineteenth century. Novel predictions regarding urban density across space line up relatively well with available data. Predicted agricultural productivity gaps in recent times are also of reasonable magnitude.

Agricultural productivity growth is shown to be crucial for the results, since it reduces the price of land at the urban fringe and frees up resources to be spent on housing. As a consequence, while workers reallocate away from agriculture, cities grow faster in area than in population and land prices do not rise very rapidly. Faster commuting modes also play an important and complementary role but only when combined with rural growth and structural change. When rural productivity is high, they allow households to live further away from their workplace and enjoy larger homes, contributing significantly to the decline in urban density, particularly at the city center.

Our baseline framework assumes a monocentric urban structure where all workers commute from their residential location to the city center. While French cities exhibit the qualitative features of monocentric cities, such an urban structure certainly remains an approximation. In particular, data shows that commuting distance increases with residential distance to the center but less than one for one. This suggests that workers sort into jobs and residential locations that are closer to each other. We believe that relaxing further the monocentric structure remains an important step to better account for the expansion of cities and the evolution of density across urban locations. However, we leave for future research a theory that jointly determines firms and workers location decisions across the urban space within our framework.

Relatedly, our work focuses on the reallocation of economic activity from the rural to the urban sector, abstracting from the reallocation that takes place within the urban sector. Admittedly, we could extend our framework to also take into account the transition from manufactures to services in the later part of our sample. We do not think our aggregate results would change much but we believe it would matter for the cross-section of cities in recent times. Some services are provided at a local level, especially in large cities, implying that workers do not have to commute to the city center. We also leave this extension for future research.

We also believe that our approach can be used to study the aggregate implications of policies regulating land use and urban planning. Such policies are likely to play a role in explaining the evolution of housing prices in recent years, which our current setup cannot fully replicate. To the extent that these land-use policies prevent cities from growing as much as they would, they lead to greater demand for the existing housing units and to a faster rise in their prices. The general equilibrium structure of our quantitative spatial model makes it well suited to conduct such policy counterfactuals.

A Data

A.1 Agricultural Land Use

Data sources and definitions. Data for the land used in agriculture are available in various secondary sources based on the French Agricultural Statistics (Statistique Agricole). We checked the consistency of the measures across the different sources.

The variable of interest is the area of land used for agriculture (SAU, for 'Surface Agricole Utilisée'). It is important to note that it includes land that is cultivated but excludes all land that is not (woods and forests, rocky land unfit for agriculture, mountains, swamps...).

Post World War 2 (WW2), data for the SAU are provided by the Ministry of Agriculture (data available in [Desriers \(2007\)](#) until 2000 by decade and available on annual basis since 2000 on the website of the Ministry (Agreste)).

Before WW2, agricultural statistics on land use are also available but on a very irregular basis.⁴⁵ Through a search across various sources, we compute a measure for the SAU from the first Agricultural Census in 1840 until today. It is worth noting that one must be cautious with such a measure before WW2 in the earlier periods. While it is quite clear that the share of land used in agriculture fell over the whole period, the variations throughout the 19th century (before the 1882 Census) must be taken with caution.

The main difficulty is to make the data presented in various sources comparable across years. First, woods and forest, accounting for 15-20% of French land in the 19th century (and more than 25% today) were initially included in the cultivated agricultural land. We made sure to exclude them from the SAU consistently over the whole time period considered. A second difficulty arises because the French territory varied since 1790: some variations being due to measurement, some due to the loss (or addition) of some parts of France — loss of Alsace and Moselle after the war of 1870 until 1918 and addition of Savoye and Comté de Nice in 1860 (see discussion in [Augé-Laribé \(1945\)](#)). This makes the across-time comparison difficult, even though we show our measure of the SAU as a share of the French territory at the time. A third difficulty for the early periods (before 1882), detailed below, regards the treatment of pasture and grazing fields in a consistent way across years.

Period 1945-2015. Let us start with the most recent period where the data are arguably of better quality and coherent across time and then present our measures going further back in time. Since 1945, the land used in agriculture has clearly been falling over the period 1950-2015: while land used for agriculture accounted for 62% of total French land post-WW2, this numbers falls to 52% in 2015.

⁴⁵In the 19th century, starting 1840, France aimed at organizing every decade a detailed data collection of agricultural statistics (Agricultural Census, 'Statistique Agricole'). See for instance description in [Fléchet \(1898\)](#) and [Augé-Laribé \(1945\)](#). A comparison across years during the 19th century is available in the report of the 1892 Census. Before 1840, Lavoisier provides the first measure of land use in France, in 1790, as described in.

Interwar Period. In between the world wars, we could find measures for the years 1929 and 1937. Two slightly different measures are available for 1929: one in [Toutain \(1993\)](#) and one in [Mauco \(1937\)](#). We take the average between the two, a SAU of 34 483 thousands of ha in 1929. A measure, very similar to 1929, is available in [Augé-Laribé \(1945\)](#) for 1937: 34 207 thousands of ha and 33 285 if one excludes Alsace-Moselle for comparison with earlier periods. This corresponds to about 62% of the French territory.⁴⁶

Nineteenth century. Before World War 1, we have measures in 1882 and 1892 ([Mauguin \(1890\)](#), [Fléchet \(1898\)](#), [Hitier \(1899\)](#) and [Toutain \(1993\)](#) for further details). Both measures are consistent across sources, including the main results of the 1892 Agricultural Census as a more primary source.⁴⁷ This gives an SAU of 34 882 thousands of ha in 1882 and 34 720 in 1892—slightly higher than the values in between the wars despite a smaller French territory. Figure 20 provides the details of the measurement for the 1892 Agricultural Census.⁴⁸

The measurement in 1840 constitutes our first observation. However, in the 1840 data, an important difficulty is the treatment of meadows, pasture and grazing fields (prés, herbages, pâturages,...). These should be included in the SAU to the extent that the land is used for agricultural purposes (feeding cattle). As grazing fields and meadows account for a large share of French agricultural land (up to 11% in 1892), their inclusion (or not) in the cultivated part of agricultural land (SAU) matters. However, in 1840, a significant share of grazing fields ('pâturages', 'pâtis communaux/vaines pâtures') is excluded from the SAU. The non-cultivated part of agricultural land thus appears to be a much larger measured area than in all subsequent years.⁴⁹ As discussed in the results of the 1892 Agricultural Census, comparison across years is difficult due to the reallocation of grazing fields into the cultivated part of French land over the period 1840-1880. This reallocation is quite artificial—mostly a statistical artefact coming from the earlier exclusion of common pasture. Excluding entirely the measured non-cultivated part from the SAU in 1840 gives thus a lower bound, while including it entirely to account for all grazing fields gives an upper bound. To solve this issue, [Toutain \(1993\)](#) provides an estimate of agricultural land in 1840, in between these two values, of 35 500 thousands of ha. While this is just a matter of definition and any solution is somehow arbitrary, we proceed in a similar fashion as [Toutain \(1993\)](#) and assume that the grazing fields later reallocated in the cultivated part are part of the SAU in 1840. This gives a land use in agriculture of 35 497 thousands of ha in 1840—a very similar number to [Toutain \(1993\)](#). Proceeding exactly in

⁴⁶[Mauco \(1937\)](#) compares to the 1892 value and find very similar numbers than ours once woods are excluded from his measurement. [Augé-Laribé \(1945\)](#) compares to the 1882 value and the measure given for 1882 is also consistent with our data.

⁴⁷Statistique Agricole de la France: Résultats généraux de l'Enquête Décennale de 1892. The online archives are available at: <https://gallica.bnf.fr/ark:/12148/bpt6k855121k/f1.item>

⁴⁸Comparison of land use as a share of total French land across the 19th century is also available in the report of the 1892 Census.

⁴⁹As shown in Figure 20, in 1892, the non-cultivated part includes moor and rocky land arguably unfit for agriculture, accounting for about 11% of French land. The corresponding non-cultivated part in 1840 accounts for 17% of French land as it includes a significant share of grazing fields.

RÉSUMÉ DES CULTURES.

A. — SITUATION EN 1892.

1. TERRITOIRE.

Nous donnons ci-après, par grandes catégories, la répartition du territoire de la France, telle qu'elle résulte des relevés opérés en 1892 :

CATÉGORIES DU TERRITOIRE.		SUPERFICIES.	RÉPARTITION et PROPORTIONS.	
		hectares.	p. 100.	
1^o TERRITOIRE AGRICOLE.				
Superficie cultivée.	Terres labourables.	Céréales.....	14,827,085	28.06
		Grains autres que les céréales.....	319,705	0.60
		Pommes de terre.....	1,474,144	2.68
		Autres tubercules et racines pour l'alimentation humaine.....	128,238	0.24
		Cultures industrielles.....	531,508	1.00
		Cultures fourragères ⁽¹⁾	4,736,394	9.08
		Jardins potagers et maraîchers.....	386,827	0.73
		Jachères.....	3,367,518	6.37
		Terres labourables.....	25,771,419	48.76
		Vignes.....	1,800,489	3.40
	Prés naturels.....	4,402,836	8.33	
	Herbages pâturés ⁽²⁾	1,810,608	3.42	
Bois et forêts.....	9,521,568	18.03		
Cultures arborescentes, etc.....	934,800	1.76		
	Cultures permanentes non assolées.....	18,470,301	34.94	
	TOTAUX de la superficie cultivée.....	44,241,720	83.70	
Superficie non cultivée.	Landes, pâtis, bruyères.....	3,898,530	7.37	
	Terrains rocheux et montagneux, incultes.....	1,972,994	3.73	
	Terrains marécageux.....	316,373	0.60	
	Tourbières.....	38,292	0.07	
	TOTAUX de la superficie non cultivée.....	6,226,189	11.77	
	TOTAUX DU TERRITOIRE AGRICOLE.....	50,467,909	95.47	
	2^o TERRITOIRE NON AGRICOLE.....	2,389,290	4.53	
	Totaux généraux du Territoire.....	52,857,199	100.00	

⁽¹⁾ Non compris les cultures dérobées.

⁽²⁾ Y compris les herbages alpestres.

Figure 20: Land Use in the 1892 Recensement Agricole.

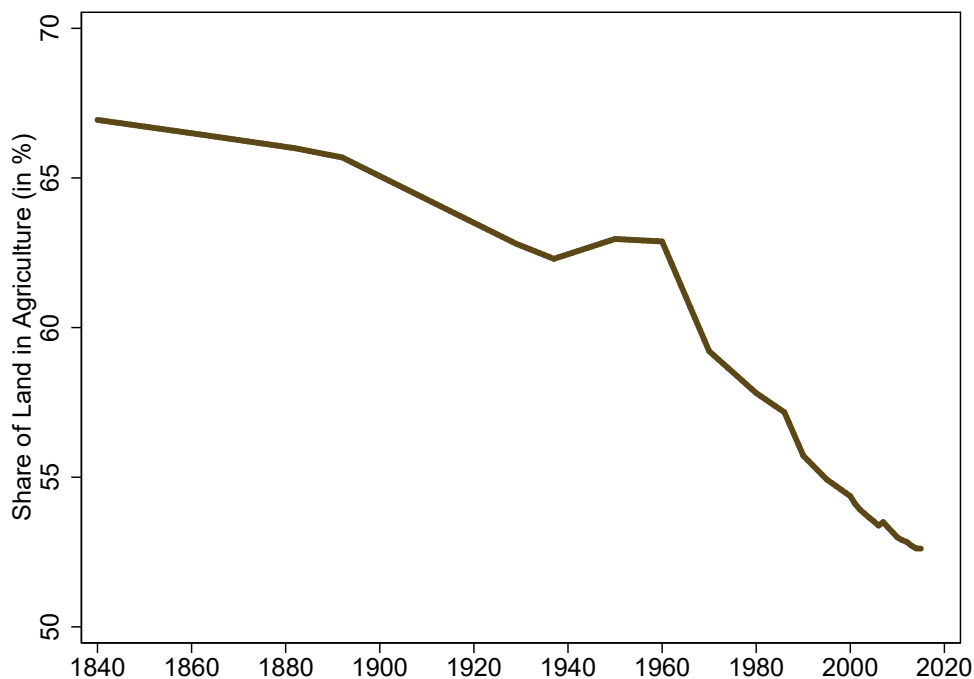


Figure 21: Shares of Land used in Agriculture (1840-2015).

the same way for the year 1862 gives an SAU of 36 088 ha—a higher value but for a larger territory. Both values correspond to about two thirds of French land used in agriculture.

The measured cultivated agricultural land (as a share of French territory) over the period 1840-2015 is summarized in Figure 21.

Pre-1800. Lastly, Lavoisier provided in 1790 the very first measure of French agricultural land before the creation of the Agricultural Census. Comparison of Lavoisier’s measurement with the later ‘Statistiques Agricoles’ is however difficult. Like for the later measurements, a large fraction of land (‘vaines patûres’) includes grazing fields as well as rocky land and moor unfit for agriculture (see [Mauguin \(1890\)](#) for an attempt to compare with the 1882 Census). Excluding woods but including the ‘vaines patûres’ (common pasture) in 1790 gives a surface of almost 40 000 thousands of ha. Excluding all the ‘vaines patûres’ provides a lower bound of about 31 000 thousands of ha. This gives a reasonable but fairly wide bracket for the total land used for agriculture. Assuming that the non-cultivated part due to rocky land is comparable to the later measures gives a SAU in 1790 around 34 000 thousands of ha—comparable to the later years (on a smaller territory)—about 65% of French land measured at the time. While this measure should be taken with great caution, it is nevertheless comforting that we find a value in same ballpark as our first measure in 1840 using the Agricultural Census.

A.2 Sectoral employment

Sources. Data on employment are available in three different sources covering different time periods: [Marchand and Thélot \(1991\)](#) ('Deux siècles de travail en France') for the period 1806-1990; [Herrendorf et al. \(2014\)](#) for the period 1856-2006; OECD for the period 1950-2018. When overlapping, the different sources are largely consistent with each other.⁵⁰ We use the three sources allowing to span the entire 1806-2018 period. For the pre-WW2 period, data available in [Marchand and Thélot \(1991\)](#) and [Herrendorf et al. \(2014\)](#) are on an irregular basis—typically one or two observations per decade (corresponding to Census years). Annual data are available from 1950 onwards.

Over the nineteenth century (until 1901), we use the data from [Marchand and Thélot \(1991\)](#) as the series goes further back in time. Over the period 1901-1950, we use the data from [Herrendorf et al. \(2014\)](#). Over the period 1950-2018, we use data provided by the OECD on an annual basis, where the measure of employment is expressed in full-time equivalent.

Share of employment in agriculture. This gives the share of employment in agriculture over the entire period (1806-2018) in Figure 22. Data are linearly interpolated in between two values when data are not available on an annual basis (pre-1950). It starts with about 2/3 of the employment in agriculture in 1806 and falls progressively to 3% in 2018. One can notice the acceleration in the process of reallocation post WW2. In the matter of three decades, the employment share in agriculture went from 36% in 1946 to 10% in 1976.

A.3 Sectoral National Accounts and Prices

Sources. Data on value added at the sectoral level together with aggregate value added (GDP) at current prices are available in two different sources covering different time periods. Historical national accounts from [Toutain and Marczewski \(1987\)](#) are used to cover the period 1815-1938. They are directly available at the Groningen Growth and Development Centre (Historical National Accounts Database, <http://www.ggdc.net/>).

Post WW2, INSEE provides sectoral value added at current prices for the period 1949-2019. For both series, we use agricultural value added and aggregate GDP at current prices. Using both sources covers the entire period 1815-2019. The series are interrupted at war times: observations are missing for the periods 1914-1919 and 1939-1948.

[Toutain and Marczewski \(1987\)](#) also provides volume indices for GDP in agriculture and for aggregate GDP over the period 1815-1982 (also available Groningen Growth and Development Centre). The series for agricultural volumes is extended in [Toutain \(1993\)](#) until 1990. Together with the value added at current prices, these series will be used to compute an agricultural price deflator and a GDP deflator.

⁵⁰[Marchand and Thélot \(1991\)](#) gives a slightly lower share of employment in agriculture in the first half of the 20th century relative to [Herrendorf et al. \(2014\)](#). Our results do not depend on the use of one series or the other.

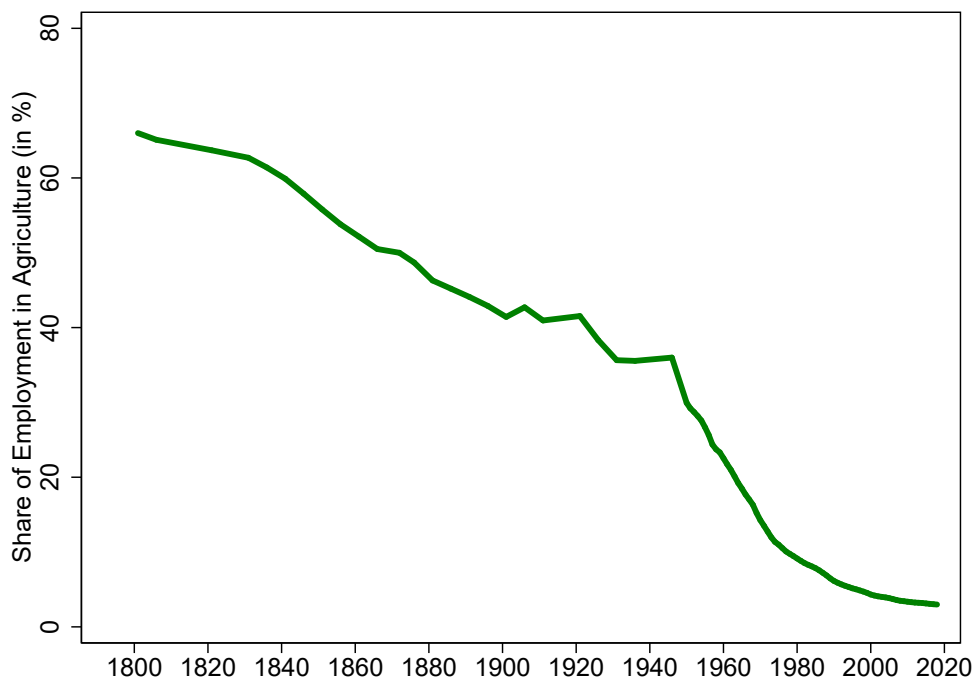


Figure 22: Shares of Employment in Agriculture (1806-2018).

Sources for sectoral prices. Data on agricultural producer prices are available over the period 1815-2019 using two different data sources: one derived from the national accounts in value added and volume from Toutain (1987, 1993) and one from INSEE post-1949.

Using Toutain (1993), we compute a price index of agricultural goods using the value added in agriculture divided by the production volume index in agriculture (period 1815-1990). Post WW2, INSEE directly provides a producer price index for agricultural goods (Indice des prix agricoles à la production, IPPAP)—the series can be retropolated back to 1949.⁵¹ These two series will be used to construct a price index for agriculture goods over the period 1815-2019 (with interruptions at war times). Similarly, a GDP deflator over the period 1815-1960 can be computed using GDP at current prices and a GDP volume index from Toutain and Marczewski (1987). Post-1960, we use the GDP deflator from the World Bank.⁵² The price index for agricultural products and the GDP-deflator are both normalized to 100 in 1949.

Relative price for agricultural goods. Using the computed historical time-series for the agricultural producer price index and the GDP-deflator, one can take the ratio of the two series to shed some lights on the evolution of the relative prices of agricultural goods. The series for the relative price based on Toutain production data (solid green) over the period 1815-1990 and the

⁵¹The IPPAP series is the 'Base 2000 rétopolée' available in Insee Méthodes 114 (INSEE (2006)). Until 1970, the retropolated series from INSEE excludes fruits and vegetables. The series including fruits and vegetables and the one excluding them are almost identical when both are available.

⁵²We checked consistency with the consumer price index available over the period 1820-2015 (INSEE). Inflation is very similar in both series.

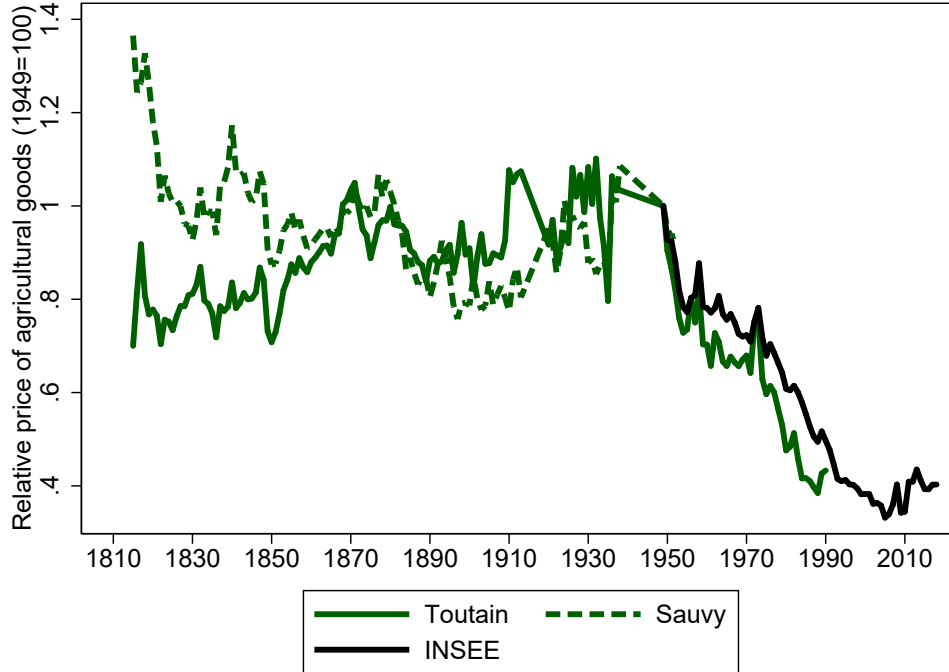


Figure 23: Relative prices of agricultural goods, 1949=100 (1815-2019).

INSEE producer price (solid black) starting 1949 are shown in Figure 23. While the relative price of agricultural goods appears fairly stable until 1910, it exhibits later a clear downward trend over the twentieth century. Both series show a similar trend post WW2.

Our baseline price index of agricultural goods (denoted P_{agri}) uses the series computed using the national accounts of Toutain prior to WW2 (1815-1938) and the agricultural producer prices by INSEE post WW2 (1949-2019). The two series are linked by the same normalization to 100 in 1949. The final series for P_{agri} is only interrupted during the wars.

The model counterpart of our data is the relative price of rural/agricultural goods over the price of urban/non-agricultural goods. The latter is not observed but can be backed out using the GDP-deflator. Let us denote $P_{agri,t}$ the price index for agricultural goods at date t , $P_{non-agri,t}$ the price index for non-agricultural goods, and $P_{GDP,t}$ the GDP-deflator. The GDP-deflator can be written as

$$\frac{1}{P_{GDP,t}} = \frac{s_{agr,t}}{P_{agr,t}} + \frac{1 - s_{agr,t}}{P_{non-agr,t}}, \quad (30)$$

where $s_{agr,t}$ is the share in value-added of agricultural goods computed using historical national accounts. Since we observe in the data all the variables but $P_{non-agri,t}$, we can invert Eq. 30 to back out a price index for non-agricultural goods (urban goods including manufacturing and services),

$$P_{non-agri,t} = \left(\frac{1}{P_{GDP,t}} \frac{1}{1 - s_{agr,t}} - \frac{1}{P_{agr,t}} \frac{s_{agr,t}}{1 - s_{agr,t}} \right)^{-1}.$$

We are now equipped with a price index for agricultural goods, non-agricultural goods, and a GDP

deflator over the period 1815-2019.

Sensitivity analysis for the price of agricultural goods. Before WW2, the Statistique Generale de France (the predecessor of INSEE), in particular thanks to the work of Alfred Sauvy, provides an alternative series for the price of agricultural goods: 'indice des prix de gros agricoles' which is constituted by a basket of 19 raw agricultural commodities (food related).⁵³ The series is retroplated back to 1810 by A. Sauvy (see [Sauvy \(1952\)](#)). This data includes some foreign commodities (e.g. English and US corn prices) and is in part computed using customs price data. For this reason, we use the price of agricultural goods computed using production data of Toutain pre WW2 as baseline. This said, the 'indice des prix de gros agricoles' still contains useful information regarding the price of agricultural goods in France before WW2. Comparison with the price computed using production data from Toutain indicates that the two series exhibit very similar patterns starting 1850. Prior to this date, the 'indice des prix de gros agricoles' from [Sauvy \(1952\)](#) exhibits a significant downward trend, while our baseline from Toutain stays roughly stable (see [Figure 23](#)).⁵⁴ Our baseline price series for agricultural goods uses the series based on Toutain for the period pre WW2. However, results are robust using data from Sauvy since our quantitative estimation starts in 1840 and both series roughly coincide over this time period.

A.4 Sectoral Productivities

Equipped with sectoral value added at current prices, sectoral price indices, sectoral employment and land use data, one can back out the sectoral productivities (in the agricultural and non-agricultural sector) that are the counterpart of the model (the θ s) up to a constant of normalization. Our measure of land use in agriculture necessary to estimate rural productivity starts in 1840. Thus, we compute sectoral productivities for the period post 1840 and focus on the period 1840 until today for the quantitative analysis.

Urban Productivity. Let us start with the urban/non-agricultural sector. According to the model production function, $\theta_u = \frac{Y_u}{L_u}$. We observe the value added in the non-agricultural sector at current prices. Deflating this series by the constructed price index for non-agricultural goods gives Y_u . Dividing the latter variable by employment in the non-agricultural sector, $L_{non-agri,t}$, allows us to back out the empirical counterpart of $\theta_{u,t}$,

$$\theta_{u,t} = \frac{VA_{non-agri,t}}{P_{non-agri,t}L_{non-agri,t}}.$$

Due to the mere presence of a price index, this series is defined up to a multiplicative constant. We normalize $\theta_{u,t}$ to unity in the first period considered (1840). This gives the time-series for $\theta_{u,t}$

⁵³Details about the index can be found in the 'Etudes spéciales' of the 'Bulletin de la Statistique générale de la France' in 1911. Available online at: <https://gallica.bnf.fr/ark:/12148/bpt6k96205098/f73.image>

⁵⁴We also compare those series with the relative price of corn. While significantly more volatile, the latter is also fairly consistent with the other series. A period of volatile relative corn price but fairly constant on average until the early 20th century, followed by a downward trend. The downward trend is however more pronounced.

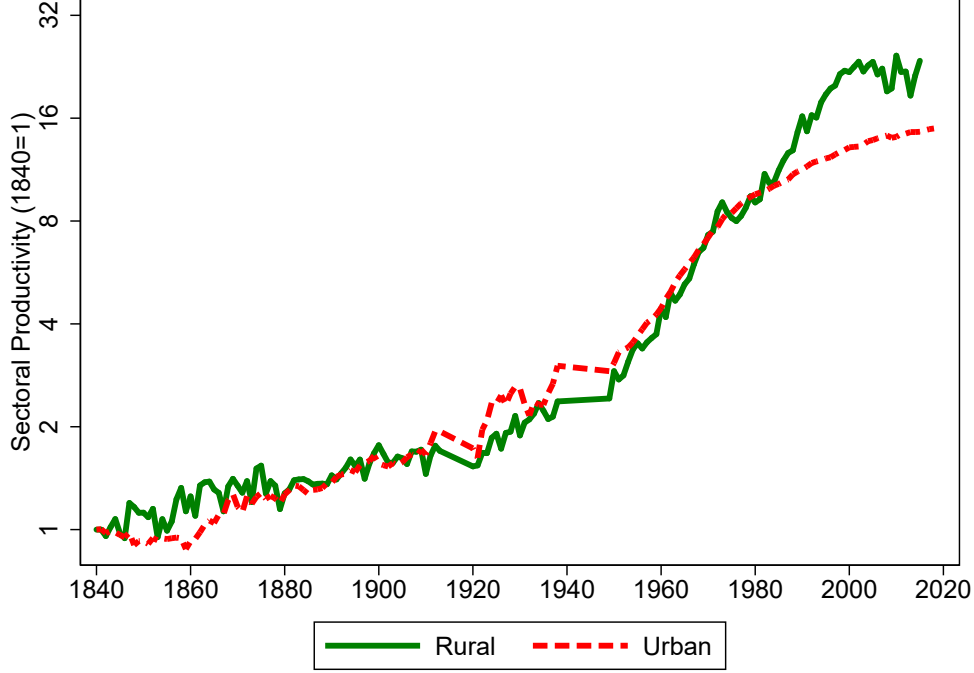


Figure 24: Rural and Urban Productivity, 1840=1 (1840-2019).

plotted in Figure 24 (dashed red line). This will be our baseline exogenous urban/non-agricultural productivity series. It is important to note that the measured urban labor productivity includes technological advances in the non-agricultural sector but also factor accumulation rising labor productivity (physical and human capital accumulation).

Rural Productivity. We proceed in a similar fashion to compute the model's counterpart of the rural productivity, $\theta_{r,t}$, with one important difference: the agricultural output per worker in the rural sector depends also on the land per worker available for agriculture,

$$\frac{Y_r}{L_r} = \theta_r \left(\alpha + (1 - \alpha) \left(\frac{S_r}{L_r} \right)^{\frac{\sigma-1}{\sigma}} \right)^{\frac{\sigma}{\sigma-1}} = \theta_r F \left(\frac{S_r}{L_r} \right). \quad (31)$$

Thanks to the data on land use in agriculture, one can back out from the data the land per worker in agriculture at each date: it is simply the cultivated area (SAU) divided by employment in agriculture, $\frac{S_r}{L_r} = \frac{SAU}{L_{agri}}$. Using Eq. 31, one can compute the rural productivity parameter, $\theta_{r,t}$, at each date,

$$\theta_{r,t} = \frac{VA_{non-agri,t}}{P_{non-agri,t} L_{non-agri,t}} \frac{1}{F \left(\frac{SAU_t}{L_{agri,t}} \right)}.$$

With a unitary elasticity of substitution between land and labor ($\sigma = 1$), this gives,

$$\theta_{r,t} = \frac{VA_{agri,t}}{P_{agri,t} L_{agri,t}} \left(\frac{SAU_t}{L_{agri,t}} \right)^{\alpha-1}.$$

Due to the mere presence of a price index, this series is defined up to a multiplicative constant. Like $\theta_{u,t}$, we normalize $\theta_{r,t}$ to unity in the first period (1840). This gives the time-series for $\theta_{r,t}$ plotted in Figure 24 (solid green line). This will be our baseline exogenous rural/agricultural productivity shifters.

Comments. Comparing urban and rural productivity, one notices the important common component: this can be due to technological advances benefiting both sectors but also to physical and human capital accumulation, which increase labor productivity across the board. Focusing on the more sectoral specific component, it is visible that non-agricultural productivity grew faster from the late 19th century until WW2. Post WW2, agricultural productivity starts growing at a faster speed, catching-up with the non-agricultural one and eventually outpacing it. This is consistent with Bairoch’s view that starting with the agricultural crisis in late nineteenth century, technological progress in the French agriculture is slow and delayed relative to other countries, before catching up post WW2. The period 1945-1985 period is more broadly characterized by a very fast technological progress in agriculture across developed countries (see Bairoch (1989)). A productivity slowdown is later observed in both sectors.

A.5 Consumption expenditures

Sources. Data on consumption expenditures are available using two different data sources. Pierre Villa provided data on consumption expenditures across 24 different categories of goods for the period 1896-1939.⁵⁵ INSEE provides data over the period 1959-2017 on personal consumption expenditures (‘Consommation effective des ménages par fonction aux prix courants’) across 12 broad categories (food, drinks, clothing, housing, transportation,...) and about 100 narrower categories. INSEE Data are from the Comptes nationaux (Base 2014).⁵⁶

Expenditure shares. We compute expenditure shares on three broad categories: food/drinks, housing and the remaining goods. The expenditure share outside food, drinks and housing includes manufacturing goods and services. The expenditure share on food/drinks is computed by adding all the good categories corresponding to food and drinks consumption divided by aggregate household expenditures (for the pre and post WW2 data). However, it excludes consumption in restaurants that will enter the remaining category (urban goods). The housing expenditure shares include housing related expenses: rents (effective and imputed), energy expenditures, some housing services (garbage, cleaning, repair, ...) but also housing equipment (furniture, tableware, household appliances...)⁵⁷

⁵⁵Data are publicly available thanks to the CEPII. For details and documentation, see <http://gesd.free.fr/villadoc.pdf>. See also Villa (1993).

⁵⁶Over the period 1950-1958, the CREDOC was providing data on consumption expenditures across broad categories for French households. These data have not been made compatible with the INSEE data post-1959, when INSEE revised the methodology. Investigating data in reports by CREDOC provides some additional insights on consumption expenditure shares in the 1950s across broad categories. As expected, these shares are in between the ones computed using the data from Villa right before WW2 and the later national accounts data of INSEE.

⁵⁷We include housing equipment as (partly) furnished/equipped houses/flats are quite common—even in the early

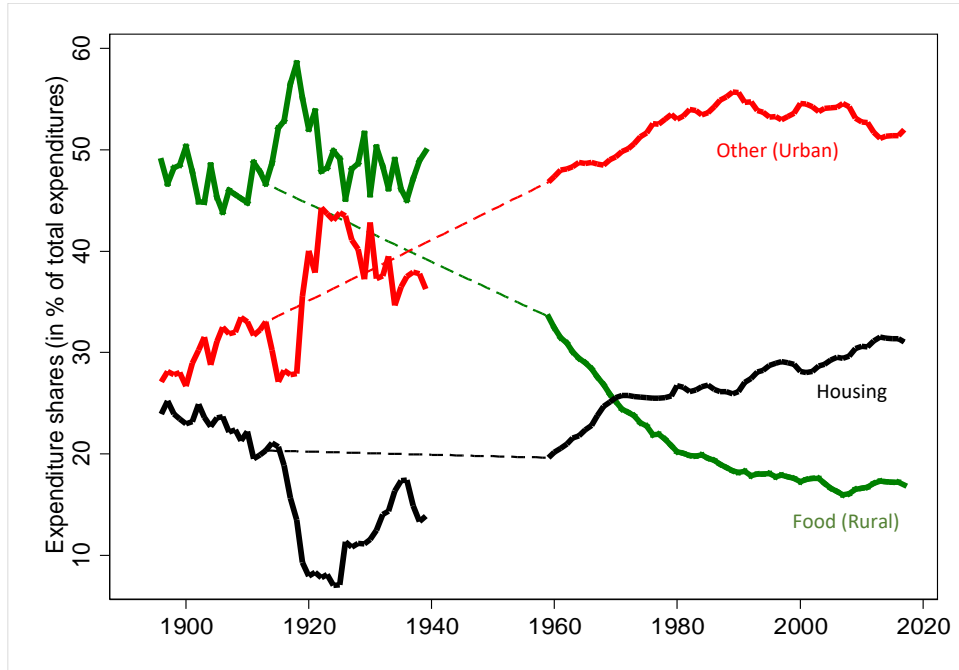


Figure 25: Spending Shares for Rural, Urban and Housing goods.

Notes: The observations around WW2 missing due to difficulties in data collection.

Data on expenditure shares across these three broad categories are shown in Figure 25. Comparing the initial periods in the late nineteenth century to today gives the following broad facts: the food share went down from almost 50% of expenditures to 17%; the housing share increased slightly to 23% to 31%; the share of expenditure on other goods increased as a consequence from 27% to more than 50%. This reallocation of expenditures away from rural goods towards housing and urban goods fits well with the process of structural transformation.

Rent control and the housing expenditure share. An important issue is the significant and persistent dip of the housing expenditure share starting at WW1. This evolution is largely due to the presence of rent controls that were put in place at the beginning of WW1 in France. As the French government wanted families to be able to afford their home during the war, it decreed that rents would be blocked (in nominal terms). As inflation picked up, this generated a large fall in real housing rents. As rents were very cheap, it freed up resources for households that could be spent on other goods (rural and urban). This is immediately visible on Figure 25, where the share of expenditures on housing went down from 21% in 1914 to less than 10% at the end of the war in 1919—other expenditure shares increasing simultaneously. While the measure was meant to be temporary, rent control lasted effectively during the whole interwar period despite various modification in the laws. It was eventually profoundly reformed post WW2 in 1948.⁵⁸ The reform

20th century. Small furnished flats/bedrooms were very common in large cities in the interwar period ('garnis'). However, excluding the latter category from housing expenses does not affect our results.

⁵⁸Rents did increase in real terms during the interwar period. However, regulations still significantly limited the rent increases. The reform of 1948 still kept some housing with regulated cheap rents. Rents could be changed for

of 1948 led to a sluggish adjustment of rents and it took some further years before one can reasonably argue that the rent control put in place in 1914 starts playing a more minor role.⁵⁹ Given this, our aim is to match the long-run evolution of spending shares while abstracting from the fluctuations in between 1914 and 1959 (first year of observation in the series provided by INSEE), as illustrated by the dashed lines on Figure 25.

A.6 Land and Housing Wealth

Land and housing wealth data is from [Piketty and Zucman \(2014\)](#), which can be obtained in the World Inequality Database (<https://wid.world/fr/accueil/>).

The data provide the value of agricultural land (as a share of national income) and the value of housing (as a share of national income) in France, roughly every ten years since 1810. The value of housing incorporates the value of land used for housing as well as the value of the capital stock used for housing (buildings and structure). To confront the data to our model, one needs to separate the value of land from the value of capital. Data on the share of land in housing is only available since 1979 for France (also available in the World Inequality Database). Due to lack of historical data on the share of land in housing, we assume a constant share over the whole period and take the average for the period 1979-2019. We find an average of 0.32 over the period 1979-2019. The value of urban/housing land is thus computed as 32% of the total value of housing. Note that this value of 0.32 is consistent with [Combes et al. \(2021\)](#) which computes a land share in housing of 0.35. It is also consistent with the model’s predictions given the calibrated supply elasticities of housing (the model gives an average value of 0.3 for this period).

A.7 Urban Area and Population Measurement - Manual and GHSL Data

As explained in Section 2.2 in the main text, we consider the 100 most populated cities in the census of 1876 as our sample. We constrain this list to contain only cities which are still independent entities nowadays.⁶⁰ With the master list of cities in place, we proceed as follows to obtain two measures for each city: the extent of urban area in square kilometers, and population count. Depending on the period, we consider different data sources. The earliest measure uses the Carte d’Etat Major for urban area (1866) and the census for urban population counts (1876), while the second measure uses 1950 aerial photographs and the 1954 population census. Due to the lack of other data sources, we regard 1866 and 1876 we well as 1950 and 1954 as the same points in time, and we will refer to 1870 and 1950 for simplicity. In subsequent years, the Global Human Settlement Layer (GHSL) provides built up area and population data for the 1975, 1990, 2000 and 2015.

new renters. Few housing with very cheap rents under the special regime of 1948 still subsists.

⁵⁹Data from CREDOC in the early 1950s suggests a fairly housing spending share at that time—around 15%.

⁶⁰This concerns Roubaix (today part of Lille), Versailles (Paris), Tourcoing (Lille), Saint-Denis (Paris), Levallois-Perret (Paris), Boulogne-Billancourt (Paris), Neuilly-sur-Seine (Paris), Clichy (Paris) and Saint-Germain-en-Laye (Paris). Our hand-collected data are published online at https://docs.google.com/spreadsheets/d/e/2PACX-1vS02WpT0e7YTtS6f-svIXR3sURjiMRw7kBgfH1XF8LRre_dhPD0Y80y67cU_L4Q2FHg0r711ffB3XYm/pubhtml?gid=0&single=true

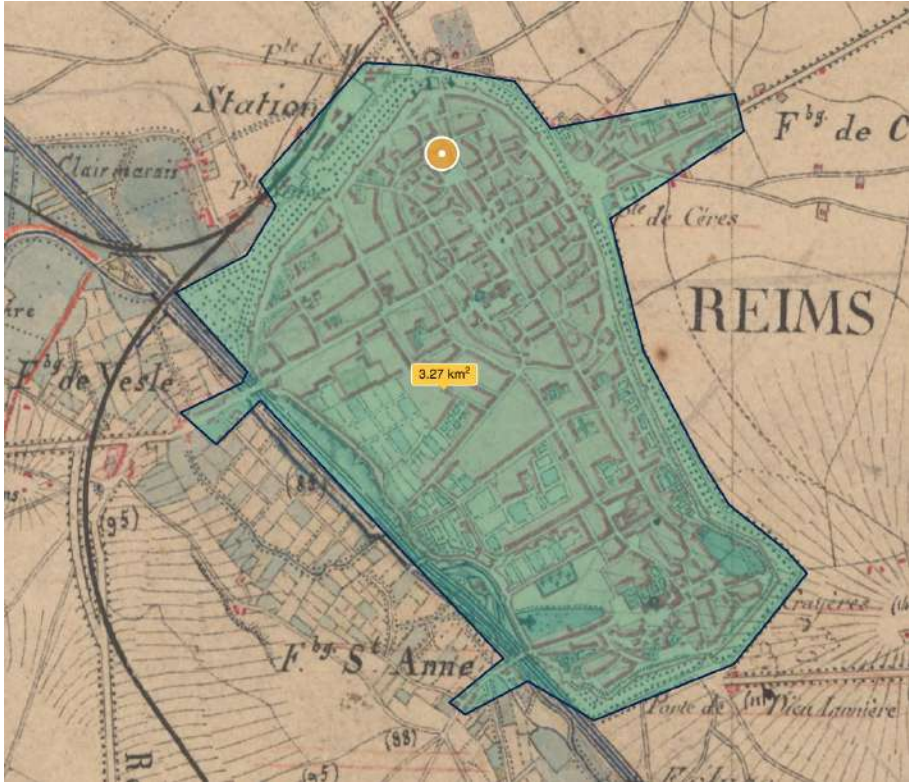


Figure 26: Area measurement of Reims using Etat Major map

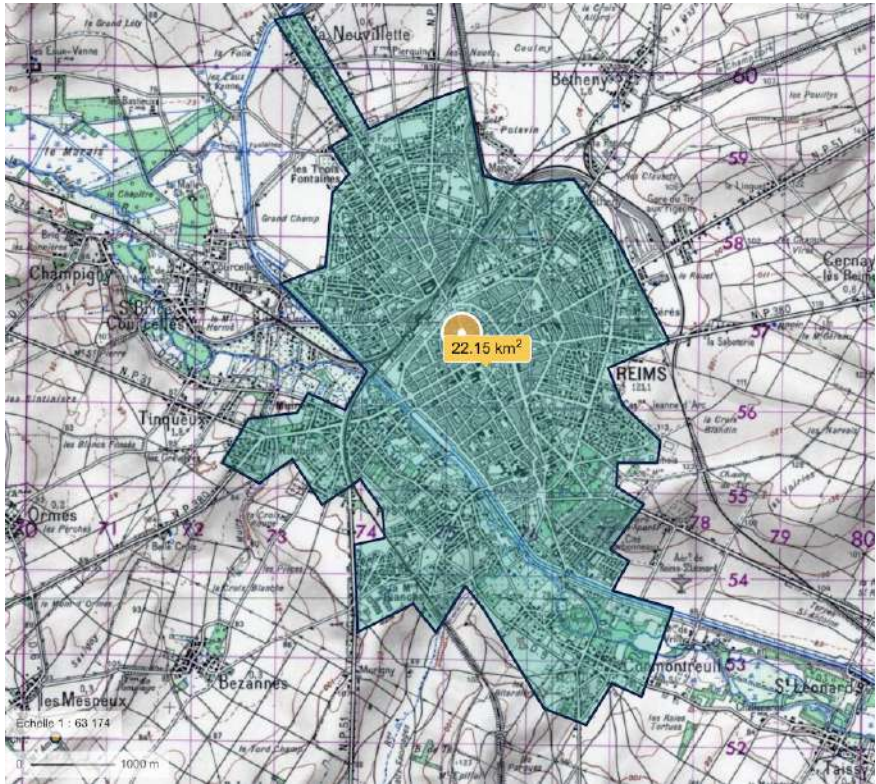


Figure 27: Area measurement of Reims using 1950 map

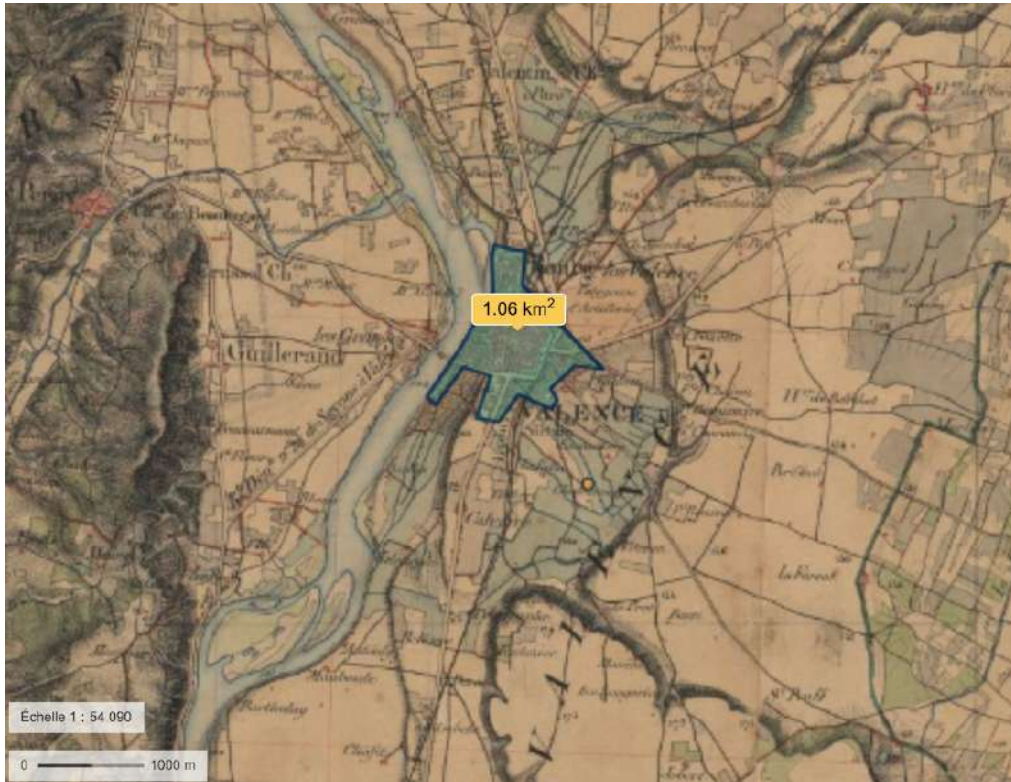


Figure 28: Area measurement of Valence using Etat Major map

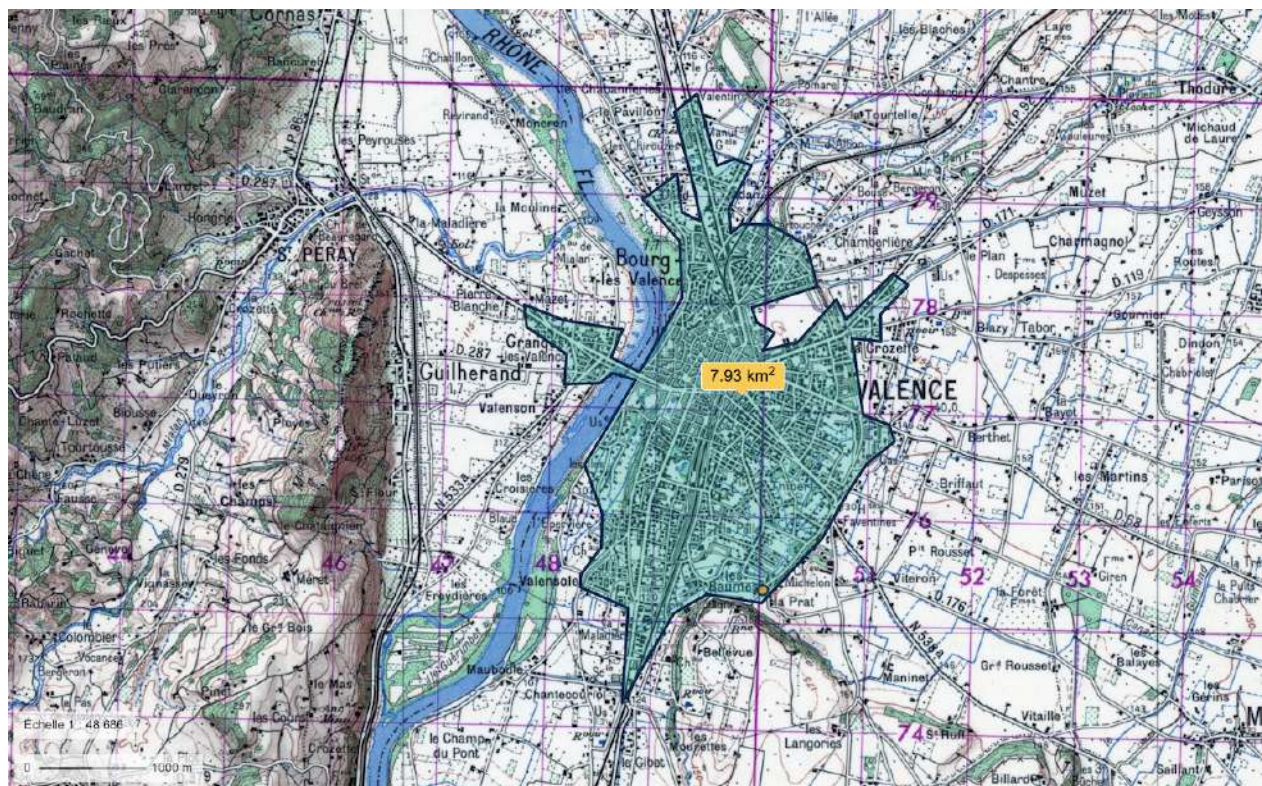


Figure 29: Area measurement of Valence using 1950 map

A.7.1 Manual Urban Area Measurements 1870 and 1950

We rely on georeferenced maps provided via <https://www.geoportail.gouv.fr> to take area measures of our cities. This website is run by the Institut national de l'information géographique et forestière (IGN) and offers a large variety of map layers and measurement tools (distance, area, etc). We use the layer *Carte d'Etat Major 1820-1866* (EM henceforth), *Photographies aériennes 1950-1965* or *Cartes 1950* (depending on which allows better classification), as well as contemporary *Photographies aériennes* to cross-check our measures with what the satellite measures will produce for the later periods (see Section A.7.5).⁶¹ We hence use the tools on geoportail.fr to delineate the urban area of the EM and 1950 aerial photos maps manually on screen, taking a screenshot of each measurement. The criteria to classify as urban area are such that they coincide with the criteria which will be applied to the automated satellite measures in later periods. We classify an area as part of a city, if:

1. We observe contiguous housing structure in a grid cell of 250m by 250m. This means disconnected municipalities or smaller parishes will not be considered as part of the main city. Given there are no grid cells displayed on the historical maps, the analyst has to be careful to consider different scales for different size cities in this step.
2. Density of built-up environment: We try to enforce a 30% built-up threshold as in the automated approach in order to distinguish low-density suburbs from city proper. This means that areas which are contiguous to the main city, but significantly less dense because of interspersed gardens and rural land, will be excluded from the main city area.

We note that there is some degree of arbitrariness in this manual measurement procedure and that a fully automated approach like in Combes et al. (2021) is more rigorous. We verify that our approach is on average accurate and consistent with the automated procedure to be outlined below. We show some examples for Reims (figures 26, 27) and Valence (figures 28, 29).

A.7.2 Manual Population Measurements 1870 and 1950

In order to collect population counts for each city, we resort to the 1876 census as published by INSEE at <https://www.insee.fr/fr/statistiques/3698339>. This procedure is unambiguous, because all cities in our sample are contained within their administrative boundaries in the initial period.

The next data point for the 1950 cities is obtained from the census in 1954. Given the area measure obtained for 1950 as described in A.7.1, we verify for each city whether the total classified area falls within the administrative boundaries of the main city. If this is the case, we take the population measure directly from the census file, as before. If this is not the case (concerning in particular larger cities which incorporate surrounding villages by 1950, and in particular Paris), we carefully

⁶¹contemporary photographs are taken between 2016 and 2020: https://www.geoportail.gouv.fr/depot/fiches/photographies-aeriennes-RVB/geoportail_dates_des_prises_de_vues_aeriennes-RVB.pdf

check which administrative areas (i.e. former independent villages) have now become part of our 1950 city area, and we sum the corresponding population counts for the concerned areas. The mapping of villages to cities is given in Table ?? and the one of Paris administrative areas is shown in Table ??.

Table 3: Paris 1950 Population Classification

CODGEO	REG	DEP	LIBGEO	year	population	date
75101	11	75	Paris 1er Arrondissement	1954	38926	1954-01-01
75102	11	75	Paris 2e Arrondissement	1954	43857	1954-01-01
75103	11	75	Paris 3e Arrondissement	1954	65312	1954-01-01
75104	11	75	Paris 4e Arrondissement	1954	66621	1954-01-01
75105	11	75	Paris 5e Arrondissement	1954	106443	1954-01-01
75106	11	75	Paris 6e Arrondissement	1954	88200	1954-01-01
75107	11	75	Paris 7e Arrondissement	1954	104412	1954-01-01
75108	11	75	Paris 8e Arrondissement	1954	80827	1954-01-01
75109	11	75	Paris 9e Arrondissement	1954	102287	1954-01-01
75110	11	75	Paris 10e Arrondissement	1954	129179	1954-01-01
75111	11	75	Paris 11e Arrondissement	1954	200440	1954-01-01
75112	11	75	Paris 12e Arrondissement	1954	158437	1954-01-01
75113	11	75	Paris 13e Arrondissement	1954	165620	1954-01-01
75114	11	75	Paris 14e Arrondissement	1954	181414	1954-01-01
75115	11	75	Paris 15e Arrondissement	1954	250124	1954-01-01
75116	11	75	Paris 16e Arrondissement	1954	214042	1954-01-01
75117	11	75	Paris 17e Arrondissement	1954	231987	1954-01-01
75118	11	75	Paris 18e Arrondissement	1954	266825	1954-01-01
75119	11	75	Paris 19e Arrondissement	1954	155028	1954-01-01
75120	11	75	Paris 20e Arrondissement	1954	200208	1954-01-01
93001	11	93	Aubervilliers	1954	58740	1954-01-01
93005	11	93	Aulnay-sous-Bois	1954	38534	1954-01-01
93006	11	93	Bagnolet	1954	26792	1954-01-01
93007	11	93	Le Blanc-Mesnil	1954	25363	1954-01-01
93008	11	93	Bobigny	1954	18521	1954-01-01
93010	11	93	Bondy	1954	22411	1954-01-01
93013	11	93	Le Bourget	1954	8432	1954-01-01
93014	11	93	Clichy-sous-Bois	1954	5105	1954-01-01
93015	11	93	Coubron	1954	1039	1954-01-01
93027	11	93	La Courneuve	1954	18349	1954-01-01

Table 3: Paris 1950 Population Classification (*continued*)

CODGEO	REG	DEP	LIBGEO	year	population	date
93029	11	93	Drancy	1954	50654	1954-01-01
93030	11	93	Dugny	1954	6932	1954-01-01
93032	11	93	Gagny	1954	17255	1954-01-01
93033	11	93	Gournay-sur-Marne	1954	2141	1954-01-01
93045	11	93	Les Lilas	1954	18590	1954-01-01
93046	11	93	Livry-Gargan	1954	25322	1954-01-01
93047	11	93	Montfermeil	1954	8271	1954-01-01
93048	11	93	Montreuil	1954	76239	1954-01-01
93049	11	93	Neuilly-Plaisance	1954	13211	1954-01-01
93050	11	93	Neuilly-sur-Marne	1954	12798	1954-01-01
93051	11	93	Noisy-le-Grand	1954	10398	1954-01-01
93053	11	93	Noisy-le-Sec	1954	22337	1954-01-01
93055	11	93	Pantin	1954	36963	1954-01-01
93057	11	93	Les Pavillons-sous-Bois	1954	16862	1954-01-01
93059	11	93	Pierrefitte-sur-Seine	1954	12867	1954-01-01
93061	11	93	Le Pré-Saint-Gervais	1954	15037	1954-01-01
93062	11	93	Le Raincy	1954	14242	1954-01-01
93063	11	93	Romainville	1954	19217	1954-01-01
93064	11	93	Rosny-sous-Bois	1954	16491	1954-01-01
93066	11	93	Saint-Denis	1954	80705	1954-01-01
93070	11	93	Saint-Ouen	1954	48112	1954-01-01
93071	11	93	Sevran	1954	12956	1954-01-01
93072	11	93	Stains	1954	19028	1954-01-01
93074	11	93	Vaujours	1954	3972	1954-01-01
93077	11	93	Villemomble	1954	21522	1954-01-01
93078	11	93	Villepinte	1954	5503	1954-01-01
93079	11	93	Villetaneuse	1954	3937	1954-01-01
94001	11	94	Ablon-sur-Seine	1954	3220	1954-01-01
94002	11	94	Alfortville	1954	30195	1954-01-01
94003	11	94	Arcueil	1954	18067	1954-01-01
94015	11	94	Bry-sur-Marne	1954	6660	1954-01-01
94016	11	94	Cachan	1954	16965	1954-01-01
94017	11	94	Champigny-sur-Marne	1954	36903	1954-01-01
94018	11	94	Charenton-le-Pont	1954	22079	1954-01-01

Table 3: Paris 1950 Population Classification (*continued*)

CODGEO	REG	DEP	LIBGEO	year	population	date
94019	11	94	Chennevières-sur-Marne	1954	4032	1954-01-01
94021	11	94	Chevilly-Larue	1954	3861	1954-01-01
94022	11	94	Choisy-le-Roi	1954	32025	1954-01-01
94028	11	94	Créteil	1954	13793	1954-01-01
94033	11	94	Fontenay-sous-Bois	1954	36739	1954-01-01
94034	11	94	Fresnes	1954	7750	1954-01-01
94037	11	94	Gentilly	1954	17497	1954-01-01
94038	11	94	L'Haÿ-les-Roses	1954	10278	1954-01-01
94041	11	94	Ivry-sur-Seine	1954	48798	1954-01-01
94042	11	94	Joinville-le-Pont	1954	15657	1954-01-01
94043	11	94	Le Kremlin-Bicêtre	1954	15618	1954-01-01
94046	11	94	Maisons-Alfort	1954	40358	1954-01-01
94052	11	94	Nogent-sur-Marne	1954	23581	1954-01-01
94058	11	94	Le Perreux-sur-Marne	1954	26745	1954-01-01
94067	11	94	Saint-Mandé	1954	24522	1954-01-01
94068	11	94	Saint-Maur-des-Fossés	1954	64387	1954-01-01
94069	11	94	Saint-Maurice	1954	11134	1954-01-01
94073	11	94	Thiais	1954	10028	1954-01-01
94076	11	94	Villejuif	1954	29280	1954-01-01
94079	11	94	Villiers-sur-Marne	1954	9205	1954-01-01
94080	11	94	Vincennes	1954	50434	1954-01-01
94081	11	94	Vitry-sur-Seine	1954	51507	1954-01-01
92002	11	92	Antony	1954	24512	1954-01-01
92004	11	92	Asnières-sur-Seine	1954	77838	1954-01-01
92007	11	92	Bagneux	1954	13774	1954-01-01
92009	11	92	Bois-Colombes	1954	27899	1954-01-01
92012	11	92	Boulogne-Billancourt	1954	93998	1954-01-01
92014	11	92	Bourg-la-Reine	1954	11708	1954-01-01
92019	11	92	Châtenay-Malabry	1954	14269	1954-01-01
92020	11	92	Châtillon	1954	12526	1954-01-01
92022	11	92	Chaville	1954	14508	1954-01-01
92023	11	92	Clamart	1954	37924	1954-01-01
92024	11	92	Clichy	1954	55591	1954-01-01
92025	11	92	Colombes	1954	67909	1954-01-01

Table 3: Paris 1950 Population Classification (*continued*)

CODGEO	REG	DEP	LIBGEO	year	population	date
92026	11	92	Courbevoie	1954	59730	1954-01-01
92032	11	92	Fontenay-aux-Roses	1954	8642	1954-01-01
92033	11	92	Garches	1954	10450	1954-01-01
92035	11	92	La Garenne-Colombes	1954	26753	1954-01-01
92036	11	92	Gennevilliers	1954	33137	1954-01-01
92040	11	92	Issy-les-Moulineaux	1954	47433	1954-01-01
92044	11	92	Levallois-Perret	1954	62871	1954-01-01
92046	11	92	Malakoff	1954	28876	1954-01-01
92048	11	92	Meudon	1954	24729	1954-01-01
92049	11	92	Montrouge	1954	36298	1954-01-01
92050	11	92	Nanterre	1954	53037	1954-01-01
92051	11	92	Neuilly-sur-Seine	1954	66095	1954-01-01
92060	11	92	Le Plessis-Robinson	1954	13147	1954-01-01
92062	11	92	Puteaux	1954	41097	1954-01-01
92063	11	92	Rueil-Malmaison	1954	32212	1954-01-01
92064	11	92	Saint-Cloud	1954	20668	1954-01-01
92071	11	92	Sceaux	1954	10601	1954-01-01
92073	11	92	Suresnes	1954	37149	1954-01-01
92075	11	92	Vanves	1954	21679	1954-01-01
92078	11	92	Villeneuve-la-Garenne	1954	4035	1954-01-01

A.7.3 Automatic Area and Population Measurement via GHSL

For years 1975, 1990, 2000 and 2015 we can rely on satellite data provided by the [Global Human Settlement Layer \(GHSL\)](#) project. We use two products, the multitemporal built-up grid [GHS-BUILT](#) (see [Corbane et al. \(2018\)](#)) and the multitemporal population grid [GHS-POP](#), see [Schiavina et al. \(2019\)](#). We first give a brief overview of the GHSL data, which is a global raster dataset to measure human activity over space and time (see [Florczyk et al. \(2019\)](#)).⁶² Then we will outline our strategy to derive area and population measures for our 100 French cities.

GHS-BUILT Area Classification. We rely on the multitemporal (years 1975, 1990, 2000, 2015) grid [GHS_BUILT_LDSMT_GLOBE_R2018A](#) which uses satellite imagery of various Landsat generations. The methodology to classify a certain pixel as built-up or not is described in [Corbane et al. \(2019\)](#). The task at hand is a classical supervised learning, or classification, task, whereby an automated

⁶²https://ghsl.jrc.ec.europa.eu/documents/GHSL_Data_Package_2019.pdf

Table 2: France 1950 Population Classification. Cities containing more than one INSEE administrative area by 1950.

CODGEO	DEP	LIBGEO	components
02691	2	Saint-Quentin	Saint-Quentin, Harly , Gauchy
03185	3	Montluçon	Montluçon , Désertines
03190	3	Moulins	Moulins, Yzeure
14366	14	Lisieux	Lisieux , Saint-Désir
28085	28	Chartres	Chartres , Mainvilliers, Luisant
29151	29	Morlaix	Morlaix , Saint-Martin-des-Champs
33063	33	Bordeaux	Bordeaux , Talence , Bègles , Le Bouscat
36044	36	Châteauroux	Châteauroux, Déols
42207	42	Saint-Chamond	Saint-Chamond, L’Horme
43157	43	Le Puy-en-Velay	Le Puy-en-Velay , Vals-près-le-Puy
44109	44	Nantes	Nantes, Rezé
51108	51	Châlons-en-Champagne	Châlons-en-Champagne, Saint-Memmie
51454	51	Reims	Reims , Cormontreuil
57463	57	Metz	Metz , Montigny-lès-Metz , Longeville-lès-Metz
59122	59	Cambrai	Cambrai , Proville , Neuville-Saint-Rémy
59178	59	Douai	Douai, Dechy
59350	59	Lille	Lille , La Madeleine
59606	59	Valenciennes	Valenciennes , Marly , Saint-Saulve , La Sentinelle , Anzin , Trith-Saint-Léger , Beuvrages , Raismes , Bruay-sur-l’Escaut , Petite-Forêt , Aulnoy-lez-Valenciennes
62041	62	Arras	Arras , Achicourt
62160	62	Boulogne-sur-Mer	Boulogne-sur-Mer , Saint-Martin-Boulogne, Outreau , Le Portel
62193	62	Calais	Calais , Coulogne
63113	63	Clermont-Ferrand	Clermont-Ferrand, Chamalières
67482	67	Strasbourg	Strasbourg , Schiltigheim, Bischheim , Hoenheim
69123	69	Lyon	Lyon , Villeurbanne , Caluire-et-Cuire, Oullins
76231	76	Elbeuf	Elbeuf , Caudebec-lès-Elbeuf , Saint-Aubin-lès-Elbeuf
76351	76	Le Havre	Le Havre , Sainte-Adresse
83137	83	Toulon	Toulon , La Valette-du-Var

procedure learns from a labeled dataset (the training dataset) how to label new and unseen data. The method used here is called *Symbolic Machine Learning* (SML), and it outperforms other methods such as Maximum Likelihood, Logistic Regression, Linear Discriminant Analysis, Naive Bayes, Decision Tree, Random Forest and Support Vector Machine both in terms of accuracy and in terms computing cost. We refer to [Corbane et al. \(2019\)](#) for greater details concerning accuracy assessment. We end up using the 250m resolution data in Mollweide projection, where a grid cell is characterized by a numeric (Float32) value in $[0, 100]$ representing the percentage of area in the cell which is *built up*. Finally, note that

the concept of “built-up area” applied in the GHSL is compliant with the definition of the “building” abstraction in the Infrastructure for Spatial Information in Europe (INSPIRE). The “built-up area” as defined in the GHSL framework is “the union of all the satellite data samples that corresponds to a roofed construction above ground which is intended or used for the shelter of humans, animals, things, the production of economic goods or the delivery of services”. ([Corbane et al. \(2019\)](#) page 141)

GHs-POP Population Grid. We use the product `GHS_POP_MT_GLOBE_R2019A` in this part. For later periods (after 2000), GHs-POP uses the [Gridded Population of the World \(v4.10\)](#) dataset produced by CIESIN/SEDAC. For the earlier years 1975 and 1990 it takes as input the GHs-BUILT grid and disaggregates population data from census enumerations according to a simple model. The disaggregation starts from knowledge of population counts in certain census areas, and then uses the building density from GHs-BUILT to distribute the census population into GHs-POP cells which constitute the concerned census area. We use again the 250m resolution in Mollweide projection, where a grid cell is characterized by a numeric value $[0, \infty]$ representing population count – notice that given the fixed geography (a box 250m by 250m), the measure is synonymous for *population density* in this instance. For more details on the generation of GHs-POP data please refer to [Freire et al. \(2016\)](#).

GHSL Measurement Procedure. We first describe the exact data products we use, and then how we process them in order to obtain area and population measurements for all grid cells which are part of our list of 100 French cities. We begin by downloading the data via <https://ghsl.jrc.ec.europa.eu/download.php?ds=bu>, selecting the tiles covering continental France (tiles 18_3 and 17_3). The precise data versions we use are as follows:

GHs-POP `GHS_POP_E1975_GLOBE_R2019A_54009_250_V1_0_18_3` and `GHS_POP_E1975_GLOBE_R2019A_54009_250_V1_0_17_3`

GHs-BUILT ...

year < 2015 `GHS_BUILT_LDS1975_GLOBE_R2018A_54009_250_V2_0_17_3` and `GHS_BUILT_LDS1975_GLOBE_R2018A_54009_250_V2_0_18_3`

year == 2015 GHS_BUILT_LDS2014_GLOBE_R2018A_54009_250_V2_0_18_3 and GHS_BUILT_LDS2014_GLOBE_R2018A_54009_250_V2_0_17_3

We proceed as follows with the data:

1. Read results of manual measurement (see ??) to obtain list of cities and historical measures.
2. Crop GHS rasters to bounding boxes containing cities.
3. For each GHS-year, measure area from GHS-BUILT and population from GHS-POP. We delineate city extent based exclusively on GHS-BUILT, as follows:
 - (a) Classify all grid cells with built-up proportion greater than threshold `cutoff` as *urban*. The baseline value for this parameter is 30%, and we present sensitivity analysis below in Section A.7.6.
 - (b) For larger cities we have to decide what the *main* city is, as there may be disconnected parts of urbanized area outside the main city’s boundary. We select the largest connected set of grid cells, where connection is established via *queen’s case* directional movement (i.e. connected in any direction).
 - (c) We count the so-classified grid cells of GHS-BUILT in order to obtain total urban area, and we sum the corresponding cells of GHS-POP in order to get urban population.

A.7.4 Density Measurement Results

Built-up and Density Measures. We show example output for built-up area classifications for two cities in figures 31 and 32. Example measures of resulting urban densities can be seen in figures 34 for the top 5 cities as well as in Figure 33 for the entire distribution.

Within-city Density Gradients. For each grid cell of our GHSL data (2015), we define its distance from the center of the corresponding city, where the center is defined as location of the townhall by the the French National Institute of Geography (IGN). We cut each city into 50 bins of distance of equal size from the center and measure the average density across cells in each bin of distance. Thus, for each city i , we compute the density $D_{i,\ell}$ at distance ℓ from the city center. The set of distances ℓ varies across cities, as they are of different size.

Figure 30a illustrates the negative relationship between density and distance for the monocentric city of Lyon. Note that this relationship is quite different in a polycentric city such as Lille as shown in Figure 30b.

We define the density gradient of city i , b_i , as the absolute value of slope coefficient of $\ln(D_{i,\ell})$ on ℓ ,

$$D_{i,\ell} \approx a_i \exp(-b_i \ell), \tag{32}$$

where a_i and b_i are both positive. We use such a functional form as it fits very well the data for

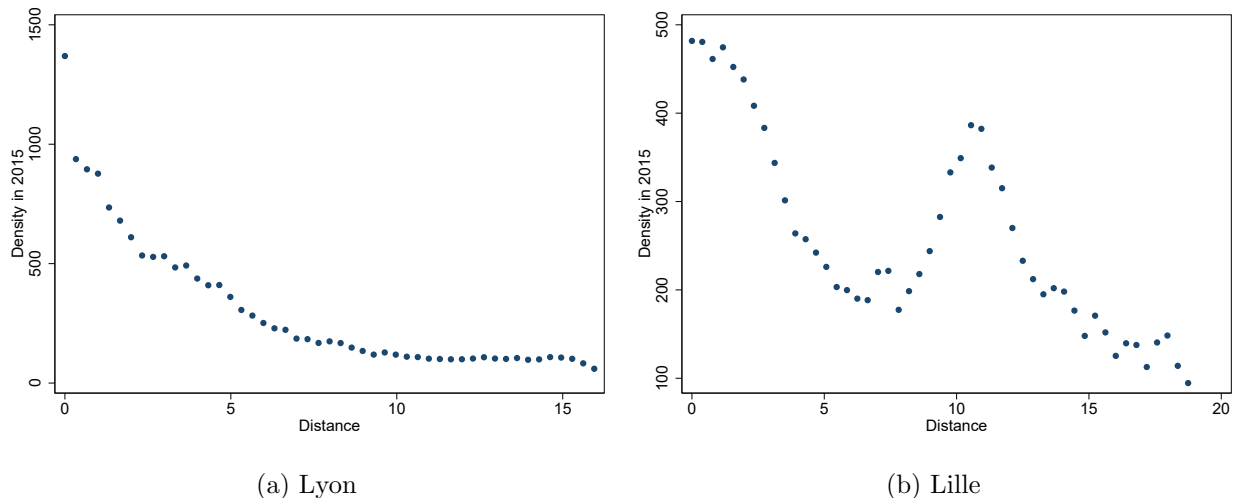


Figure 30: Density gradients.

Notes: Figures show the density (number of residents per 250m by 250m) at a given distance (in km) from the city center. GHSL data 2015.

all French cities—apart few polycentric ones such a Lille. This gradient can be computed for every city in our sample.

The unweighted mean of gradients is equal to 0.200, while the population-weighted mean is equal to 0.121. This reflects the lower values of the gradient in larger cities as they are more likely to be polycentric. These two values provide reasonable bounds for average value of the gradient across cities.

Our sample contains few large polycentric cities (Lille, Nice, Paris, Saint-Etienne, Toulon and Toulouse) where density as a function of distance is clearly non-monotonic. One way to deal with the issue is to compute the the population-weighted mean of gradients, excluding large polycentric cities. This gives a value of 0.176 for the average gradient. Another way to deal with large polycentric cities is to adjust the gradients for those cities by cutting the city at a given threshold of distance, abstracting from the rise in density further away from the center. If we compute the gradient within the first 10kms of distance from the center for those cities, we obtain a population-weighted gradient of 0.146. A slightly higher value of 0.152 is obtained if the gradient is computed only on the central part of the most polycentric ones (below 6kms distance from the center). If we consider only the first 10kms from the center for all cities in the sample, we get a gradient of 0.154.

Thus, according to our empirical estimates, we find a density gradient ranging from 0.14 to 0.18 for the average city in our sample and the value of 0.15 constitutes our baseline estimate. Note that beyond the value for this average density gradient, our empirical investigation also shows that the exponential shape of Eq. 32 provides a very accurate description of the density data within cities.

From data to model’s counterpart. The estimated density gradients correspond to a distance expressed in kms and the value is sensitive to the unit. Thus, one need to convert this value in

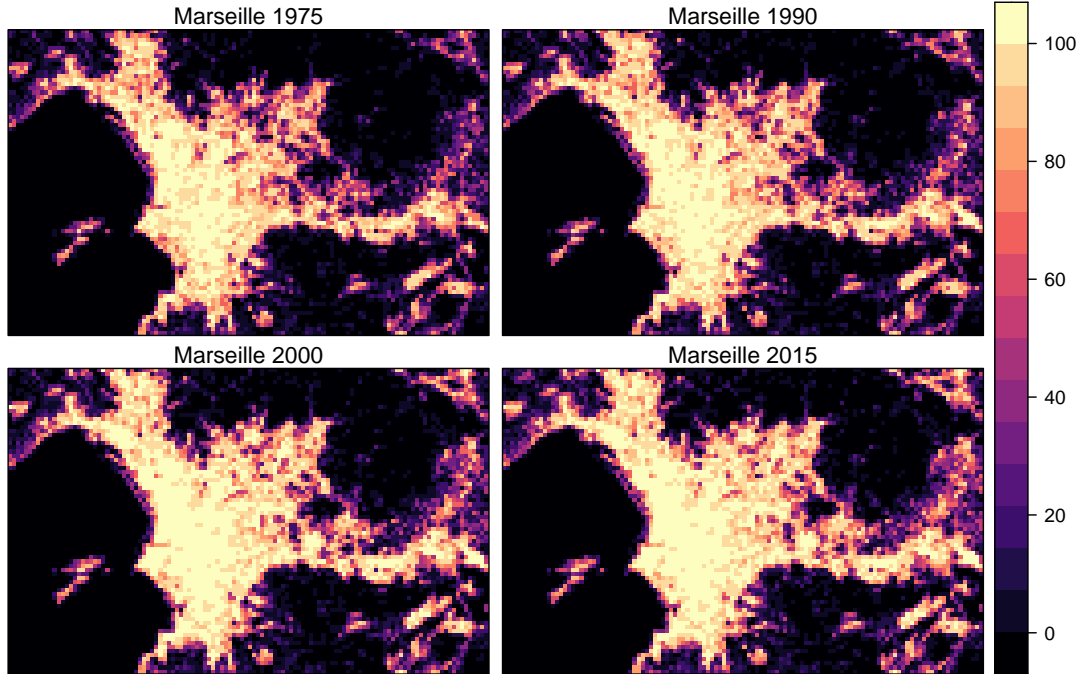


Figure 31: GHS-BUILT raster map of Marseille. The color scale represents percentage built-up in each grid cell.

a unit that can be confronted to our model. To do so, we measure the average radius of cities in our sample as the population-weighted mean of the largest distance bin in each of the 100 cities. This gives a mean radius of 21.43 kms. One can cut this radius into 20 equal size bins of 1.072 kms. Converting the density gradient of 0.15 in bin-unit gives a gradient of 0.16. This value can be compared to the gradient obtained in our model if we cut the radius ϕ of the city into 20 bins of equal distance increment.

A.7.5 Consistency of Area Measures across Methods and Sources

We have aerial photography from 2016 available (see an example for the city of Reims in Figure 35), which we use to also measure area of cities manually. The main purpose of this exercise is to show the consistency across methods (manual measurement and the automatic measure using satellite data). We report the relationship between manual 2016 and automatic 2015 measures in Figure 36. Results are comforting. Both measures give similar estimates and are very highly correlated across cities.

Additionally, we can rely on historical data compiled by Shlomo Angel and co-authors for Paris (amongst many other cities), see Angel et al. (2012) and Angel et al. (2010). We report in Figure 37 that our manual measures correspond closely to their obtained measures despite different measurement strategies.

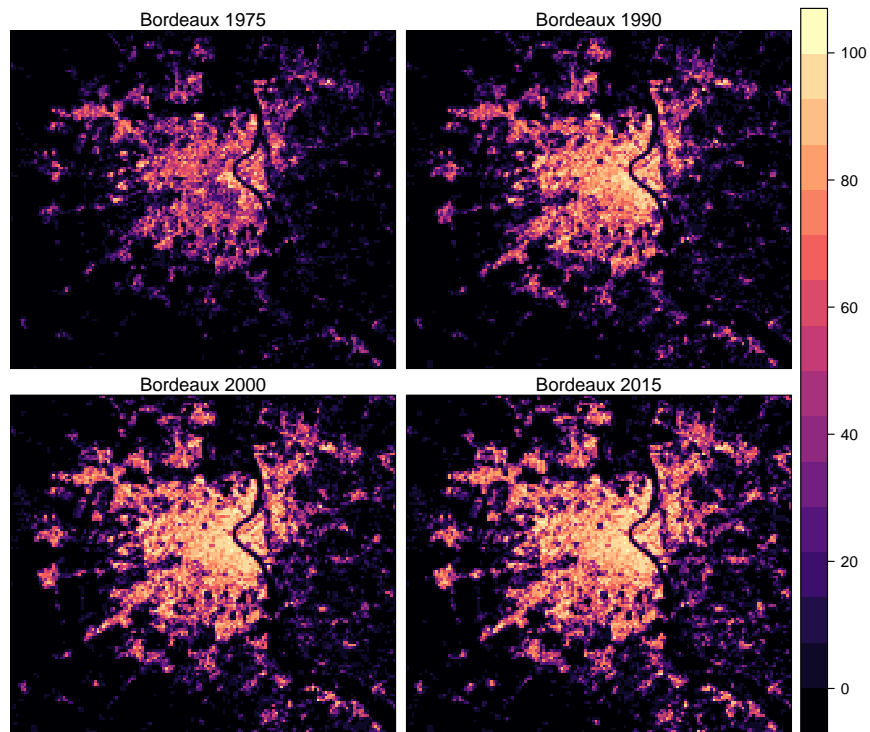


Figure 32: GHS-BUILT raster map of Bordeaux.

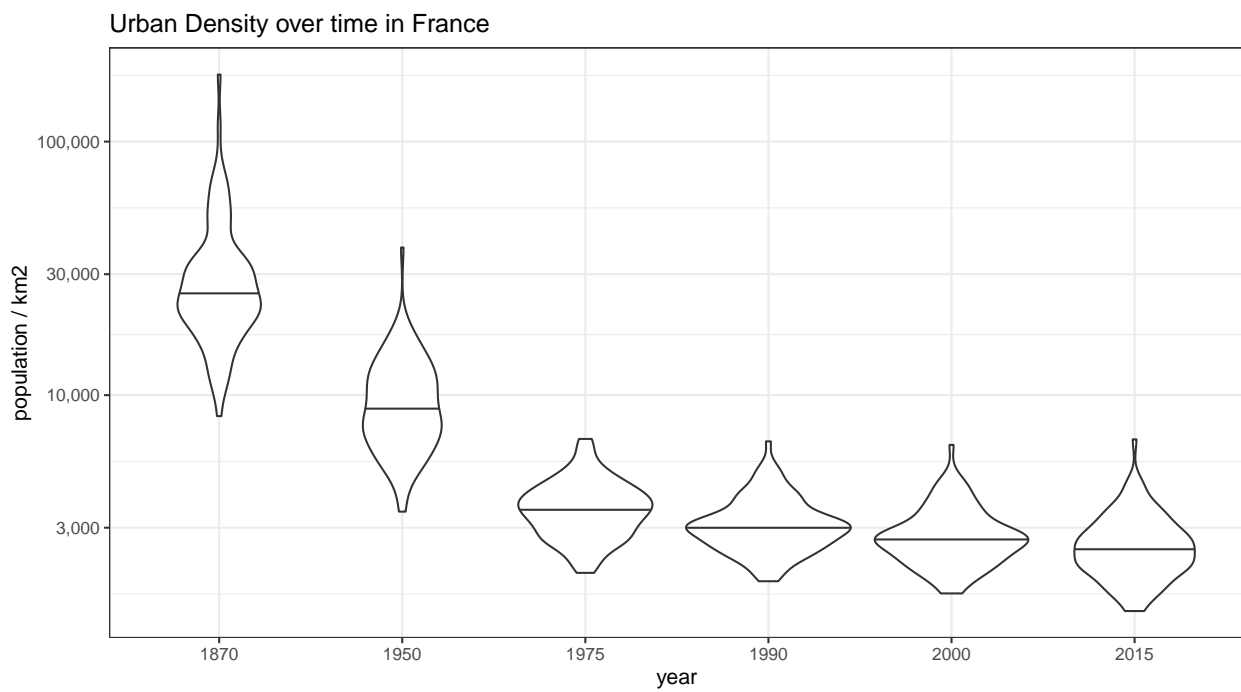


Figure 33: Distribution of Urban Density over Time. This *violin plot* represents the distribution of densities at each date, labeling the extreme values. The horizontal line denotes the median value.

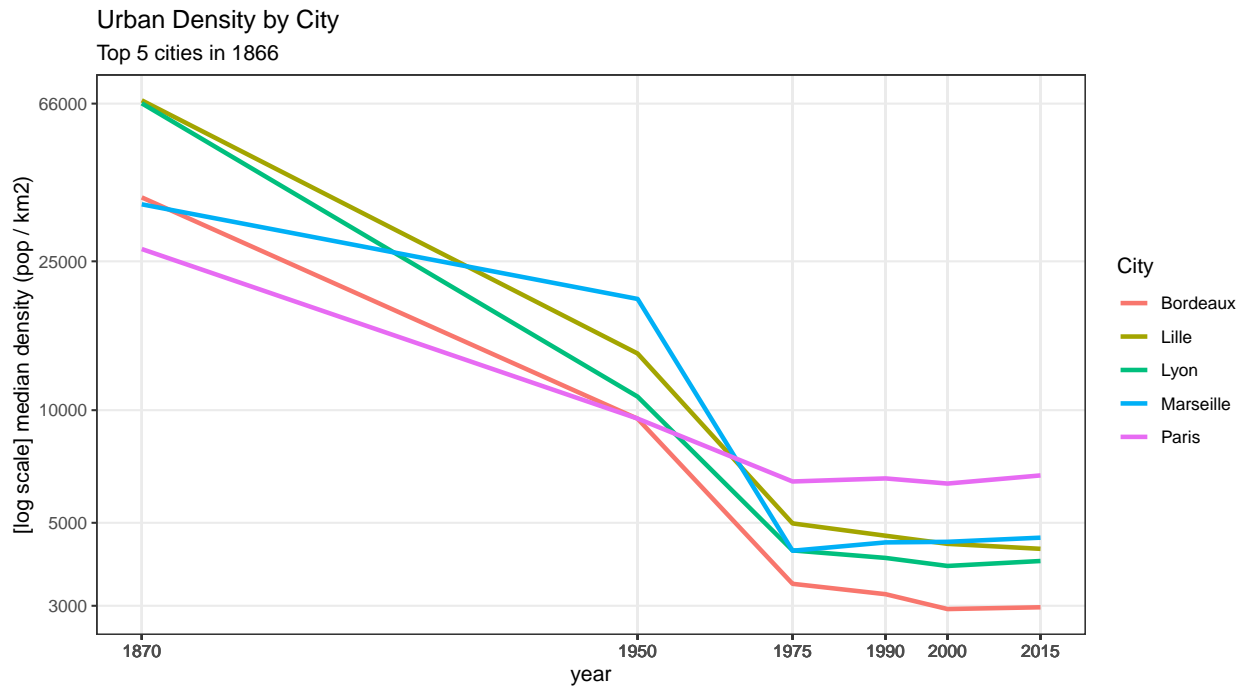


Figure 34: Density in the largest five cities in 1876 over time.

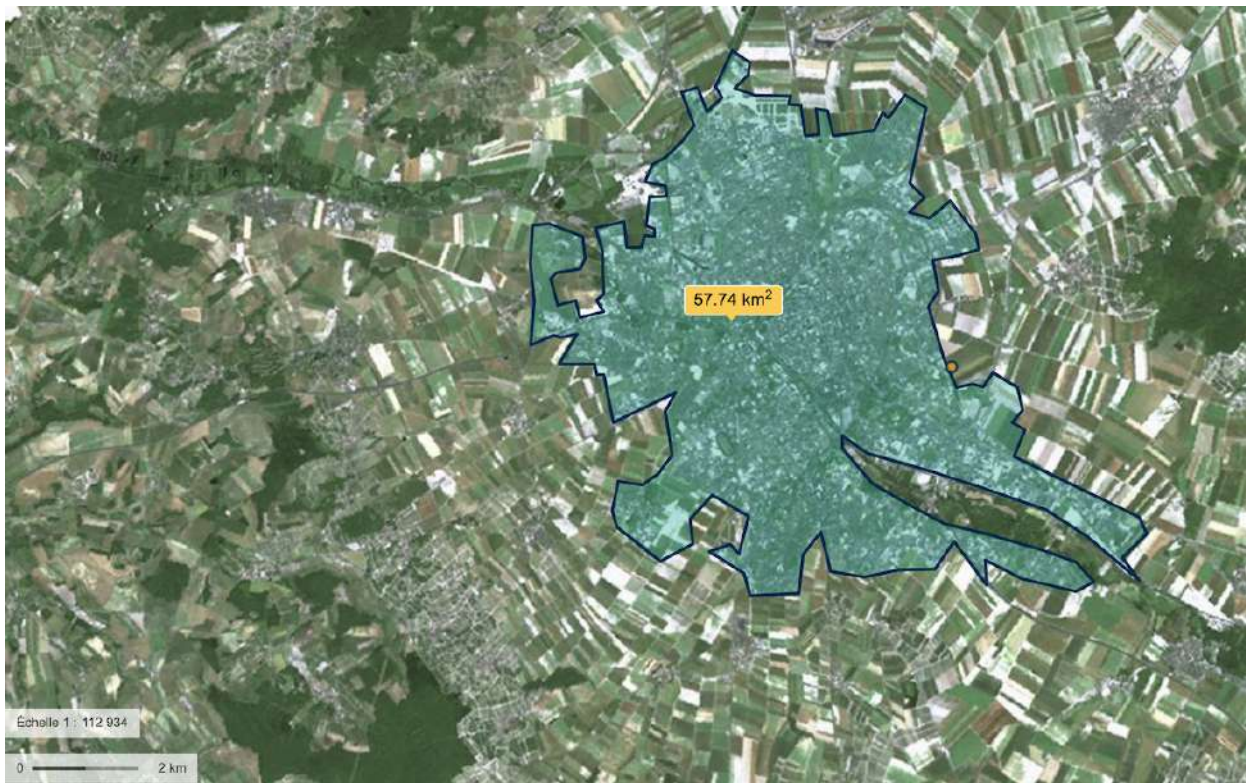


Figure 35: Area measurement of Reims using modern day photograph - used only for cross-checking GHSL measures.

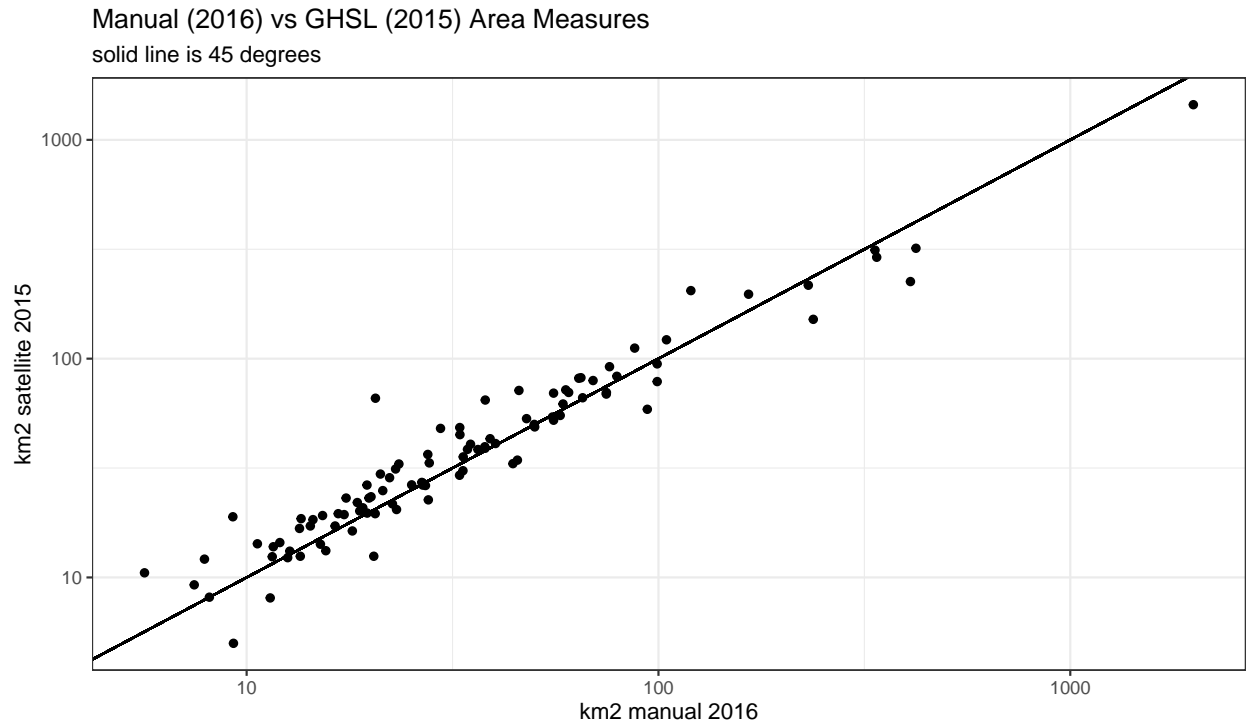


Figure 36: Comparing manually obtained area measures for each of our cities with automatically obtained ones via GHSL data.

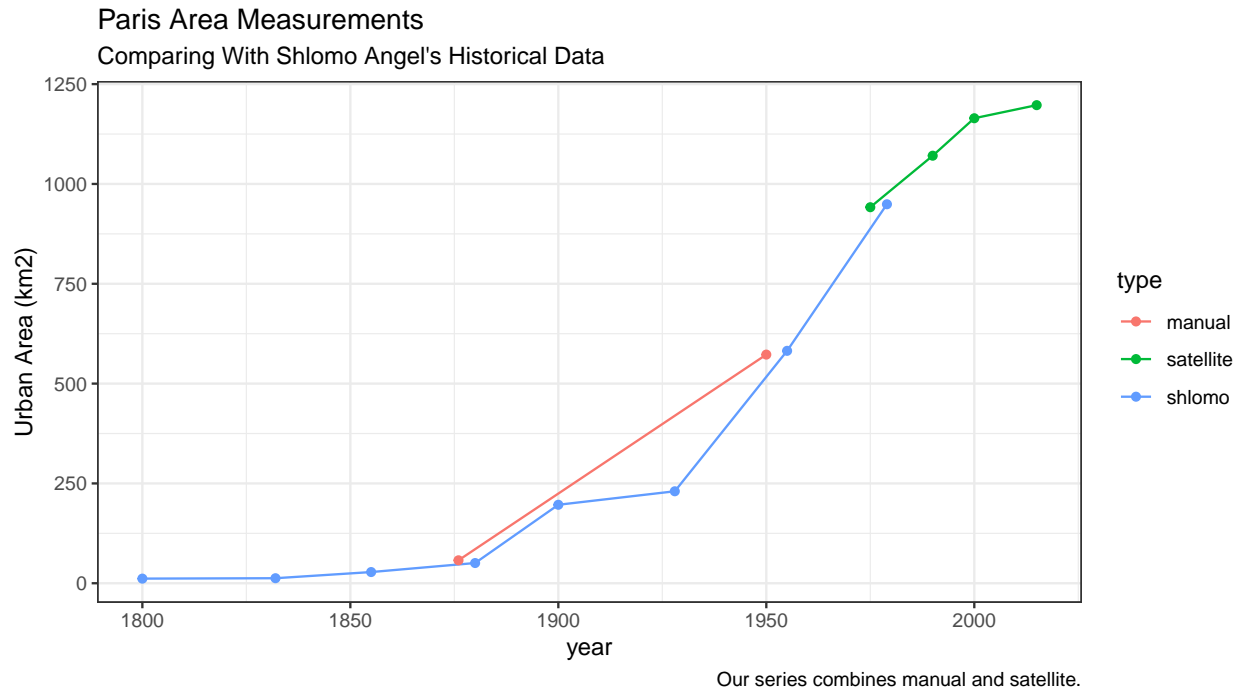


Figure 37: Comparing our measures with Shlomo Angel's data used in [Angel et al. \(2012\)](#) and [Angel et al. \(2010\)](#). We are reassured that our manual measurement exercise aligns closely with what they obtained. Also, their final data point is reassuringly close to our first satellite measure.

A.7.6 GHSL cutoff Parameter Sensitivity

As mentioned earlier, we chose a cutoff of 30% built up in a grid cell to discriminate urban from rural area in terms of building density. The purpose of this parameter is to decide what type of suburbanization should be considered to be still part of the city. In rough terms, our default setting would keep a property with 90 m^2 roofspace and 300 m^2 lot area (e.g. 210 m^2 garden) as part of the city. The criterion to classify an area as urban or not is necessarily subjective to some degree. We try to be as pragmatic as possible in choosing 30% and presenting how measured outcomes measure for a range of different cutoff values. De Bellefon et al. (2019) for example use a different approach which considers the distribution of grid cell density over the entire country and chooses a cutoff on that distribution as criterion (e.g. the 95-th percentile). The fundamental problem (value of the cutoff) remains. With this in mind, we present in figures 38 and 39 our derived statistics about median and population-weighted average urban density, using different values for the cutoff parameter. We are reassured that towards the lower range of values, the density measure is rather stable. Very large values (less than half of a gridcell built up being excluded from *urban*) increase density more importantly. Our main data moment from this exercise – the ratio in (population-weighted) average urban density between 1876 and 2015 – is only minimally affected by the choice of `cutoff`.

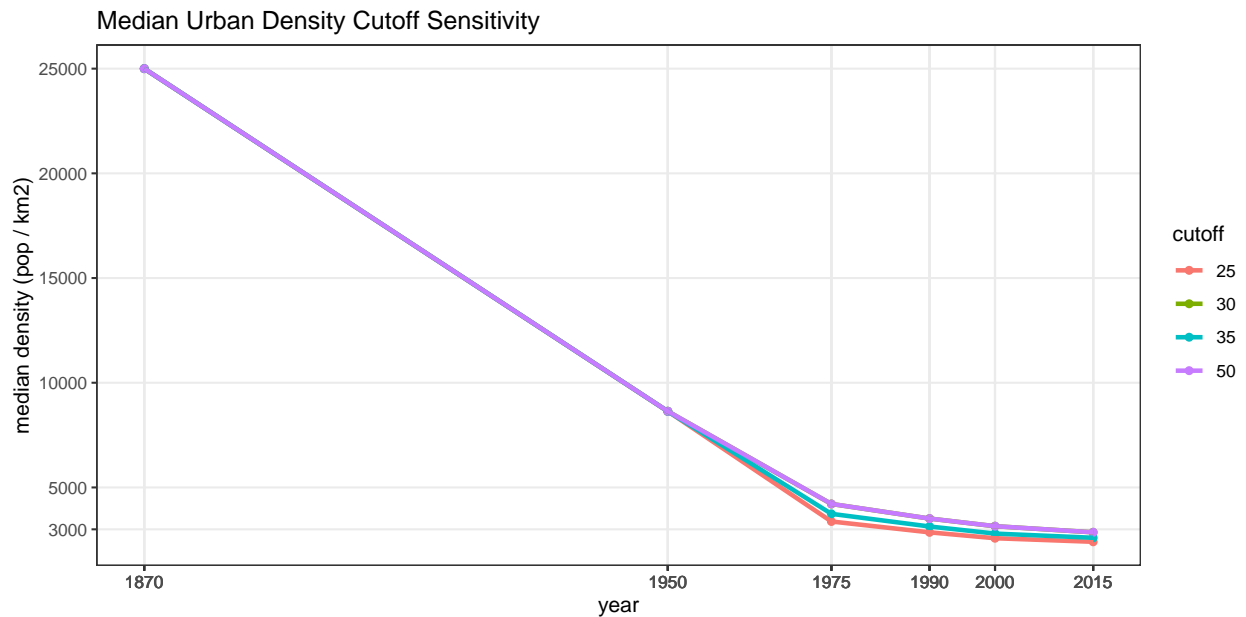


Figure 38: Median urban density for different cutoff parameter values. The parameter indicates the percentage of a grid cell (250x250 meter) that has to be built-up in order to be classified as *urban area*.

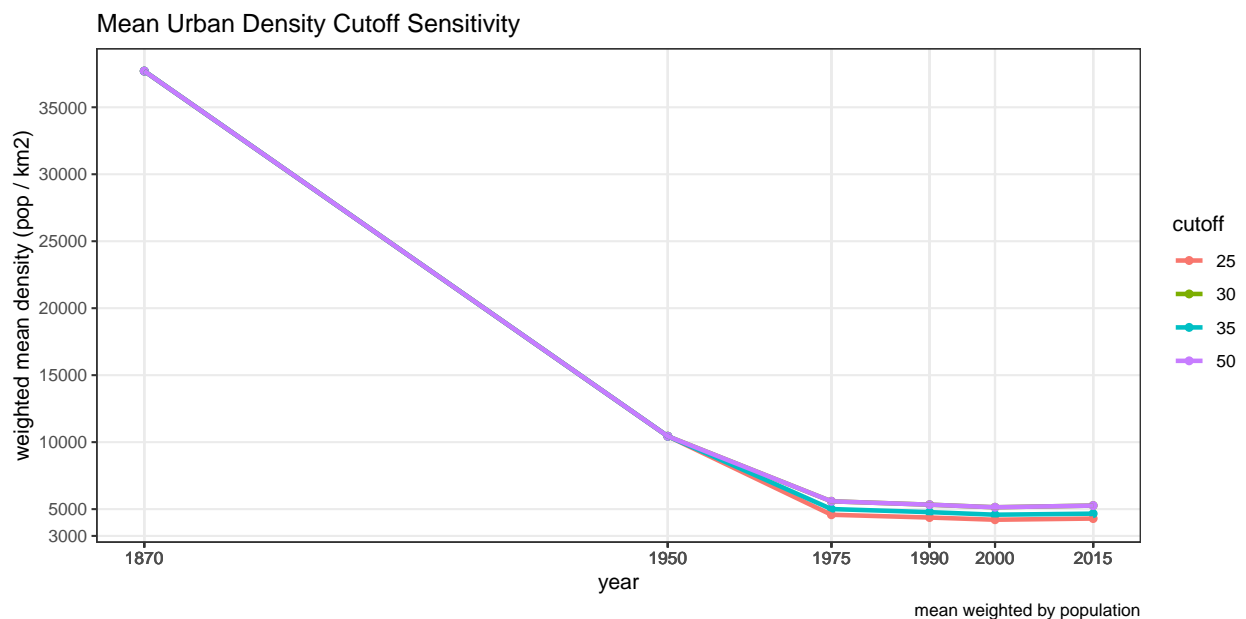


Figure 39: Weighted mean urban density for different cutoff parameter values. The parameter indicates the percentage of a grid cell (250x250 meter) that has to be built-up in order to be classified as *urban area*.

A.8 CORINE Land Cover (CLC) 2018 Data

We use CLC data to substantiate the claim made in Section 2.2 of the main text that land outside our top 100 French cities is to a large extent used for agricultural purpose nowadays. We rely on the 2018 edition of the European Land Monitoring Service called **CORINE Land Cover (CLC)** based on Sentinel-2 and Landsat satellite imagery [European Union \(n.d.\)](#). The geometric accuracy is better than 100m and the thematic accuracy is greater than 85%. We refer for all technical issues to the user manual of CLC available at <https://land.copernicus.eu/user-corner/technical-library/clc-product-user-manual>.

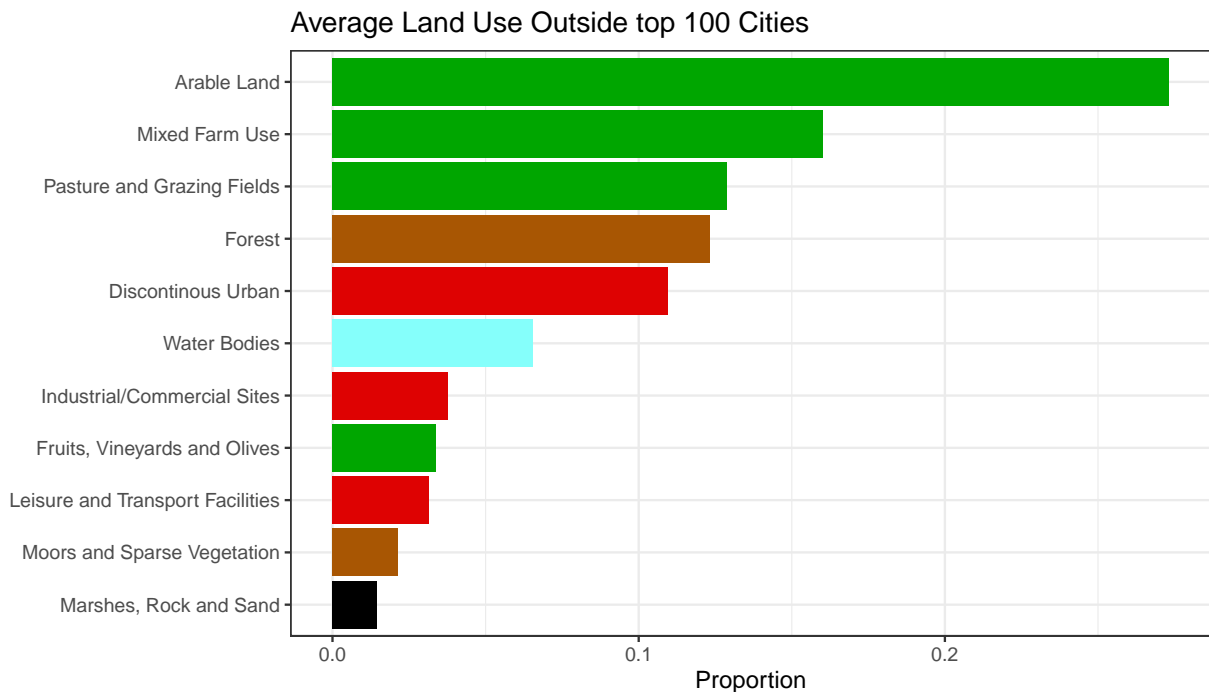


Figure 40: Average land use measure from CLC data for our sample of top 100 French cities. This plot uses our own aggregation from 45 CLC labels into 11 exhaustive classes. We group all categories corresponding to agriculture into green bars.

Our usage of the data is very similar to the GHSL above. In fact, we crop CLC to a bounding box of continental France and then cut out the respective bounding boxes of our 100 cities. Care has to be taken to convert to the same coordinate reference system in this operation. Once the box around each city is contained, we report the proportion with which each of 41 land use types occurs. We show the resulting average in Figure 40 and an example for Reims in Figure 41.

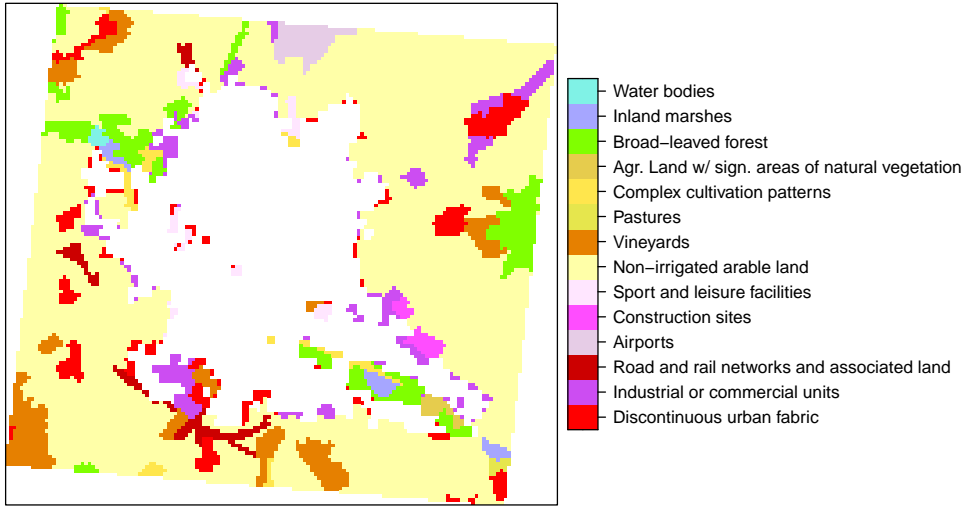


Figure 41: Land use measures from CLC data for Reims. The white area represents our definition of the Reims Urban area in the last GHLS periods (2015), hence it is our definition of *inside vs outside* of the city. For instance, the red areas labelled *discontinuous urban fabric* are not part of our definition of the city

A.9 Individual Commuting Data

We present here data from the "Enquête National du Logement (ENL)" as well as from the "Déclaration annuelle des données sociales" (DADS) in order to investigate individual commuting behaviour over space and time.

A.9.1 ENL: Enquête National du Logement

We obtain confidential access to the ENL and use it to measure commuting speed as a function of commuting distance. The ENL asks respondents questions about commuting behaviour, mode of commute, and importantly, duration of commute in minutes.

We use the waves 1984 (sample size $n = 9433$), 1988 ($n = 8910$), 2006 ($n = 12390$) and 2013 ($n = 7860$) where all required measures are observed. We subset the data to workers who work outside their home and to be the the reference person in each household. We observe workplace and residence at the commune level. We can therefore compute an approximation to commuting distance by taking the straight line distance between the central location of an individual's commune of residence and their commune of work. The central location is indicated by the IGN as *Chef Lieu* for each commune (most of the times the town hall). The variable *speed in km/h* is then implied by dividing our measure of commuting distance by each individual's commuting time (variable GTT1, reported in minutes) divided by 60. We drop all observations where reported commuting time or residence-workplace combination implies a commute of more than 100 km (or implied speeds of more than 100 km/h). We use the provided sampling weights for all computations. Figures 42 and

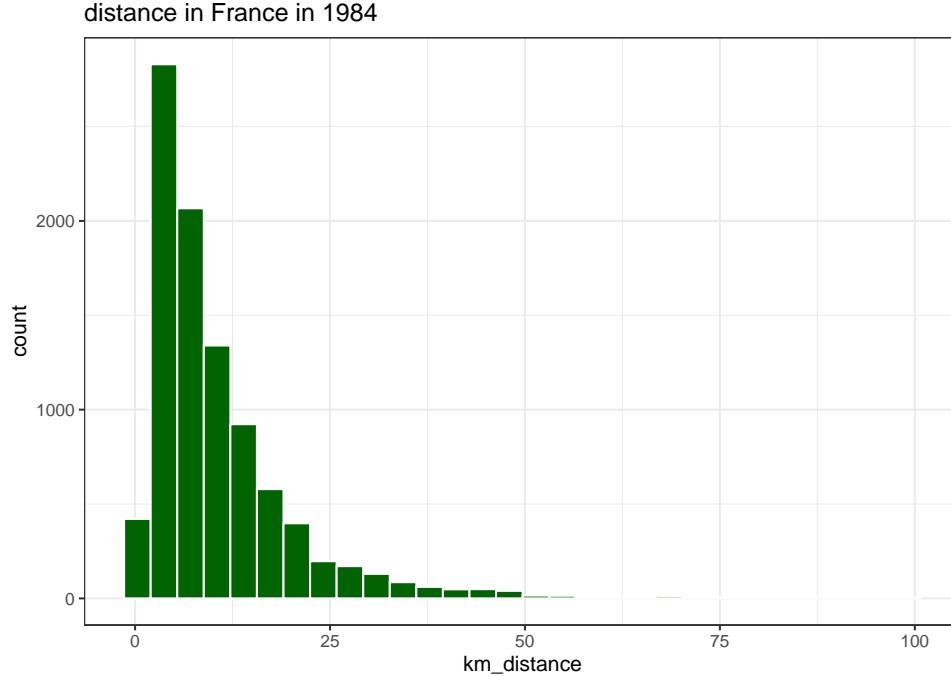


Figure 42: ENL: Distribution of Commuting Distances for a representative French Sample in 1984.

43 illustrate the distributions of our commuting distance variable.

We find that from 1984 to 2013, the average commuting distance increased by 3.2km, while the average commuting speed increased by 6km/h. Note that the increase in average speed over time is arguably the outcome of two forces: the use of faster commutes for a given commuting distance and an increasing importance of longer distance commutes for which workers use faster modes. The subsequent analysis aims at disentangling how speed changes over time for a given commuting distance and how speed varies with commuting distance at a given date.

We are interested in the cross-sectional elasticity of speed w.r.t commuting distance in a given year, controlling for as many individual characteristics as possible. This is reported in tables 4 and 5 for the years 1984 and 2013 (we omit the 1988 and 2006 waves for brevity but results are very similar across years). We can see that across specifications with different control variables and across different years of data, the elasticity of speed with respect to distance is in the range of 0.438 (regional fixed effect specification in 2013) and 0.506 (simple regression of log speed on log distance in 1984). Since our preferred estimates with controls and regional fixed effects range from 0.43 to 0.47, we use 0.45 as baseline value to calibrate externally ξ_ℓ . This yields a value of $1 - 0.45 = 0.55$ for ξ_ℓ .

We also want to know how the average commuting speed has evolved, controlling for commuting distance, between 1984 and 2013. To achieve this, we pool both cross sections from 1984 and 2013

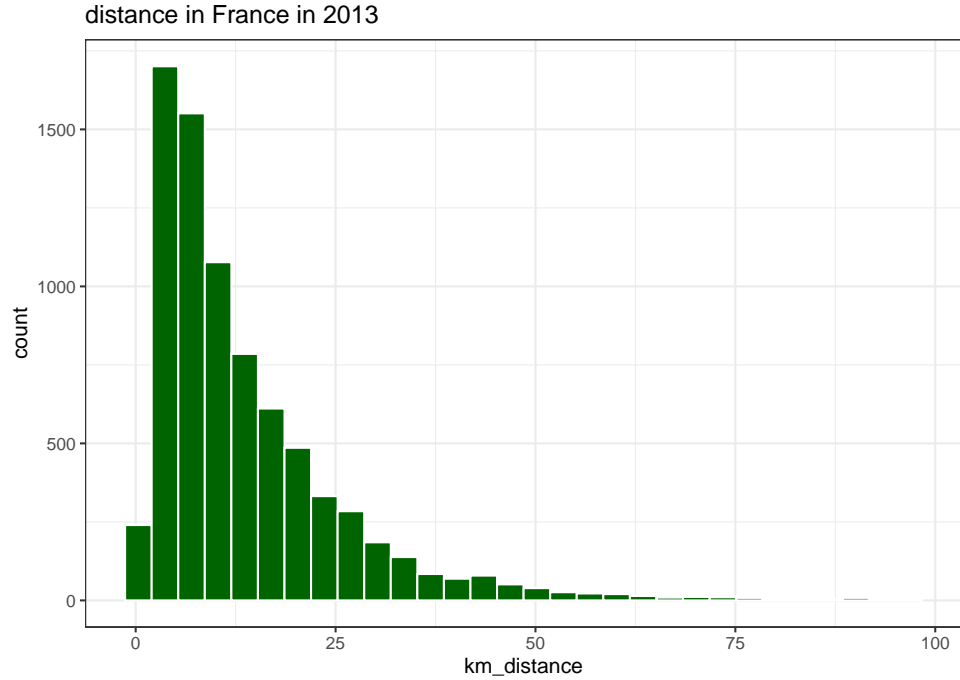


Figure 43: ENL: Distribution of Commuting Distances for a representative French Sample in 2013.

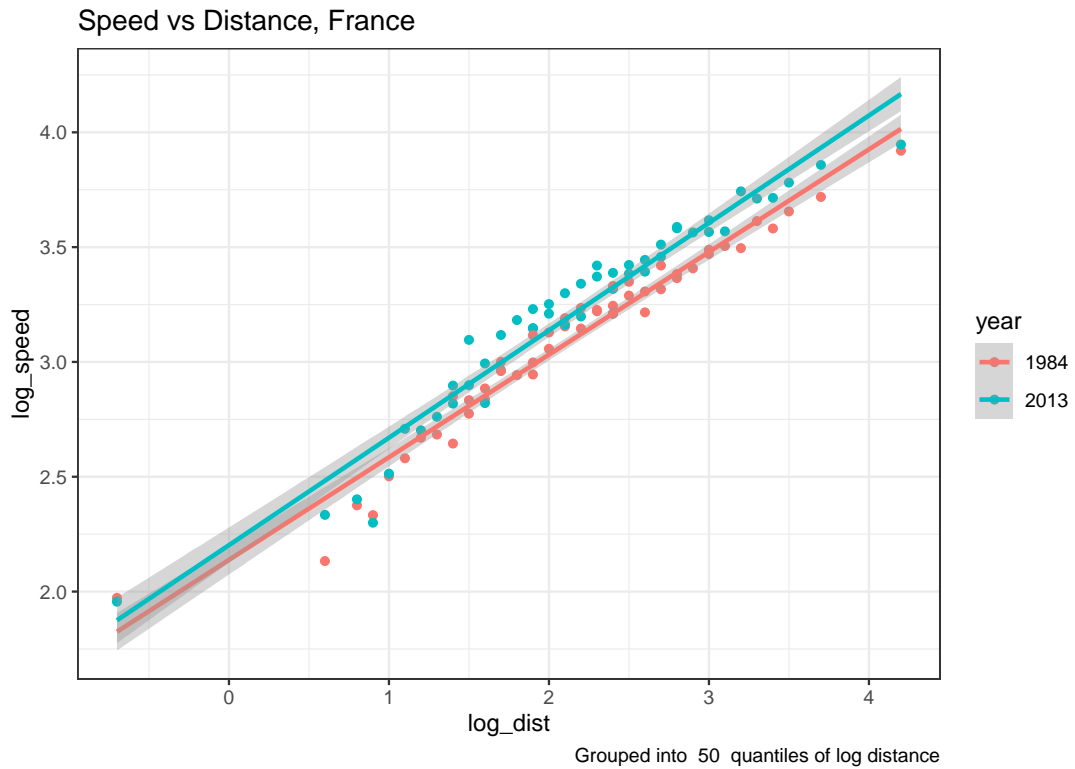


Figure 44: ENL: Commuting speed for 50 bins of commuting distance (in log).

	log(speed) in 1984				
	(1)	(2)	(3)	(4)	(5)
log(km_distance)	0.506 *** (0.007)	0.505 *** (0.007)	0.498 *** (0.007)	0.502 *** (0.007)	0.470 *** (0.006)
r.squared	0.357	0.357	0.372	0.376	0.549
nobs	9199	9199	9189	9199	9189

*** p < 0.001; ** p < 0.01; * p < 0.05.

Table 4: Cross sectional regression of Speed on Commuting Distance using ENL 1984 data. Columns specify control variables as follows: Column (1) has no additional controls; (2) adds log income, (3) adds age and education class to (2), (4) adds adds age and SES to (2), and (5) adds age, education, SES and a regional fixed effect to (2).

	log(speed) in 2013				
	(1)	(2)	(3)	(4)	(5)
log(km_distance)	0.476 *** (0.007)	0.478 *** (0.007)	0.469 *** (0.007)	0.474 *** (0.007)	0.438 *** (0.006)
r.squared	0.361	0.362	0.397	0.410	0.570
nobs	7795	7795	7773	7795	7773

*** p < 0.001; ** p < 0.01; * p < 0.05.

Table 5: Cross sectional regression of Speed on Commuting Distance using ENL 2013 data. Columns are specified as in table 4.

and run a simple regression of the form

$$\ln \text{speed}_{it} = \beta_0 + \beta_1 \ln \text{dist}_{it} + \beta_2 \text{year}_{it} + u_{it}$$

This is reported in Table 6. We group the data into 50 bins of log distance, shown in Figure 44. Then we run a simple regression on this grouped data to measure the size of intercept shift, which will be our measure of *average increase in commuting speed at given commuting distance* between 1984 and 2013. We obtain a value of 0.109 on the dummy variable indicating `year == 2013`, hence the (approximate) marginal effect of being in year 2013 is given by a 10.9% increase in speed – controlling for commuting distance. This number is used in the quantitative model to calibrate parameter ξ_w as described in the calibration Section 4.1 in the main text.

	log_speed
(Intercept)	2.116 *** (0.027)
log_dist	0.457 *** (0.011)
factor(year)2013	0.109 *** (0.019)
r.squared	0.951
nobs	98

*** p < 0.001; ** p < 0.01; * p < 0.05.

Table 6: ENL Data. Measuring average increase in commuting speed between 1984 and 2013, controlling for commuting distance. This is done on data grouped into 50 bins of commuting distance. The coefficient of ‘year==2013’ is the size of the horizontal shift in figure 44.

A.9.2 DADS: Déclaration annuelle des données sociales

The monocentric model implies that the location of residence ℓ maps one for one into commuting distance. Extension C.5 developed below (see Section 4.4 in the main text) relaxes this assumption. We will introduce in a reduced-form way the following relationship between commuting distance $d(\ell)$ and distance from the city center ℓ ,

$$d(\ell) = d_0(\phi) + d_1(\phi) \cdot \ell \tag{33}$$

where $d_0(\phi)$ and $d_1(\phi)$ are parametric functions of the city radius as detailed in extension C.5— with $d_0(\phi)$ increasing in ϕ and positive and $d_1(\phi)$ decreasing in ϕ and between 0 and 1. Data on residential and work locations are necessary to validate our reduced-form approach and discipline the calibration of $d_0(\phi)$ and $d_1(\phi)$.

We thus make use of confidential access to the DADS “Tous Salariés” (DADS-DSN) dataset for 2018 in order to investigate how commuting distance vary with residential location conditionally on city size in a large sample of the population. The DADS-DSN dataset contains all salaried workers in France, both private and public sector.

We start by reading the full dataset with 62 million records. We drop records which are in overseas territory, or which have as a residence or workplace identifier the code 75056.⁶³ This reduces the sample to 60 million records. From this, we extract a 50% random sample. Next we obtain all unique pairs of residence and workplace communes (variables COMR and COMT) and compute straight-line distance for each pair. Then we add the distance of each commune to the center of their urban area. The urban area classification is officially given by INSEE and we use the AU2010 (Aire Urbaine 2010) classification. We end up with 18 million observations.

⁶³this stands for the entire commune of Paris and is the default value if Parisian Arrondissement is not available. This concerns only a small number of Parisian observations.

We aim to investigate how commuting distance varies with the distance from the center across different city sizes. We restrict our sample to individuals who do indeed conform to the INSEE definition of *aire urbaine* and whose workplace lies within their urban area, leaving us with 15 million observations. We also drop observations with commutes longer than 100 km, which concerns roughly 80000 workers. We have 15,317,995 observations left. Using the commuting distance (`distance_commute`) and the residential distance from the city center (`distance_center`) for each individual, we perform the following regression,

$$\text{distance_commute}_i = \gamma_{0,C(i)} + \gamma_{1,C(i)} \cdot \text{distance_center}_i + u_i \quad (34)$$

where i indexes an individual in DADS, $C(i)$ is the city (urban area) to which i belongs, and u_i is a mean-independent error term. $\gamma_{0,C(i)}$ and $\gamma_{1,C(i)}$ are city-specific coefficients (758 urban areas). We also perform the same regression by grouping cities into brackets of different sizes (with population above 3 millions, between 1 and 3 millions, between 50 000 and 1 million, ...).

Figure 45 plots the distribution of the intercept coefficient $\gamma_{0,C(i)}$ across all 758 urban areas. The mean across urban areas is 0.4 km and the mean weighted by the population of urban areas is 2.6 kms, significantly different from zero. Figure 46 plots the distribution of the slope coefficient $\gamma_{1,C(i)}$ across all 758 urban areas. The distribution exhibits a mode around 0.7, while the population weighted mean is close to 0.5. Overall, residential distance from the city center is a very strong and robust predictor of commuting distance, even though commuting distance move less than one for one with residential distance from the center.

We also inspect the value of the estimates as a function of the size of the city. The intercept $\gamma_{0,C(i)}$ increases with city size, from about 0.2 km for the smallest urban areas to more than 4 kms for Paris. The slope coefficient $\gamma_{1,C(i)}$ decreases with city size—ranging from around 0.4 for Paris to more than 0.7 for small urban areas.

These results validate our reduced-form parametrization (Eq. 33), where commuting distance $d(\ell)$ increases less than proportionately with residential location ℓ , and less so for larger cities (larger radius ϕ). We use these findings in Section C.5 to parametrize $d_0(\phi)$ and $d_1(\phi)$.

Distribution of Intercepts over 758 Urban Areas

mean = 0.361, wtd. mean = 2.611, median = 0.056

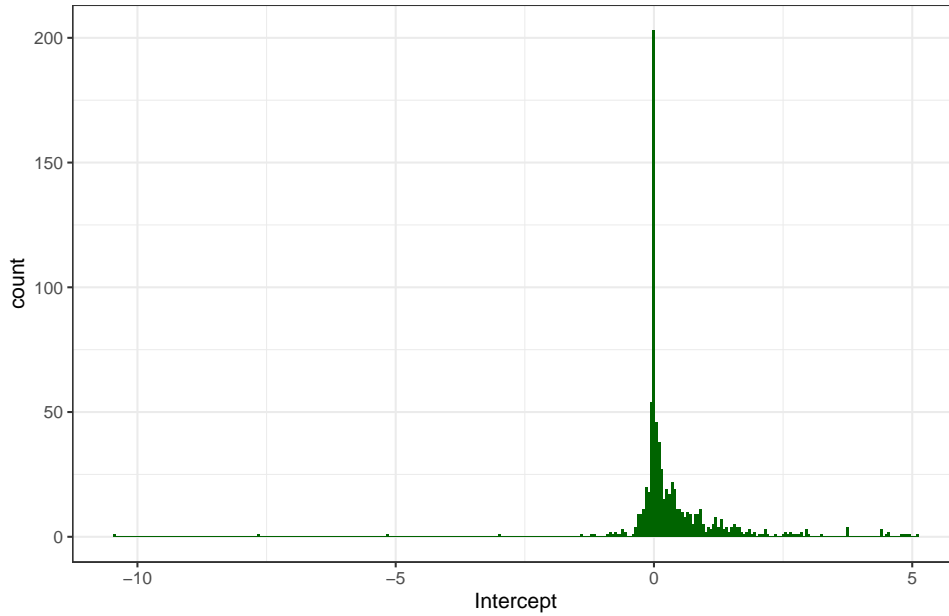


Figure 45: Distribution of DADS intercept estimates

Notes: City-specific intercepts $\gamma_{0,C(i)}$. City is defined as *Aire Urbaine (AU)* by INSEE. Results from individual level regression of commuting distance on distance from city center using DADS.

Distribution of Slopes over 758 Urban Areas

mean = 0.711, wtd. mean = 0.507, median = 0.708

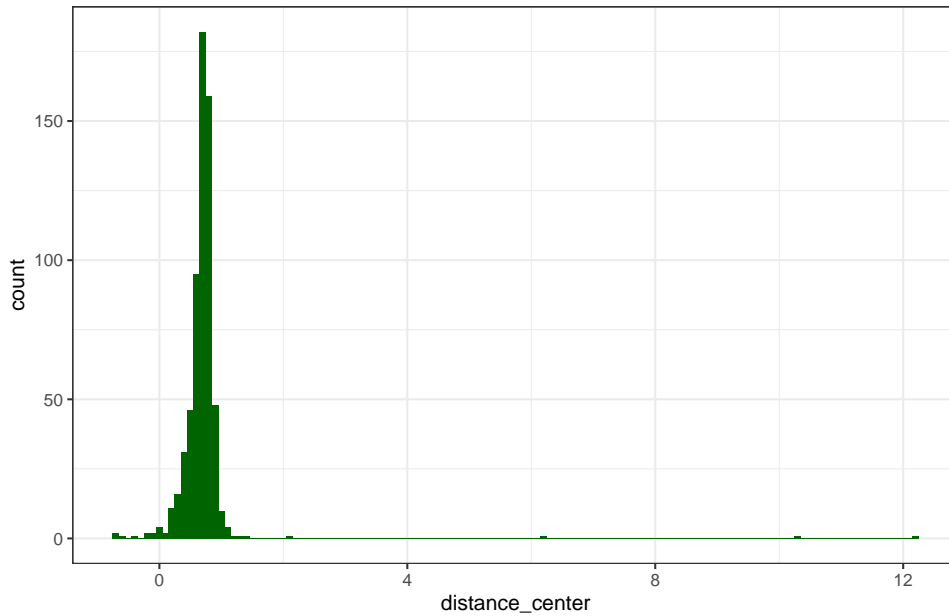


Figure 46: Distribution of DADS slope estimates

Notes: City-specific slopes $\gamma_{1,C(i)}$. City is defined as *Aire Urbaine (AU)* by INSEE. Results from individual level regression of commuting distance on distance from city center using DADS.

A.9.3 Historical commuting speed in Paris

We aim at providing estimates of the evolution of the average commuting speed for working trips in the Parisian urban area since 1840. These estimates are used to compare with the model's predictions (Figure 14a)). To do so, we use survey data (individual commuting data) in the Parisian urban area for the post-WW2 period. These data give the main mode used for working trips and well as the corresponding speed. Pre-WW2 (1840-1940), such individual surveys are not available. However, historical data on traffic by public transport modes and on registered private vehicles helps us to build estimates of the distribution of mode use over the whole period. Given estimates of the speed of each transportation mode, one can back out historical estimates of the average commuting speed.

Two main caveats are in order. First, the strategy developed only provide *estimates* since 1840 of the average commuting speed. These estimates depend on assumptions to convert historical data on traffic and registered vehicles into their modal use for work commutes and on assumptions regarding the speeds of the various modes. While some measurement error is unavoidable, our estimates provide a reasonable order of magnitude of the historical evolution of commuting speed in Paris. Second, due to historical data availability, we must focus on the Parisian urban area rather than France as a whole. Paris is arguably special. In the recent period, public transport is more widely used in Paris.⁶⁴ Paris might also be more congested than other French cities. Overall, one needs to be cautious with our estimates. However, it is clearly reassuring that estimates for Paris and model's predictions give very similar order of magnitude since the former were not targeted in the calibration.

Commuting data post-WW2. The first survey on commuting for work in the Parisian urban area was conducted in 1959 (on a representative sample of more than 20,000 individuals). While the original data are not available, secondary sources provide a detailed summary of the results (see Bertrand and Hallaire (1962)). For our purpose, this gives us the distribution of mode use in Parisian area in 1959. The majority of Parisian workers (50.2%) were using public transport (ventilated between metro, autobus and train); 21.5% were using a private mean of transportation (8.5% a private car, the rest for the most part a bicycle or a motorbike); the remaining 28.3% are walking.⁶⁵ The 1959 data do not provide the speed of each mode and we impute the speed measured in the later survey (1976) to compute the average commuting speed in the Parisian area in 1959. We use the 'Enquête Global Transport (EGT)' for the years 1976, 1983, 1991, 2001 and 2010. The EGT provides individual commuting data for a representative sample of the Parisian urban area: distance of commuting trips, time, speed and modal use. We restrict our attention to trips to the work location to extract the distribution of mode use and their respective speeds to compute the

⁶⁴Note that the effect on commuting speed is however ambiguous. Cars are faster than public transport for longer distances but the large availability of public transports in Paris makes commuting easier for shorter distances.

⁶⁵Note that less than 10% of surveyed individuals use a private car—reflecting the low level of car equipment in France in the 1950s. This number is up to 20.2% in 1967, 36.8% in 1976, 42.6% in 1983 and close to 50% since 1990.

average commuting speed.⁶⁶ Note that the speed measured from these surveys is based on the distance as the crow flies and is measured using the time of the whole journey (including time to walk to the bus stop or metro/train station, time to park, ...). The implied speeds (around 9 km/h for the metro, 15 km/h for the train, 20 km/h for cars or motorbikes, ...) are thus significantly below the speed of the different modes when operating at full speed (see Figure 48).

Commuting data pre-WW2. Using traffic data for public transportation and numbers of registered private vehicles, we propose a strategy to estimate the distribution of workers across the different modes of transportation since 1840.

Public transportation. We investigate various secondary sources to measure the traffic of the different public transport modes at different dates (1835, 1856, 1876, 1890, 1910 and 1930). For the nineteenth century, we use data from [Martin \(1894\)](#) which provides very detailed statistics on transportation in the Parisian area across the various modes. Data for 1910 and 1930 are from [Bertillon \(1910\)](#), [Brunet \(1986\)](#), [Merlin \(1997\)](#), as well as the *Annuaire statistique de la Ville de Paris* in 1929, 1930 et 1931. Traffic is expressed in number of individual trips per year. Data for the Parisian urban area are available across the different modes: omnibus, tramway, metro, autobus, train and boat. The modes used depend on the time-period: only the horse-drawn omnibus initially, then appears the horse-drawn tramway in the late 1850s with 22 lines built between 1853 and 1873, followed by the electric tramway starting 1881 and motorized omnibus in 1905.⁶⁷ The network of the tramway is fully electric by the end of the nineteenth century and reaches its peak in the 1920s (122 lines) before slowly disappearing due to the development of the metro—being fully replaced later in the 1930s by the autobus. The first metro line opens in 1900—10 lines being built before WW1. Four more lines open in between the wars together with extensions of the existing ones. Suburban trains started post-1840 (with the exception of the line Paris-Saint Germain en Laye inaugurated in 1837) with major developments towards the late 1850s-early 1860s. Before WW2, it remains a mean of transportation much less used than the others. Lastly, boats were provided to the public to reach some specific destinations along the Seine before the offer was restricted to tourists post-WW2. This mean of transportation remained very anecdotal over the whole period.

We also collected similar data on traffic for public transportation post-WW2 at various dates (1955, 1975, 1990, 2000, 2010) using data from [Bastié \(1958\)](#), the *Annuaire statistique de la Ville de Paris* (1955), [Merlin \(1997\)](#), the Annual statistics of the Paris public transport entity RATP for 1975 and 1990 and data of the Observatoire de la mobilité en Ile-de-France (OMNIL) for 2000 and 2010 (annual traffic for all modes 2000-2020 from OMNIL). These more recent data help us to convert the traffic into a proportion of workers using the various modes to commute to work. To do so, we first compute, for a given mode m , the number $N_{m,t}$ of two-way trips per worker per working day in the Parisian urban area using employment at the various dates t from Census data.⁶⁸ The main issue

⁶⁶The sample raw average commuting speed at each date gives very similar estimates.

⁶⁷The horse-drawn omnibus disappears in 1913.

⁶⁸We use all available censuses starting in 1835, initially considering the *Département de la Seine* as the Paris Urban Area; after 1975 we use INSEE's official definition of the Paris Urban Area.

arise since many of these measured trips are not made to commute to work but for other reasons (leisure, shopping, ...). Assuming that a fraction $x_{m,t} \in (0, 1)$ of these trips are work commutes. By definition, the proportion of workers using mode m to commute to work, $p_{m,t}$, is the number of (two-way) working trips per worker (per working day) using mode m ,

$$p_{m,t} = x_{m,t} \cdot N_{m,t}.$$

Thus, with some estimates of $x_{m,t}$, one can recover estimates of $p_{m,t}$ using traffic data. Note also that for the years post-WW2, $p_{m,t}$ and $N_{m,t}$ are both observed allowing us to back out $x_{m,t}$. However, some modes were abandoned post-WW2 (horse-drawn modes, tramways). Moreover, workers use sometimes more than one mode of public transportation (train + metro, ...). To avoid these issues, we assume for simplicity that $x_{m,t}$ is the same across modes. Under this assumption, the proportion p_t of workers using public transportation at date t is,

$$p_t = x_t \cdot \sum_m N_{m,t},$$

and $x_t = \frac{p_t}{\sum_m N_{m,t}}$ can be easily recover from the data for the years post-WW2—using measures of p_t in individual surveys and values for $(\sum_m N_{m,t})$ from traffic data. It is close to 1/3, relatively stable across years. Using EGT data which provides the motive for registered trips, 31% of non-walking trips in 1976 were between home and work. Such a value implies about 50% of people using public transport in 1955, in line with the corresponding survey data. Thus, prior to WW2, we set x to $\hat{x} = 31\%$.⁶⁹ This implies for each mode m at date $t = \{1835, 1856, 1876, 1890, 1910, 1930\}$,

$$p_{m,t} = \hat{x} \cdot N_{m,t}.$$

As summarized in Figure 47, the estimated fraction of workers using public transportation, $p_t = \sum_m p_{m,t}$, starts from a very low value of 4.5% in 1835 and remains fairly low throughout the nineteenth century before picking up in the twentieth century. More than 50% of workers using public transportation by 1930. This proportion starts falling post WW2, largely due to the wider usage of automobiles. It is still around 40% in the recent years.

Private transportation; Private transportation includes essentially private cars, bikes and motor-bikes.⁷⁰ To evaluate the use of private cars pre-WW2, we use data on the number of registered vehicles, whether horse-drawn or motorized for years 1890, 1910 and 1930.⁷¹ We also collected data

⁶⁹One could argue that commuting trips for leisure motives were perhaps less common in the 19th century, pushing towards setting a higher value for x . However, anecdotal evidence also emphasizes that public transportation, train in particular, were in the early years very often taken by the richer population for leisure activities.

⁷⁰Pre-WW2, it also includes rented horse-drawn coaches with a driver. Post-WW2, it also includes other private means of transportation (taxis, private means provided by the employer, and recently scooters, ...). These remaining private means are either allocated to other categories according to their speed or neglected (employer buses considered as autobus, taxis as private cars, scooters as bikes...). Results are largely unaffected when omitting these categories.

⁷¹In 1899, 288 private automobiles were registered in Paris. We set the number of automobiles in 1890 to zero. In 1930, horse-drawn vehicles had almost disappeared in Paris and their number is also set to zero.

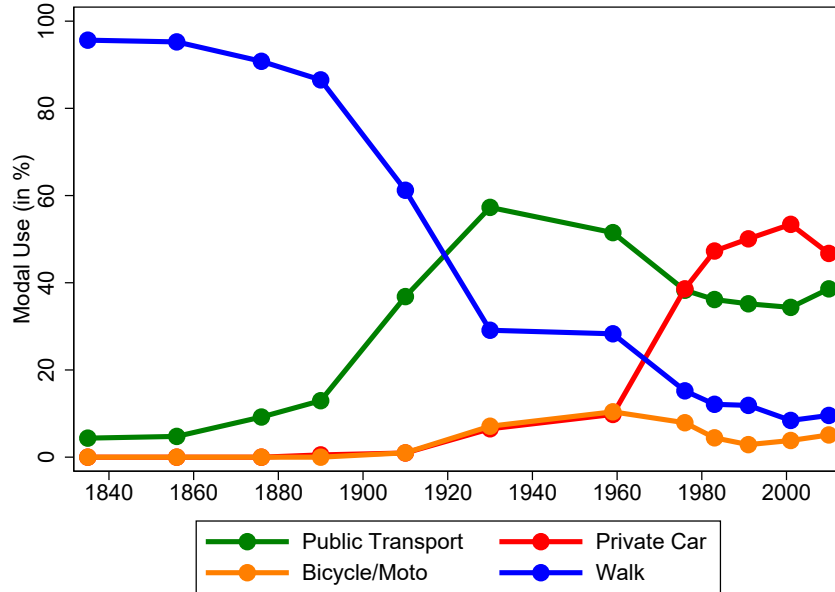


Figure 47: Transportation mode use in the Parisian urban area.

Notes: Fraction of workers using the respective transportation mode over the period 1835-2010, in %. Sources: Data from secondary sources for the dates prior to WW2 (mostly traffic of the different public modes and registered private vehicles converted into modal use). Individual survey data on the main mode used for work commutes post-WW2 (Bertrand and Hallaire (1962) for 1959 and EGT data for 1976, 1983, 1991, 2001 and 2010).

for the number automobiles post-WW2 using Merlin (1997) and the annual statistics of the RATP for the years 2000 and 2010. Using these data and employment data, we compute the number of cars per worker (horse-drawn and motorized) since 1890. While the number of horse-drawn private cars per worker remained very small (below 1 for 200 before WW2), the number of automobiles per worker increases steadily until 1990 before reaching a plateau—about 1/100 in 1910, 11/100 in 1930, 22/100 in 1955, 61/100 in 1975 and 75/100 in 1990. However, many of these cars are not used on a daily basis for work commutes. To measure the proportion of workers using their car to go to work, we use survey data post-WW2 in the same vein as our strategy for public transportation. The ratio between the proportion of workers commuting to work by private cars and the number of cars per worker measures the fraction of cars used for work commutes. Post-WW2, this number is about 45% in 1959 and then hovers between 60% and 67%, with a mean across all observations of 60%. Assuming a ratio pre-WW2 of 60% allows us to compute the fraction of workers commuting to work by private cars, less than 1% pre-WW1 and about 6% in 1930. Figure 47 summarizes the evolution of the proportion of workers using their private cars for work commutes.

The use of bikes and motorbikes was almost inexistent prior to 1890. The number of bikes in Paris is estimated to about 60 000 in 1891, 250 000 in 1901 and 285 000 in 1912 (Orselli (2008)). Unfortunately, such data are not available at a later dates and not readily available for motorbikes for the Parisian area.⁷² Given the importance of bicycles for leisure and the lack of relevant data post-

⁷²Orselli (2008) provides data on the number of registered motorbikes for France over 1899-1914. This number is about 1/100 of the number of bikes—small enough to be neglected until WW1.

WW1, it is rather difficult to measure accurately the use of these means of transportation for work commutes. Prior to 1890, it seems reasonable to assume that these modes were not used. Given the low number of motorbikes registered in France as a whole pre-WW1 (about 27 000), we also assume that this means of transportation can be neglected in 1910. Thus, one needs to provide estimates in 1910 and 1930 for bikes and in 1930 for motorbikes. Based on a retrospective surveys provided by the ENTD2008 (Enquête nationale transports et déplacements) where people were asked their main mode of transport over their lifetime, one can assess the extent of bicycle/motorbike use relative to other means for 1930. Papon et al. (2010) provides such estimates by decades—reweighting observations to control for sample attrition due to survival: in 1930-1940, 9.9% of the population were using the bicycle as main mode of transportation in France, versus 2.3% for the 1920-1930 decade. We take the average between these values, 6.1%.⁷³ For the use of bikes in 1910, it is arguably very low and we set it to 1%, below their estimated value for the 1920s. For motorbikes, there are no survivors in the retrospective survey declaring using this mode for the decade 1930-1940, versus 4.8% for the following decade. While one cannot come up with a definitive estimate, motorbikes were most likely used by at most 2-3% of the workers. We set the share of workers using a motorcycle in 1930 to 1%.⁷⁴ Certainly, one might want to be cautious with these estimates due to the small sample size of survivors. Fortunately, given that motorcycles were barely used and bikes are not much faster than walking, the quantitative implications for the estimated average speed cannot be large. Figure 47 summarizes the estimates for the share of workers using bikes/motorbikes over the whole period.

Walking. The share of workers walking to their work location is estimated as a residual—made of workers using neither a public transportation nor a private one. Figure 47 summarizes the estimates for the share of workers walking to work over the whole period. In the early years, before 1840, Paris is a walkable city, public and private means of transportation are barely starting, and about 95% of the workers commute by feet. This share has been falling since reaching about 75% in the early twentieth century, 30% around WW2 and about 10% nowadays.

Average commuting speed. Average commuting speed is estimated as the weighted average of the speed of the various modes—weighted by their modal use. For modes of transportation still used in 1976 (first date for which the speed of the various modes can be measured), we set their speed at the earlier dates to the one observed in 1976. One caveat is that we ignore that current modes of transportation (public or private) have been faster through time. For the modes of transportation that disappeared (or have been replaced by more modern modes), we estimate speed based on anecdotal evidence related mostly in Martin (1894). Horse-drawn omnibus were not much faster than walking, about 7 to 8 kms per hour. When considering the time walking and waiting when using this mode, we set the horse-drawn omnibus speed to 6 kms per hour—in between walking

⁷³For the following decades, 13% of people using bikes in 1940-1950, 13% in 1950-1960, 9.7% in 1960-1970—broadly in line with survey data for Paris available at the latest periods.

⁷⁴Traffic data for France in 1934 (Orselli (2008)) shows that the share of traffic (per km per year) due to motorcycles is about 1/5 (resp. 1/10) of the one of bicycles (resp. automobiles)—broadly in line with the chosen value.

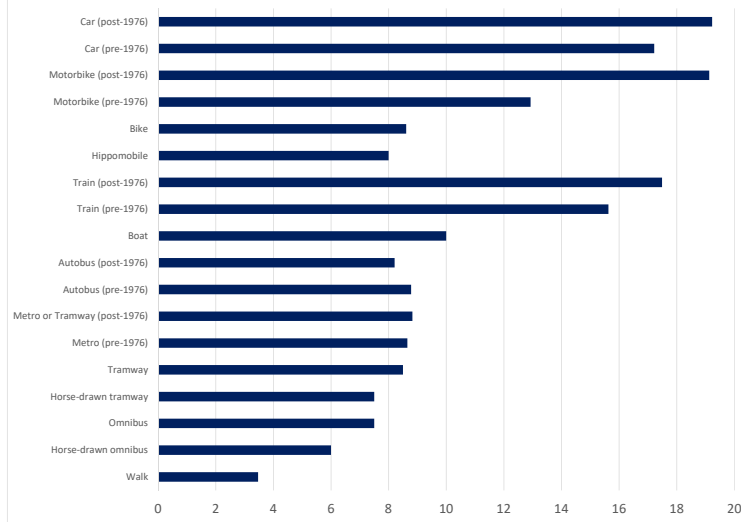


Figure 48: Speed across transportation modes.

Notes: Average speed of the different commuting modes. Measured using survey data in the Parisian urban area (EGT data) post-1976 (average over the 1983, 1991, 2001 and 2010 surveys). Values pre-1976 are based on the 1976-value from EGT data for modes still operating in 1976 and based on historical description for other modes.

speed and later measured metro speed (about 8.5 kms per hour). This is the value taken until 1890. Post-1890, we set the speed of omnibus to 7.5 kms per hour as a significant share of those were motorized. For tramways, we set the speed to 7.5 kms per hour when horse-drawn in 1876 and 8.5 kms per hour when fully electric in 1910. We use the average between these two values for 1890 since both were used. Boats were on average faster than ground transportation modes. We set their speed to 10 kms per hour but results are barely affected by this value within a reasonable range given that less than 1% of the Parisian population were using this mode when available. Lastly, we set the speed of private horse-drawn cars to 8 kms per hour. Like for boats, results are barely sensitive to this value as this mode of transport for work commute was the privilege of few rich Parisians in the late nineteenth century. Figure 48 summarizes the estimated speed of the different modes, by mode at different dates. Figure 49 shows the evolution over the whole period across broader mode categories—the speed of each category (public and private) is weighted by the modal use of the different modes within the category.

B Quantitative Model, Numerical Solution and Estimation

B.1 Extensions to the baseline theory

The quantitative model expands the baseline theory of Section 3 in the main text by considering a more general production function for the rural good, a more general specification for the commuting costs, by allowing for location-specific housing supply conditions and by considering a circular city on a surface. We also introduce an intertemporal utility function to pin down the path for the real interest rate. Notice that each extension nests the previous one, such that the extension in

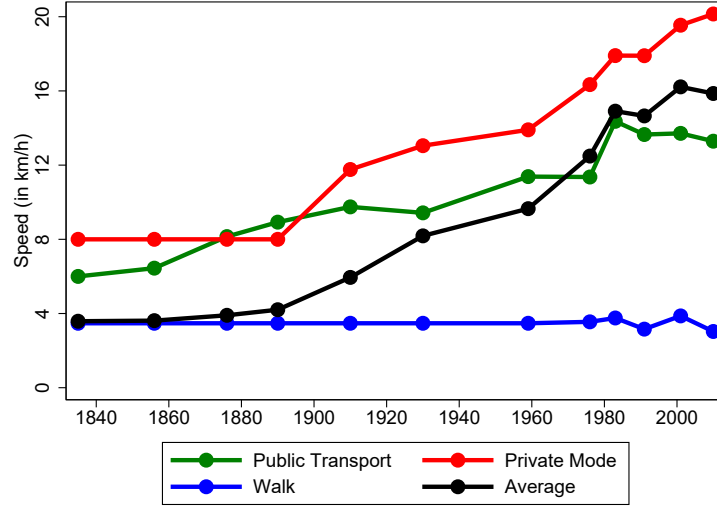


Figure 49: Evolution of average speed across mode categories.

Notes: Public includes all public transportation modes. The speed for public transportation is a weighted average of the different public modes (weighted by their modal use). Private includes private car (horse-drawn and motorized), bikes and motorbikes. The speed for private transportation is a weighted average of the different private modes (weighted by their modal use). The average speed sums the speed of the different commuting modes (walk, public, private) weighted by the computed modal use at the different dates. Average speed of the different commuting modes is measured using survey data in the Parisian urban area (EGT data) post-1976 (average over the 1983, 1991, 2001 and 2010 surveys). Values pre-1976 are based on the 1976-value from EGT data for modes still operating in 1976 and based on historical description for other modes.

Section B.1.4 contains all previous modifications and hence represents our full quantitative model for the single city case. This model will then be used for parameter estimation and main simulation results in Section B.2.5. Sensitivity analysis for some parameters values and extensions of the model around its baseline version are also developed in greater details.

The final extension in this section (see Section B.2) will introduce a multiple city version, for which we will use the estimated parameters from the single city model.

B.1.1 CES production in the rural sector

We perform sensitivity analysis with respect to the elasticity of substitution between land and labor in the rural sector. We hence upgrade the model from the main text with a CES technology where the production of the rural good uses labor and land according to the following constant returns to scale technology

$$Y_r = \theta_r \left(\alpha (L_r)^{\frac{\sigma-1}{\sigma}} + (1-\alpha) (S_r)^{\frac{\sigma-1}{\sigma}} \right)^{\frac{\sigma}{\sigma-1}},$$

where L_r denotes the number of workers working in the rural (agricultural) sector, S_r the amount of land used for production and θ_r a Hicks-neutral productivity parameter. $0 < \alpha < 1$ is the intensity of labor use in production. $\sigma \geq 0$ is the elasticity of substitution between labor and land, $\sigma = 1$ corresponding to the baseline version. Rural workers and land are paid their marginal productivities

such that main text equations (2) and (3) become

$$w_r = \alpha p \theta_r \left(\alpha + (1 - \alpha) \left(\frac{S_r}{L_r} \right)^{\frac{\sigma-1}{\sigma}} \right)^{\frac{1}{\sigma-1}} \quad (35)$$

$$\rho_r = (1 - \alpha) p \theta_r \left(\alpha \left(\frac{L_r}{S_r} \right)^{\frac{\sigma-1}{\sigma}} + (1 - \alpha) \right)^{\frac{1}{\sigma-1}} \quad (36)$$

where w_r is the rural wage and ρ_r the rental price of land anywhere in the rural sector and p the relative price of the rural good in terms of the numeraire urban good. Note that it is useful to express the price of land relative to wages,

$$\rho_r = \left(\frac{1 - \alpha}{\alpha} \right) w_r \left(\frac{L_r}{S_r} \right)^{\frac{1}{\sigma}}. \quad (37)$$

Note that due to the CES technology, the rental price of land increase with (rural) wages with a unitary elasticity and with population working in the rural sector L_r with an elasticity $1/\sigma$ —stronger complementarities between land and labor implying a larger fall of land prices if workers are reallocated to urban production.

B.1.2 Commuting Costs

We adopt a more general specification for the commuting costs f . The cost $f = f(\ell, m, w_u)$ depends on the transportation mode/speed, the location ℓ and labor costs w_u . Faster and longer commutes are more expensive and $f(\ell, m, w_u)$ is increasing in m and ℓ , with $\frac{\partial^2 f}{\partial^2 \ell} \leq 0$. The latter technical assumption makes sure that the importance of the cost f (relative to the opportunity cost of time) decreases as the commuting distance increases. The cost f also increases with the labor costs, w_u , with $\frac{\partial^2 f}{\partial^2 w_u} \leq 0$. This gives the following expression for the commuting costs, similar to Eq. 5,

$$\tau(\ell) = f(\ell, m, w_u) + 2\zeta w_u \cdot \left(\frac{\ell}{m} \right). \quad (38)$$

For tractability, we will use the following functional form for f ,

$$f(\ell, m, w_u) = \frac{c_\tau}{\eta_m} \cdot m^{\eta_m} \cdot \ell^{\eta_\ell} \cdot w_u^{\eta_w}, \quad (39)$$

with $\eta_m > 0$, $0 \leq \eta_\ell < 1$, $0 \leq \eta_w < 1$ and c_τ a cost parameter measuring the efficiency of the commuting technology.

An individual in location ℓ chooses the mode of transportation corresponding to speed m in order to minimize the commuting costs $\tau(\ell)$. This equalizes the marginal cost of a higher speed m to its

marginal benefits in terms foregone wage,

$$\frac{\partial f}{\partial m} = 2\zeta \cdot w_u \left(\frac{\ell}{m^2} \right).$$

Using Eq. 39, the optimal chosen mode/speed satisfies

$$m = \left(\frac{2\zeta}{c_\tau} \right)^{\frac{1}{1+\eta_m}} \cdot w_u^{1-\xi_w} \cdot \ell^{1-\xi_\ell}, \quad (40)$$

where $\xi_w = \frac{\eta_m + \eta_w}{1 + \eta_m} \in (0, 1]$ and $\xi_\ell = \frac{\eta_m + \eta_\ell}{1 + \eta_m} \in (0, 1]$. Using Eqs. 38-40, we get that equilibrium commuting costs satisfy,

$$\tau(\ell) = a \cdot w_u^{\xi_w} \cdot \ell^{\xi_\ell}, \quad (41)$$

where $a = \left(\frac{1 + \eta_m}{\eta_m} \right) c_\tau^{\frac{1}{1+\eta_m}} (2\zeta)^{\frac{\eta_m}{1+\eta_m}} > 0$. Commuting costs are falling with improvements in the commuting technology (a lower a). They are increasing with the wage rate (the opportunity cost of time) and the distance of commuting trips with constant elasticities. Expression (41) is the resulting commuting cost function which appears in the model solution. It is also important to note that the parameters ξ_w (resp. ξ_ℓ) directly maps into elasticities of commuting speed to income (resp. commuting distance) through Equation 40. We use this link to directly parametrize both ξ_w and ξ_ℓ .

B.1.3 Location-specific housing supply conditions

As shown in Baum-Snow and Han (2019), the elasticity of housing supply to prices is lower closer to the CBD than at the urban fringe. We allow in this extension for location-specific housing supply conditions. To do so, we assume that in each location ℓ , land developers supply housing space $H(\ell)$ per unit of land with a convex cost

$$\frac{H(\ell)^{1+1/\epsilon(\ell)}}{1 + 1/\epsilon(\ell)}$$

paid in units of the numeraire, where $1/\epsilon(\ell)$ can depend on the location. This is meant to capture that it might be more costly for developers to build closer to the city center than in the suburbs or the rural part of the economy. Profits per unit of land of the developers are

$$\pi(\ell) = q(\ell)H(\ell) - \frac{H(\ell)^{1+1/\epsilon(\ell)}}{1 + 1/\epsilon(\ell)} - \rho(\ell),$$

where $\rho(\ell)$ is the rental price of a unit of land in location ℓ . Similarly to the housing price $q(\ell)$ above, for locations beyond the fringe ϕ , the land rent is constant, hence $\rho_r = \rho(\ell \geq \phi)$.

Maximizing profits gives the following supply of housing $H(\ell)$ in a given location ℓ ,

$$H(\ell) = q(\ell)^{\epsilon(\ell)}, \quad (42)$$

where the parameter $\epsilon(\ell)$ is the price elasticity of housing supply in location ℓ . More convex costs to build intensively on a given plot of land reduces the supply response of housing to prices. In the rural area, the housing supply elasticity is assumed constant, $\epsilon_r = \epsilon(\ell \geq \phi)$.

Lastly, free entry imply zero profits of land developers. This pins down land prices in a given location,

$$\rho(\ell) = \frac{q(\ell)H(\ell)}{1 + \epsilon(\ell)} = \frac{q(\ell)^{1+\epsilon(\ell)}}{1 + \epsilon(\ell)}, \quad (43)$$

Arbitrage across land usage imply that the latter land price must be in equilibrium above the marginal productivity of land for production of the rural good (Equation (36)), where the condition holds with equality in the rural part of the economy, for $\ell \geq \phi$,

$$\rho_r = \frac{(q_r)^{1+\epsilon_r}}{1 + \epsilon_r} = (1 - \alpha)p\theta_r \left(\alpha \left(\frac{L_r}{S_r} \right)^{\frac{\sigma-1}{\sigma}} + (1 - \alpha) \right)^{\frac{1}{\sigma-1}}. \quad (44)$$

This last equation shows that a fall in the relative price of rural goods and/or a reallocation of workers away from the rural sector lowers the price of urban land at the fringe of cities.

Consider first locations within the city, $\ell \leq \phi$. Market clearing for housing in each location implies $H(\ell) = D(\ell)h(\ell)$, where $D(\ell)$ denotes the density (number of urban workers) in location ℓ . Within the city, the density $D(\ell)$ follows,

$$D(\ell) = \left(\frac{q_r^{1+\epsilon(\ell)}}{1 + \epsilon(\ell)} \right) \frac{1}{\gamma_\ell} (w(\phi) + r + \underline{s} - p\underline{c})^{-1/\gamma_\ell} (w(\ell) + r + \underline{s} - p\underline{c})^{1/\gamma_\ell - 1}, \quad (45)$$

where $\gamma_\ell = \frac{\gamma}{1+\epsilon(\ell)}$ represents the spending share on housing adjusted for the supply elasticity in location ℓ and the fringe housing price q_r satisfies $\rho_r = \frac{(q_r)^{1+\epsilon_r}}{1+\epsilon_r}$. Integrating density defined in Eq. 45 across urban locations gives the total urban population,

$$L_u = \int_0^\phi D(\ell)d\ell = \int_0^\phi \left(\frac{q_r^{1+\epsilon(\ell)}}{1 + \epsilon(\ell)} \right) \frac{1}{\gamma_\ell} (w(\phi) + r + \underline{s} - p\underline{c})^{-1/\gamma_\ell} (w(\ell) + r + \underline{s} - p\underline{c})^{1/\gamma_\ell - 1} d\ell \quad (46)$$

Note that with homogeneous supply conditions across locations, $\epsilon(\ell) = \epsilon_r = \epsilon$, Equation (46) simplifies into (22) of the main text, which we give again:

$$L_u = \int_0^\phi D(\ell)d\ell = \rho_r \int_0^\phi \frac{1 + \epsilon}{\gamma} (w(\phi) + r + \underline{s} - p\underline{c})^{-\frac{1+\epsilon}{\gamma}} (w(\ell) + r + \underline{s} - p\underline{c})^{\frac{1+\epsilon}{\gamma} - 1} d\ell.$$

In the rural area, $\ell \geq \phi$, market clearing for residential housing imposes

$$L_r \gamma (w_r + r + \underline{s} - p\underline{c}) = S_{hr} (q_r)^{1+\epsilon_r} = S_{hr} (1 + \epsilon_r) \rho_r,$$

where S_{hr} is the amount of land demanded in the rural area for residential purposes. This leads to the following demand of land for residential purposes in the rural area,

$$S_{hr} = \frac{L_r \gamma_r (w_r + r + \underline{s} - p\underline{c})}{\rho_r}, \quad (47)$$

where $\gamma_r = \frac{\gamma}{1+\epsilon_r}$.

The market clearing condition for land, Equation (24), becomes

$$S_r = S - \phi - \frac{L_r \gamma_r (w_r + r + \underline{s} - p\underline{c})}{\rho_r}. \quad (48)$$

The last modification regards the market clearing for urban goods. The amount of urban good used to produce housing becomes location specific. Hence, Equation (28) becomes

$$c_u + \frac{1}{L} \int_0^\phi \tau(\ell) D(\ell) d\ell + \frac{1}{L} \int_0^1 \frac{\epsilon(\ell)}{1 + \epsilon(\ell)} q(\ell) H(\ell) d\ell = y_u, \quad (49)$$

where $y_u = \frac{Y_u}{L}$ denotes the production per worker of the urban good.

B.1.4 Single City On Circular Surface

We now take model B.1.3 and extended it to a surface (instead of a line), where the city is circular around its center— ϕ denotes the radius of the city. The modifications concerns for the most part the integrals used. We start with the city size Equation (46), which becomes

$$L_u = \int_0^\phi D(\ell) 2\pi \ell d\ell = \int_0^\phi \left(\frac{q_r^{1+\epsilon(\ell)}}{1 + \epsilon(\ell)} \right) \frac{1}{\gamma_\ell} (w(\phi) + r - p\underline{c})^{-1/\gamma_\ell} (w(\ell) + r - p\underline{c})^{1/\gamma_\ell - 1} 2\pi \ell d\ell \quad (50)$$

Notice again that with homogeneous supply conditions across locations, $\epsilon(\ell) = \epsilon_r = \epsilon$, this simplifies into the equivalent of the baseline model, if this were defined on a circle:

$$L_u = \int_0^\phi D(\ell) 2\pi \ell d\ell = \rho_r \int_0^\phi \frac{1 + \epsilon}{\gamma} (w(\phi) + r + \underline{s} - p\underline{c})^{-\frac{1+\epsilon}{\gamma}} (w(\ell) + r + \underline{s} - p\underline{c})^{\frac{1+\epsilon}{\gamma} - 1} 2\pi \ell d\ell.$$

Demand of land for residential purposes in the rural area is unchanged and given in (47). The market clearing condition for land (24), however, needs to be adjusted to read

$$S_r = S - \pi \phi^2 - \frac{L_r \gamma_r (w_r + r + \underline{s} - p\underline{c})}{\rho_r}. \quad (51)$$

The aggregate land rent definition also needs to be adjust for the circular area and becomes

$$rL = \int_0^\phi \rho(\ell)2\pi\ell d\ell + \rho_r \times (S_r + S_{hr}). \quad (52)$$

The aggregate per capita income y net of spatial frictions in the economy that is spent on both goods becomes,

$$y = r + \frac{L_r}{L}w_r + \frac{1}{L} \int_0^\phi w(\ell)D(\ell)2\pi\ell d\ell. \quad (53)$$

The market clearing condition for rural goods is unchanged. The last modification regards the market clearing for urban goods,

$$c_u + \frac{1}{L} \int_0^\phi \tau(\ell)D(\ell)2\pi\ell d\ell + \frac{1}{L} \int_0^\phi \frac{\epsilon(\ell)}{1 + \epsilon(\ell)} q(\ell)H(\ell)2\pi\ell d\ell + \frac{1}{L} \frac{\epsilon_r}{1 + \epsilon_r} q_r H_r = y_u, \quad (54)$$

where $y_u = \frac{Y_u}{L}$ denotes the production per worker of the urban good.

B.1.5 Dynamic Model

The value of the real interest rate in the economy is obtained from the intertemporal optimization of ex-ante identical, infinitely-lived agents. Their intertemporal utility is given by

$$U_t = \sum_{s=t}^{\infty} \beta^{s-t} \bar{u}_s,$$

where β is the discount factor and \bar{u}_t denotes the expected utility flow at period t . The expected utility flow at period t is derived from the agents' optimization, in which they maximize

$$\frac{1}{L} \int_0^\phi 2\pi\ell D(\ell) \log(C_t(\ell)) d\ell + \frac{L_r}{L} \log(C_{r,t}),$$

subject to

$$p_t c_{r,t}(\ell) + c_{u,t}(\ell) + q_t(\ell) h_t(\ell) = w_t(\ell) + r_t + R_t B_{t-1} + B_t, \forall \ell,$$

where R_t denotes the real interest rate at period t , B_t denotes the amount of risk-free asset purchased at period t , and the other variables are defined in Section 3. Using the optimal expenditures described in equations (10)–(12) and the fact that in equilibrium $B_t = 0 \forall t$, the interest rate is given by

$$R_t = \frac{1}{\beta} \frac{\widehat{u}'_t}{\widehat{u}'_{t+1}},$$

where $\widehat{u}' = \frac{1}{L} \int_0^\phi \frac{2\pi\ell D(\ell)}{w(\ell)+r+\underline{s}-p\underline{c}} d\ell + \frac{L_r}{L} \frac{1}{w_r+r+\underline{s}-p\underline{c}}$.

Once we have the value of the real interest rate for every period, we compute land and housing values at each location as the discounted sum of future land rents. We simulate the model until the

year 2350 to have at least 120 future periods in the computation. To simulate the model forward, we assume a productivity growth rate after 2000 of 1% in both sectors and a population growth rate after 2040 (last year for INSEE population projections) equal to 0.4%, which corresponds to the average growth in the period 1990-2040.

The housing price index is computed as the total value of housing in the economy divided by the total units of housing, which corresponds to average housing purchasing price. The total value of housing, W_t^h , is equal to the value of housing in the city plus the value of housing outside the city, and it is computed as

$$W_t^h = \int_0^\phi 2\pi\ell H_t(\ell) Q_t(\ell) d\ell + \int_\phi^{\sqrt{S/\pi}} 2\pi\ell \frac{S_{hr}}{S_{hr} + S_r} H_t(\ell) Q_t(\ell) d\ell,$$

where the purchasing price of a housing unit in location ℓ , $Q_t(\ell)$, is computed as the discounted sum of future rental prices until a final period T :

$$Q_t(\ell) = \sum_{s=t}^T \frac{q_s(\ell)}{R_s}.$$

The total units of housing, HH_t , is equal to the housing units in the city plus the housing units outside the city, which is computed as

$$HH_t = \int_0^\phi 2\pi\ell H_t(\ell) d\ell + \int_\phi^{\sqrt{S/\pi}} 2\pi\ell \frac{S_{hr}}{S_{hr} + S_r} H_t(\ell) d\ell.$$

Finally, the Housing Price Index is computed as

$$HPI_t = \frac{W_t}{HH_t}.$$

We then deflate this value using an implied GDP-deflator that takes the geometric average of the Laspeyres and the Paasche price index.

B.1.6 Numerical Integration over Circular City

In this subsection we define some integrals over space. We limit ourselves to the definition for the full model on a circular surface described in B.1.4, the integrals simplify accordingly for the city on a line segment.

We use Gaussian quadrature to compute numerical approximations to our integrals. To this end we use $N_j = 64$ Gauss-Legendre integration weights $\omega \in (0, 1)$ and nodes \hat{z} , which are defined in $[-1, 1]$. We map the nodes into $z \in [0, \phi]$. By way of example, consider the city size Equation (50), where we want to approximate the integral of residential density D at location ℓ over a circle with

radius ϕ :

$$L_u = \int_0^\phi D(\ell) 2\pi \ell d\ell$$

$$\approx \frac{\phi - 0}{2} \sum_{j=1}^{N_j} \omega_j D(z_j) 2\pi z_j$$

We use the second line in our numerical implementation – notice the initial fraction as a result of mapping nodes into $[0, \phi]$. The approach to integrate other expressions (integral of urban good consumption, for example) is identical. In most cases, $D(\ell)$ above is the weight attached to a given model outcome. A slight difference occurs if we compute urban-population averages – for example the average commuting speed as mentioned in the main text. Define function $m(\ell, L_u)$ as (40). To obtain the average, we have to divide by the number of urban residents to obtain the correct per-capita representation:

$$\bar{m} = \frac{1}{L_u} \int_0^\phi m(\ell, L_u) D(\ell) 2\pi \ell d\ell$$

$$\approx \frac{\phi}{2L_u} \sum_{j=1}^{N_j} \omega_j m(z_j, L_u) D(z_j) 2\pi z_j$$

B.2 Numerical Model Solution and Parameter Estimation

In this subsection we describe the numerical solution techniques to solve the single city model.

B.2.1 Timing and Productivity Series Smoothing

We run the model in time steps of 10 years, starting in 1840 and up until 2020.

A key input for the model is the estimated series of sectoral productivities $\{\theta_{u,t}, \theta_{r,t}\}_{t=1840}^{2020}$, displayed in Figure 24. In order to be useable in the model, we need to smooth the displayed data. We explain the necessary steps briefly here:

1. We obtain the estimated series at annual frequency.
2. We subset both series to start in 1840 and end in 2015 (rural productivity ends in that year)
3. We linearly interpolate the missing interwar years.
4. Smoothing is done with a **Hann window** and a 15-year window size. We experimented with the window size until high-frequency oscillations disappear.
5. Our rural productivity series get very volatile starting at the 2000s. We abstract from this noise by growing the smoothed series forward with 1% annual growth from the year 2000 onwards.

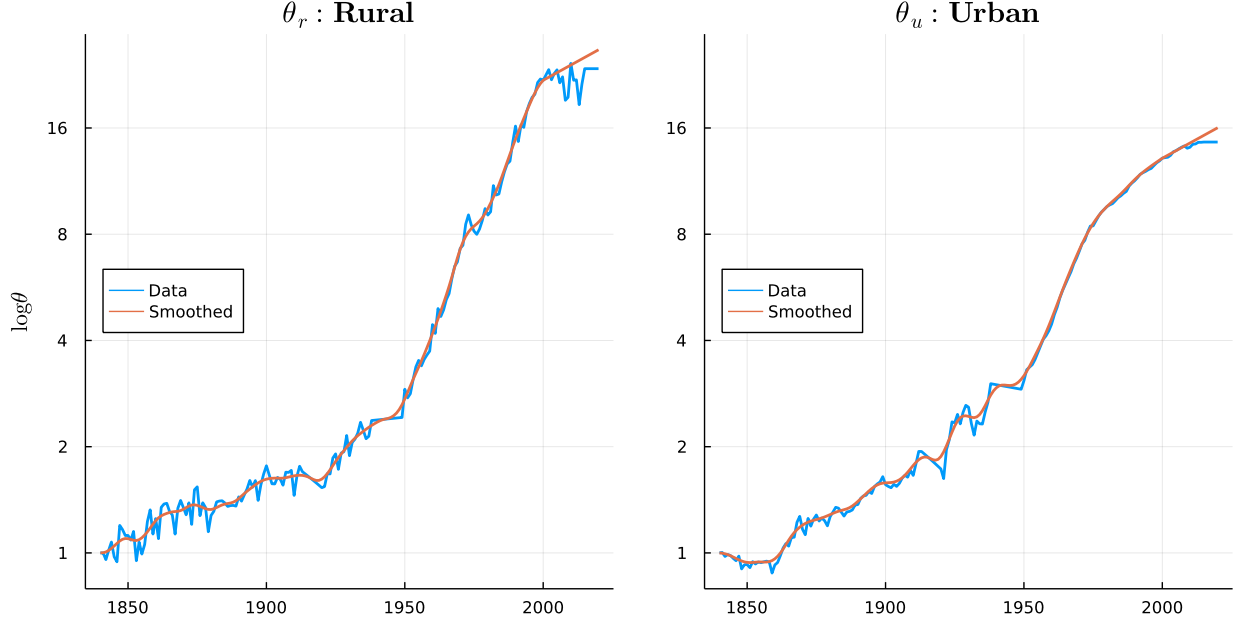


Figure 50: Smoothing Procedure applied to estimated productivity data. The rightmost panel are the series for θ which are given to the quantitative model in Section 4. Notice how the data are extrapolated from 2000 onwards assuming constant 1% growth.

This procedure yields the smoothed series displayed in Figure 50.

B.2.2 Single City Model Solution

In this section we describe the solution of the system of equations that describe the model with all extensions as enumerated in Section B.1, hence we give the equation system of model B.1.4 as

$$S = \begin{cases} (35) & w_r = \alpha p \theta_r \left(\frac{S_r}{L_r} \right)^{1-\alpha} \\ (36) & \rho_r = (1-\alpha) p \theta_r \left(\frac{L_r}{S_r} \right)^\alpha \\ (50) & L_u = \int_0^\phi D(\ell) 2\pi \ell d\ell \\ (52) & rL = \int_0^\phi \rho(\ell) d\ell + \rho_r \times (1-\phi) \\ (51) & S_r = S - \pi \phi^2 - \frac{L_r \gamma_r (w_r + r + \underline{s} - p\underline{c})}{\rho_r} \\ (54) & y_u = c_u + \frac{1}{L} \int_0^\phi \tau(\ell) D(\ell) 2\pi \ell d\ell + \frac{1}{L} \int_0^\phi \frac{\epsilon(\ell)}{1+\epsilon(\ell)} q(\ell) H(\ell) 2\pi \ell d\ell + \frac{1}{L} \frac{\epsilon_r}{1+\epsilon_r} q_r H_r \end{cases}$$

The solution proceeds by choosing values for $x = \{\rho_r, \phi, r, L_r, p, S_r\}$ which, given parameters and

two values for sectoral productivities (θ_u, θ_r) solves the system of equations \mathcal{S} . An important consideration concerns valid starting values x_0 : once a valid starting point for the first period is found, we supply the solution x_{t-1} as a starting point for period t 's algorithm. We explain generation of starting values in [B.2.3](#) below.

B.2.3 Starting Values

We generate valid starting values for the single city model in the following way.

1. Given parameters $(\alpha, \theta_u, \theta_r, \gamma, \nu, \epsilon_r, \underline{s}, \underline{c})$, specify a two-sector model (rural and agricultural production) but without commuting costs. We search over rural land rent ρ_r and rural workforce L_r in order to satisfy a land market clearing condition and a feasibility constraint on the economy. We obtain thus $(\rho_r^{(0)}, L_r^{(0)})$.
2. We can compute the remaining entries of starting vector $x^{(0)}$ with those values in hand.
3. We return $\phi/10$ to ensure the initial city is not too big to aid the first period solution.

This procedure is sufficient to run the baseline model and to explore a limited range of parameter values. For estimation of the model, however, we are confronted with convergence issues when moving too far away from the initial value generated by this simple procedure. We therefore upgrade the procedure in the following section.

B.2.4 Estimation Procedure

For estimation, we choose the vector $\Gamma \in \Theta$ with following elements and spaces:

$$\Gamma = \begin{cases} \underline{c} & \in (0.7, 0.9) \\ \underline{s} & \in (0.2, 0.26) \\ \nu & \in (0.02, 0.03) \\ a & \in (2.0, 3.0) \\ \gamma & \in (0.28, 0.33) \end{cases}$$

We create a Cartesian grid Θ over this five-dimensional space and evaluate the model at each parameter value using the procedure described in [B.2.3](#). The solution encounters invalid points in a highly irregular fashion - in particular, non-monotonic in any particular parameter's space. We therefore employ a deep learning procedure to impute the starting values for combinations of Γ which result in invalid starting values.

We train a neural network with 4 dense layers, where the first 3 have a RELU activation function and the final layer is linear, in order to map a 5-dimensional parameter vector Γ into a 6-dimensional starting point $x^{(0)}$, which produces a valid model solution. Our data are all valid starting points

obtained from our grid evaluation mentioned above. We split data into training (70%) and test samples and we use gradient descent to optimize a MSE loss function.

We can use the resulting neural network to generate starting values which allow evaluation of the model anywhere inside the above described parameter space Θ . Estimation involves solving the standard GMM optimization problem

$$\min_{\Gamma \in \Theta} L(\Gamma) = \min_{\Gamma \in \Theta} [m - m(\Gamma)]^T W [m - m(\Gamma)]$$

where m is a data moment and $m(\Gamma)$ is its model-generated counterpart. Both sets of values are displayed in Section B.2.5. We optimize this loss function with a differential evolution optimizer from the `BlackBoxOptim.jl` package.⁷⁵ Notice that we focus here solely on achieving the best fit of the model to our main data moments (leaving aside considerations related to optimal weighting for inference purposes), hence we set the weights on the diagonal of W in order to ensure that those moments do not vanish in the gradient of the moment function.

B.2.5 Estimation Results

The estimated parameter Table 7 implies the following moment fits of both targeted (Table 8 and non-targeted (Table 9) moments.

C Sensitivity Analysis and Extensions

C.1 Estimation Results with $\epsilon(0) = 2.5$

In our baseline results we used a value $\epsilon(0) = 2$ at the city center. In this section we report results if estimation is performed setting instead a value of $\epsilon(0) = 2.5$. We show resulting parameter values in Table 10, targeted moments in Table 11 as well as non-targeted moments in Table 12. Parameter estimates are close to identical w.r.t. to the baseline values in Table 7, except for the value of a , which is lower. This makes intuitive sense because a greater supply elasticity in the center would imply higher buildings in the central area, hence the city would become smaller overall. In order to satisfy the urban area data moment, the model thus decreases the base parameter of commuting costs in order to offset this effect. The resulting moments are virtually identical to the baseline model. We see from the non-targeted moments in Table 12 that by choosing $\epsilon(0) = 2.5$, we create a city that is too dense in the center: the coefficient of the exponential decay model is too large (density falls too fast, moving away from the center).

C.2 Sensitivity with constant $\epsilon = 3$

We perform sensitivity analysis assuming a housing supply elasticity ϵ equal to 3 in all locations. We use the estimated parameter values from Table 7 for this exercise. Results are displayed in Figure

⁷⁵<https://github.com/robertfeldt/BlackBoxOptim.jl>

Parameter	Description	Value
S	Total Space	1.0
L_0	Total Population in 1840	1.0
θ_0	Initial Productivity in 1840	1.0
α	Labor Weight in Rural Production	0.75
σ	Land-Labor Elasticity of Substitution	0.9999
ν	Preference Weight for Rural Consumption Good	0.0296
γ	Utility Weight of Housing	0.3017
\underline{c}	Rural Consumption Good Subsistence Level	0.7368
\underline{s}	Initial Urban Good Endowment	0.2106
β	Discount Factor	0.935
ξ_l	Elasticity of commuting cost wrt location	0.55
ξ_w	Elasticity of commuting cost wrt urban wage	0.75
a	Commuting Costs Base Parameter	2.2492
ϵ_r	Housing Supply Elasticity in rural area	5.0
$\epsilon(0)$	Housing Supply Elasticity at city center	2.0

Table 7: Parameter values

Moment	Data	Model	Weight
rural_emp_1840	0.6019	0.7029	0.01
rural_emp_1850	0.5625	0.6392	0.01
rural_emp_1860	0.5248	0.5612	0.01
rural_emp_1870	0.5018	0.5059	0.01
rural_emp_1880	0.4677	0.5158	0.01
rural_emp_1890	0.4433	0.4756	0.01
rural_emp_1900	0.4172	0.41	0.01
rural_emp_1910	0.413	0.4008	0.01
rural_emp_1920	0.4149	0.4053	0.01
rural_emp_1930	0.3618	0.3129	0.01
rural_emp_1940	0.3573	0.2644	0.01
rural_emp_1950	0.2994	0.2235	0.01
rural_emp_1960	0.2255	0.1447	0.01
rural_emp_1970	0.1427	0.0877	0.01
rural_emp_1980	0.0914	0.0713	0.01
rural_emp_1990	0.0615	0.0527	0.01
rural_emp_2000	0.0432	0.043	0.01
rural_emp_2010	0.0337	0.0413	0.01
rural_emp_2020	0.0313	0.0396	0.01
rel_city_area_2010	0.173	0.1741	10.0
housing_share_1900	0.237	0.2377	5.0
housing_share_2010	0.306	0.3028	5.0

Table 8: Moment function at optimal parameter vector in Table 7.

Moment	Data	Model
avg_density_fall	7.9	6.0405
max_mode_increase	5.0	4.8597
density_decay_coef	-0.16	-0.1641
density_decay_MSE	-	0.653

Table 9: Non-targeted moments at optimal parameter vector in Table 7. Notice that the implied city structure (fall in density as measure by the `density_decay_coef`) matches very well with the data. The `density_decay_MSE` provides a measure of goodness-of-fit of the exponential decay model.

Parameter	Description	Value
ν	Preference Weight for Rural Consumption Good	0.03
γ	Utility Weight of Housing	0.3
\underline{c}	Rural Consumption Good Subsistence Level	0.74
\underline{s}	Initial Urban Good Endowment	0.21
a	Commuting Costs Base Parameter	2.14

Table 10: Estimated parameter values when $\epsilon(0) = 2.5$. Most estimates differ after the second digit, the main difference is the value of commuting cost base parameter a .

51 for the some variables pertaining to urban expansion and density. Outcomes in the baseline simulation are shown for comparison purposes. With a housing supply elasticity ϵ equal to 3 in all locations the model again generates a city that is too dense in the center.

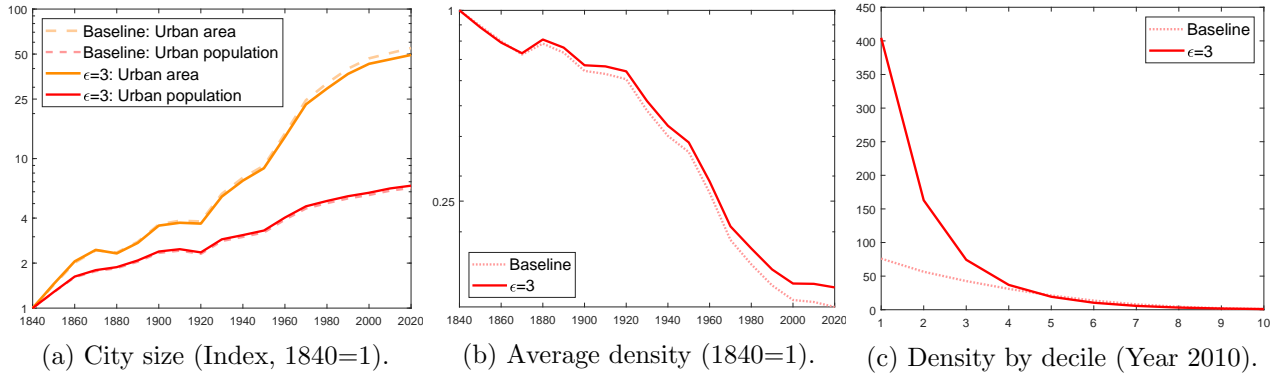


Figure 51: Constant housing supply elasticity, $\epsilon = 3$.

Notes: The housing supply elasticity ϵ is set to 3 in all locations. Other parameters set to their baseline value of Table 7. Outcomes of interest with constant elasticity, $\epsilon = 3$, are displayed with a solid line. The baseline simulation is shown with a dashed line for comparison.

C.3 Sensitivity w.r.t the elasticity of substitution between land and labor

Our baseline assumes a unitary elasticity of substitution between land and labor in the rural sector, $\sigma = 1$. Details of the derivation with a CES production in the rural sector are shown above in B.1.1. We perform sensitivity analysis with a lower value of σ equal to 0.25 and for a higher value

Moment	Data	Model	Weight
rural_emp_1840	0.6019	0.6998	0.01
rural_emp_1850	0.5625	0.6357	0.01
rural_emp_1860	0.5248	0.5573	0.01
rural_emp_1870	0.5018	0.5021	0.01
rural_emp_1880	0.4677	0.5122	0.01
rural_emp_1890	0.4433	0.4719	0.01
rural_emp_1900	0.4172	0.4062	0.01
rural_emp_1910	0.413	0.397	0.01
rural_emp_1920	0.4149	0.4017	0.01
rural_emp_1930	0.3618	0.3091	0.01
rural_emp_1940	0.3573	0.2604	0.01
rural_emp_1950	0.2994	0.2194	0.01
rural_emp_1960	0.2255	0.1405	0.01
rural_emp_1970	0.1427	0.0836	0.01
rural_emp_1980	0.0914	0.0672	0.01
rural_emp_1990	0.0615	0.0487	0.01
rural_emp_2000	0.0432	0.0392	0.01
rural_emp_2010	0.0337	0.0375	0.01
rural_emp_2020	0.0313	0.0358	0.01
rel_city_area_2010	0.173	0.1733	10.0
housing_share_1900	0.237	0.2367	5.0
housing_share_2010	0.306	0.3032	5.0

Table 11: Target moments with $\epsilon(0) = 2.5$. The values here are very similar to the ones in Table 8.

Moment	Data	Model
avg_density_fall	7.9	6.2571
max_mode_increase	5.0	4.8519
density_decay_coef	-0.16	-0.2268
density_decay_MSE	-	0.257

Table 12: Non-targeted moments with $\epsilon(0) = 2.5$. The important difference to the baseline value $\epsilon(0) = 2$ comes from the too large value of the decay coefficient – here we create a city that is too dense in the center and falls stronger than what we see in the data..

of 4. Results for variables of interest discussed in the main text are displayed on Figure 52.

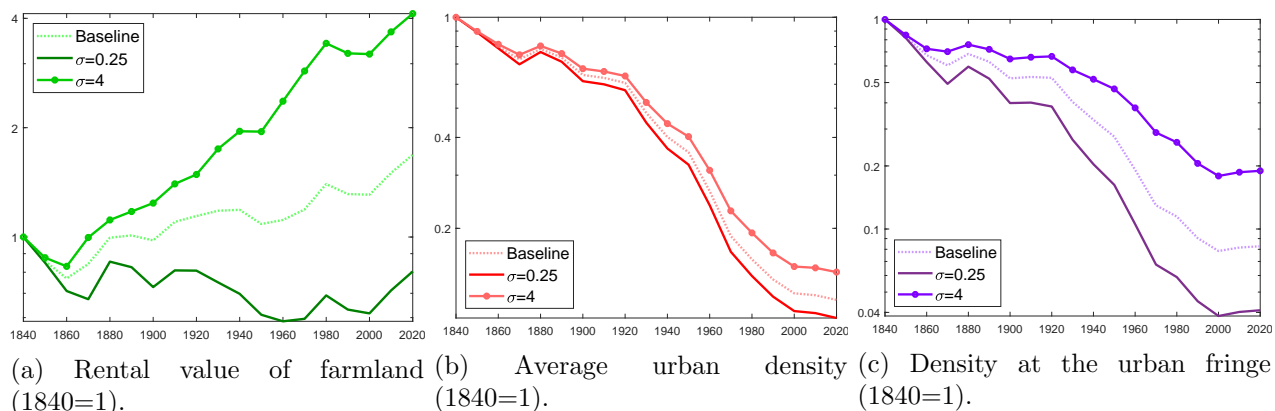


Figure 52: Sensitivity to the elasticity of substitution between land and labor σ .

Notes: The elasticity of substitution between land and labor σ is set to a low value of 0.25 (resp. a high value of 4). All other parameters are kept to their baseline value of Table 7. Simulation for the baseline calibration shown in dashed for comparison.

C.4 Agglomeration and Congestion

Agglomeration. We introduce urban agglomeration forces by assuming that the urban productivity increases externally with urban employment, $\theta_u(L_u) = \theta_u \cdot L_u^\lambda$. Urban wages, $w_u = \theta_u \cdot L_u^\lambda$, thus increase faster relative to our baseline when the city expands. Apart from the adjustment of urban wages, the model is identical to our baseline. So is the numerical solution. It is important to note though that the faster increase in urban wages makes urban workers use faster commutes as the opportunity cost of time increases faster.

We set $\lambda = 0.05$, in the range of empirical estimates for France (Combes et al. (2010)). Other parameters are left identical to the baseline for comparison, adjusting the initial value of θ_u to have the same initial urban productivity. For variables of interest, results in the presence of agglomeration forces are displayed in Figure 53 together with the baseline. While the city expands slightly more in area, there is barely no effect of agglomeration forces on urban population. The faster increase in the urban wage due to agglomeration forces increases urban housing demand and reduces urban commuting costs (as a share of income). This relocates urban households towards the suburbs where they can enjoy larger homes and the city sprawls more. However, a higher urban income makes also rural goods more valuable increasing (almost equally) rural workers' wage. General equilibrium forces thus prevent workers' reallocation towards cities. They also make rural land more valuable—mitigating the area expansion of the city. As a consequence, despite higher incomes driven by urban expansion, the economy with agglomeration forces behave quantitatively similarly to our baseline.

Congestion. We consider additional urban congestion costs by assuming that commuting costs are increasing with urban population, $a(L_u) = a \cdot L_u^\mu$. This summarizes the potential channels through which larger cities might involve longer and slower commutes for a given commuting distance. Under

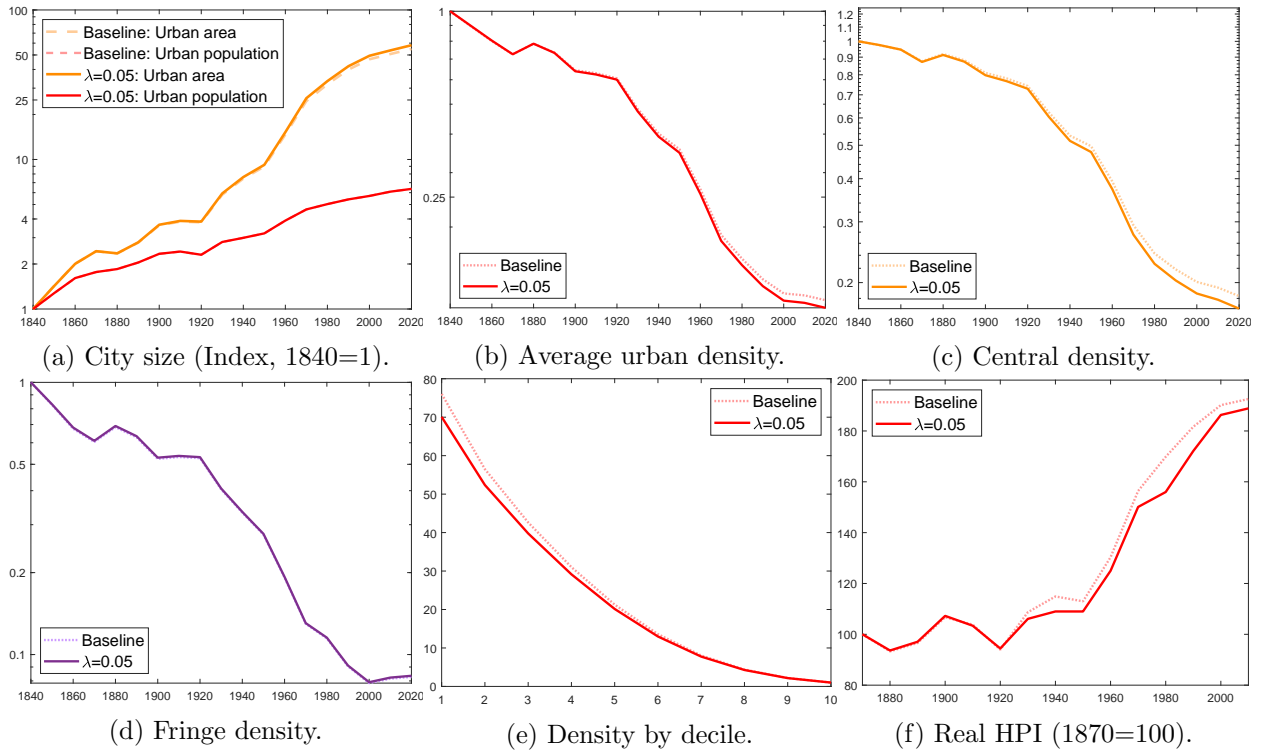


Figure 53: Positive agglomeration forces, $\lambda = 0.05$.

Notes: The urban agglomeration forces parameter λ is set to 0.05. Other parameters set to their baseline value of Table 7, while θ_u is adjusted to have the same initial urban productivity. Outcomes of interest with agglomeration forces are displayed with a solid line. The baseline simulation is shown with a dashed line for comparison.

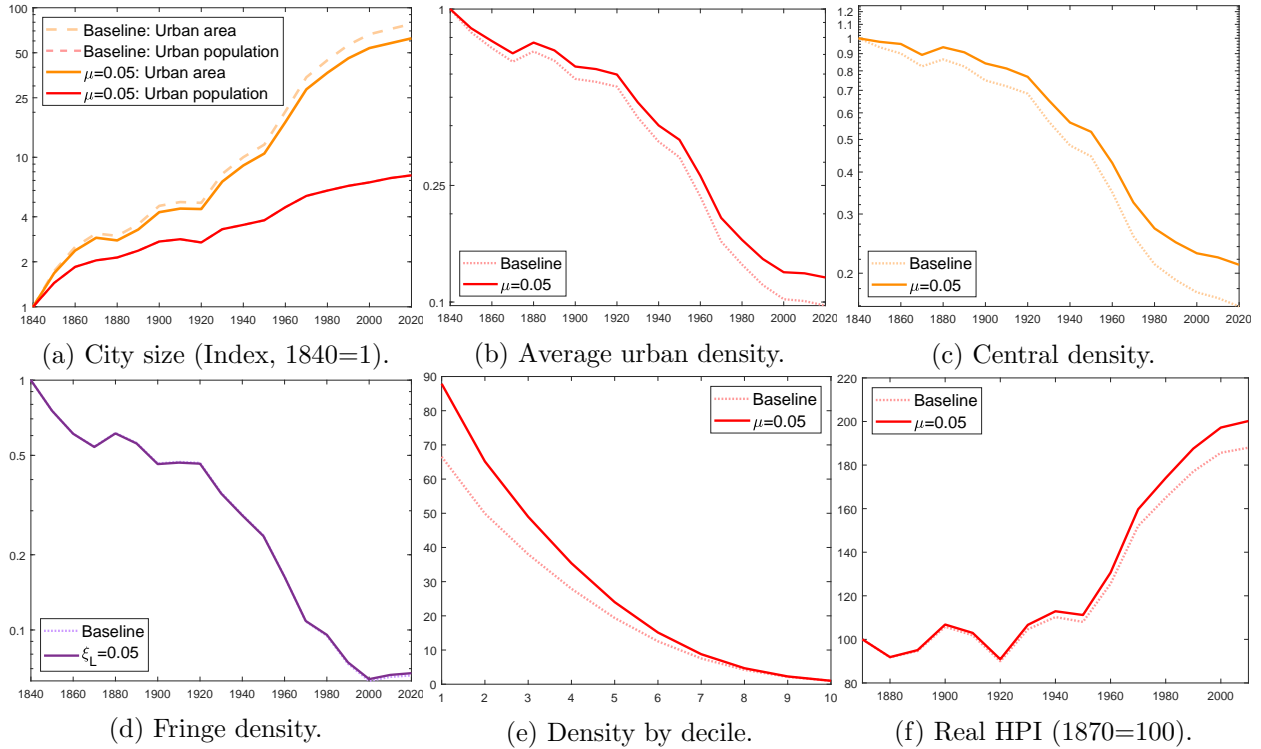


Figure 54: Congestion costs, $\mu = 0.05$.

Notes: The congestion cost parameter η is set to 0.05. Other parameters set to their baseline value of Table 7, and we re-scale the constant a to have the same initial value for the commuting costs. Outcomes of interest with congestion costs are displayed with a solid line. The baseline simulation is shown with a dashed line for comparison.

such a formulation, commuting costs in location ℓ satisfies,

$$\tau(\ell) = a \cdot L_u^\mu \cdot w_u^{\xi_w} \cdot (\ell)^{\xi_\ell}.$$

Apart from the adjustment of commuting costs, which depend on the urban population, the model is identical to our baseline. So, is the numerical solution.

We set $\mu = 0.05$ and we re-scale the constant a to have the same initial value for the commuting costs. Other parameters are set to their baseline values. The evolution of the variables of interest is shown on Figure 54 with the baseline for comparison. Congestion forces move the equilibrium in the opposite direction of agglomeration forces. They reduce the expansion in area and the extent of suburbanization. By increasing commuting costs, they also increase urban housing prices. However, via general equilibrium forces, they also make rural goods and rural land less valuable—severely mitigating the direct effect of congestion costs on urban expansion.

C.5 Commuting Distance and Residence Location

Guided by the structure of French cities, our baseline results hinge on the assumption of a monocentric model where urban individuals commute to the city center to work. While endogeneizing firms location across space is beyond the scope of the paper, one can still partly relax the monocentric assumption by assuming that commuting distance, $d(\ell)$, does not map one for one with residential distance ℓ from the central location. In line with empirical observations in Section A.9.2, we model commuting distance $d(\ell)$ in a reduced-form way as follows,

$$d(\ell) = d_0(\phi) + d_1(\phi) \cdot \ell,$$

with $d_0(\phi)$ a positive and increasing function of ϕ , satisfying $\lim_{\phi \rightarrow 0} d_0(\phi) = 0$, and $d_1(\phi)$ a decreasing function belonging to $(0, 1)$ with $\lim_{\phi \rightarrow 0} d_1(\phi) = 1$. d_0 represents the (minimum) commuting distance travelled by an individual living in the center, while d_1 is the slope between commuting distance and residential distance from the center. This specification is consistent with the data (see Section A.9.2). It also makes sure that at the limit of $\phi \rightarrow 0$, the city is monocentric as all the jobs must be centrally located. It is important to note that commuting costs are now defined as,⁷⁶

$$\tau(\ell) = a \cdot w_u^{\xi_w} \cdot (d(\ell))^{\xi_\ell}. \quad (55)$$

In the quantitative simulations, we make the following parametric assumptions: $d_0(\phi) = d_0 \cdot \phi$, with d_0 small and positive and $d_1(\phi) = \frac{1}{1+d_1 \cdot \phi}$, with $d_1 \geq 0$. The parameters d_0 and d_1 are guided by the data (Section A.9.2). Across cities, $d_0 \cdot \phi$ corresponds to the intercept of Eq. 34, ranging from 0.2 km for the smaller cities to more than 4 kms for Paris. Given that further away residential locations are typically at 5 kms of the center in smaller urban areas and up to 50 kms away from the center of Paris, d_0 should range within 4 and 8%. We set d_0 to 5% in our quantitative experiment. For a radius of about 20 kms (corresponding to the population weighted-mean of our sample of 100 urban areas), a person living in the city center ($\ell = 0$) would commute on average 1 km. Across cities, $d_1(\phi) = \frac{1}{1+d_1 \cdot \phi}$ corresponds to the slope of Eq. 34—with an estimated mode across urban areas close 0.7. Given that the model implied radius of our representative city is $\phi = 0.24$, we set $d_1 = 2$. This yields a slope coefficient of $\frac{1}{1+2 \cdot 0.24} = 0.68$ close to the empirical moment.

With these parameters values and the corresponding commuting costs, we simulate the quantitative model. Other parameters are left unchanged with the exception of the commuting costs parameter a . Changing commuting costs according to Eq. 55 implies a city area in equilibrium different from the targeted one in the baseline version of the model. Thus, for comparison purposes, a is recalibrated to make sure that the urban footprint still occupies 18% of rural land in the recent period. Results for the variables of interest are displayed in Figure 55.

We find that our results are not much affected under this alternative specification of the commuting

⁷⁶Note that this remains consistent with our calibrated value of ξ_ℓ estimated using commuting distance. The elasticity of speed $m(\ell)$ to commuting distance $d(\ell)$ being $1 - \xi_\ell$.

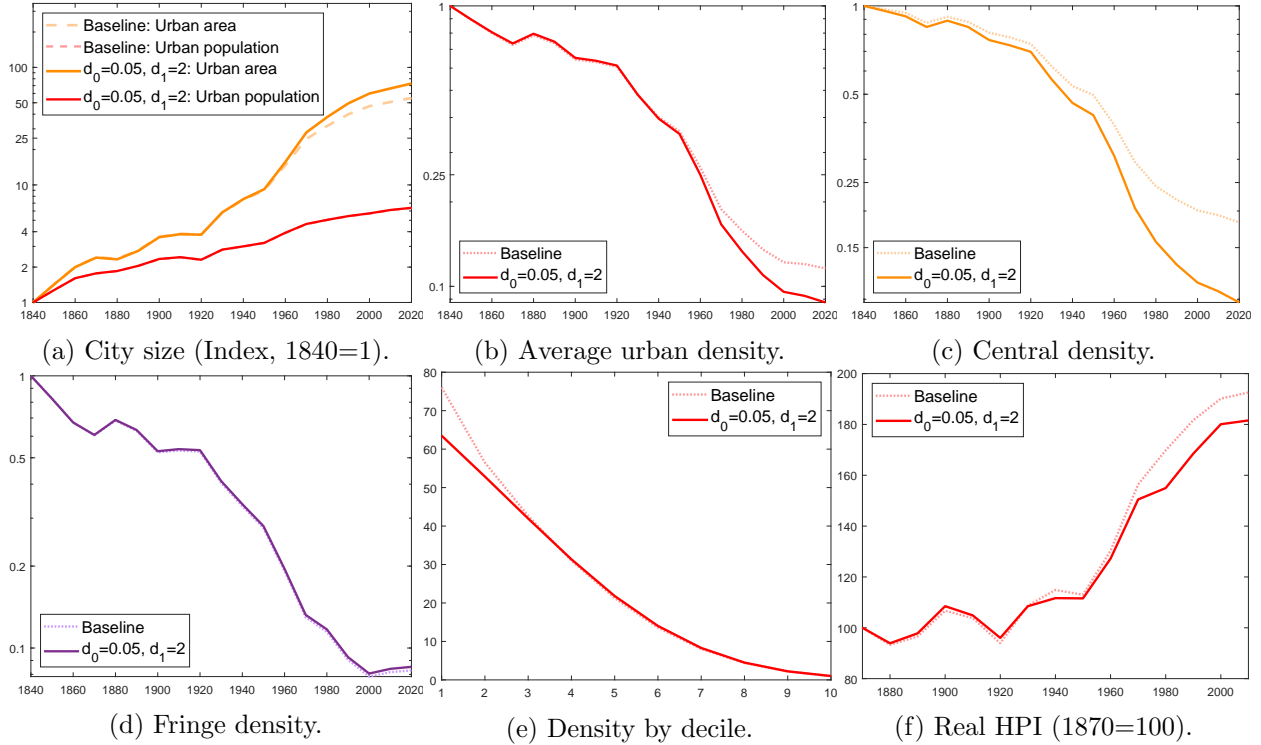


Figure 55: Alternative specification of commuting distance in the single city case, $d(\ell) = d_0 \cdot \phi + \frac{\ell}{1+d_1 \cdot \phi}$.

Notes: The solid line represents outcomes under the alternative specification of commuting distance $d(\ell)$, with parameter $d_0 = 5\%$ and $d_1 = 2$. Other parameters set to their baseline value of Table 7 up to a recalibration of the commuting cost parameter $a = 2.67$ to preserve the share of urban land in 2015. For comparison, outcomes of the baseline simulation are shown with a dashed line ($d_0 = d_1 = 0$).

costs. Quantitatively, the city expands more in area in the last decades under this specification of the commuting distance, bringing the model closer to the data. As a consequence of this larger sprawling, the average urban density falls more. This is driven by a larger fall of central density, the most noticeable difference relative to our baseline monocentric model. With urban expansion, residents in central locations end up commuting larger distances—implicitly due to the reallocation of jobs away from the center—, this makes central locations less attractive relative to suburban ones.

C.6 Multiple City Model

In this section we extend the model in Section B.1.4, which describes a single region, to allow for K different regions. The spatial structure in each region k is identical to our baseline one-city version: each region k of area S_k is made of urban and rural land, with only one (potential) city per region.⁷⁷ Regions are heterogeneous only in their urban productivity—with $\theta_{u,k}$ the urban productivity in

⁷⁷For each region, the city center (CBD) is centrally located within each region and regions are assumed large enough in area such that cities do not expand in neighbouring regions.

region/city k . Workers are freely mobile within and across regions and labor markets clear globally. Urban and rural goods are freely traded within and across regions and goods markets clear globally. For quantitative evaluation, we consider 20 regions, corresponding to the 20 largest French cities in 1870. City-specific urban productivities, $\theta_{u,k}$, are set to match the distribution of population of the different cities over the period 1870-2015, while keeping aggregate urban productivity equal to its baseline value estimated from French historical national accounts.⁷⁸ Each region is endowed with the same land area as our baseline. Aggregate population is multiplied by $K = 20$ relative to the baseline to preserve the endowment of land per head.⁷⁹ Other parameters are set to their baseline values of Table 7.

C.6.1 Multiple City Model: Setup

We will introduce index x_k to refer to variable x in region k , adding to the end of any existing indices as for example in $\theta_{u,k}$. We will make a distinction between *region* k and *location* ℓ , there the former is meant to denote one of K different subsets of total space S , and the latter to index a location *within a city* k .

Consider thus K different regions, each endowed with land area S_k , where total space is defined as $\sum_{k=1}^K S_k = S$. In each location, the productivity of the rural sector is $\theta_{r,k}$. Each region contains a potential city characterized by a level of productivity in the urban sector $\theta_{u,k}$.⁸⁰

We suppose that workers can freely move across regions k . Denote ϕ_k the radius of city k . Mobility across regions k gives the following mobility equations, equalizing the real wage of the urban and rural worker at the fringe across fringe workers in different regions,

$$\bar{C} = \kappa \frac{w_{u,k} - \tau_k(\phi_k) + r + \underline{s} - p\underline{c}}{(q_{r,k})^\gamma} = \kappa \frac{w_{r,k} + r + \underline{s} - p\underline{c}}{(q_{r,k})^\gamma},$$

where the housing rental price at the fringe of region k satisfies

$$\rho_{r,k} = \frac{(q_{r,k})^{1+\epsilon_{r,k}}}{1 + \epsilon_{r,k}} \quad (56)$$

Wages and land values are such that,

$$w_{u,k} = \theta_{u,k}, \quad (57)$$

$$\rho_{r,k} = (1 - \alpha)p\theta_{r,k} \left(\alpha \left(\frac{L_{r,k}}{S_{r,k}} \right)^{\frac{\sigma-1}{\sigma}} + (1 - \alpha) \right)^{\frac{1}{\sigma-1}}. \quad (58)$$

⁷⁸Denote Ω_k the share of urban population in city k , $\Omega_k = L_{u,k} / \sum_{j=1}^K L_{u,j}$. Measured aggregate urban productivity from historical national accounts at each date satisfies in equilibrium, $\theta_u = \sum_{j=1}^K \Omega_j \theta_{u,j}$.

⁷⁹This makes sure that, with homogeneous urban productivity, the version with multiple regions behaves like the one-city model in each region.

⁸⁰One could also consider different region specific parameters ϵ_k and τ_k .

Land must clear in every region such that,

$$S_k = S_{r,k} + \phi_k + \frac{L_{r,k}\gamma_{r,k}(w_{r,k} + r + \underline{s} - p\underline{c})}{\rho_{r,k}}. \quad (59)$$

where $\gamma_{r,k} = \frac{\gamma_k}{1+\epsilon_{r,k}}$. Labour must clear globally,

$$\sum_{k=1}^K L_k = \sum_{k=1}^K (L_{r,k} + L_{u,k}) = L. \quad (60)$$

Goods market must also clear globally

$$\sum_{k=1}^K \int_0^{S_k} c_{u,k}(l) D_k(l) 2\pi l dl + w_{u,k} \int_0^{\phi_k} \tau_k(l) D_k(l) 2\pi l dl + \int_0^{\phi_k} \frac{\epsilon_k(l)}{1 + \epsilon_k(l)} q_k(l) H_k(l) 2\pi l dl = \sum_{k=1}^K Y_{u,k} \quad (61)$$

We consider the case where housing supply conditions/rural productivity are identical across regions. In this case, one can show that $\frac{L_{r,k}}{S_{r,k}}$, $q_{r,k}$, $\rho_{r,k}$ and $w_{r,k}$ are equalized across regions (homogeneous rural sector). Then, using the mobility condition at the fringe of the different cities, one gets that the difference $\theta_{u,k} - \tau_k(\phi_k)$ is constant and equal to w_r across regions: more productive cities will be larger in area—the reason they will host a larger population in equilibrium. This can be seen using Equation (62) in region k ,

$$L_{u,k} = \int_0^{\phi_k} D(\ell) 2\pi \ell d\ell = \int_0^{\phi_k} \left(\frac{q_r^{1+\epsilon(\ell)}}{1 + \epsilon(\ell)} \right) \frac{1}{\gamma_\ell} (w(\phi_k) + r + \underline{s} - p\underline{c})^{-1/\gamma_\ell} (w(\ell) + r + \underline{s} - p\underline{c})^{1/\gamma_\ell - 1} 2\pi \ell d\ell \quad (62)$$

where q_r denotes the rural housing price equalized in all regions. This last equation pins down the relative population of cities. Together with the equalization of $\frac{L_{r,k}}{S_{r,k}}$ and the indifference condition at the fringe across regions,

$$\theta_{u,k} - \tau_k(\phi_k) = w_r, \forall k \quad (63)$$

$$\frac{L_{r,k}}{S_{r,k}} = b, \forall k \quad (64)$$

Land market clearing in all regions (59) and the city size equations (62) pin down $\{L_{u,k}, L_{r,k}, \phi_k, S_{r,k}\}$ for given aggregate prices common across regions ρ_r and p . These two aggregate prices are determined using goods and labor market clearing.

C.6.2 Multiple City Model: Numerical Solution

Solution of the multi city model is very similar to the single city case outlined in section B.2.2 with a slight modification on the sequence of urban productivities $\theta_{u,k,t}$ chosen in each period and for each city k . We formalize the problem as follows in a certain period t :

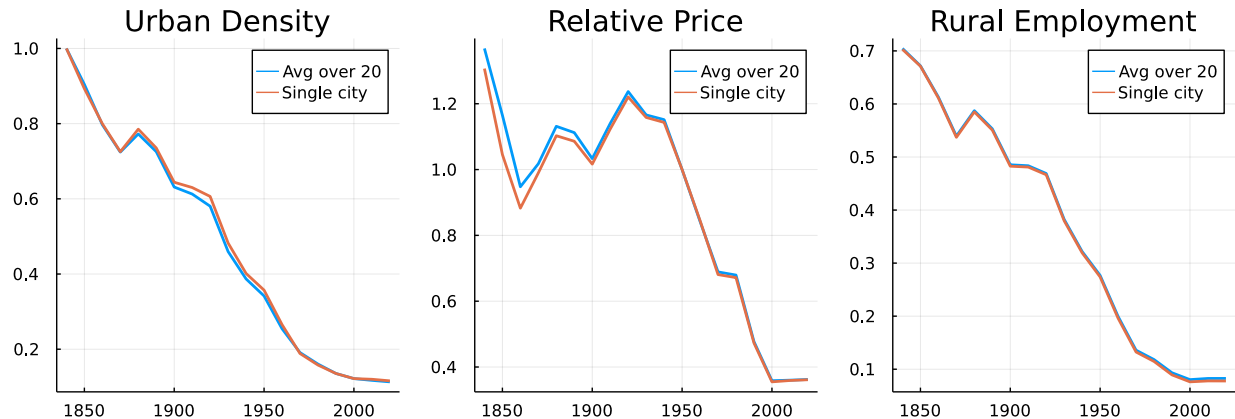


Figure 56: Comparing the average of the top 20 French cities with the single city from the baseline model. We normalize average urban density to its first value (1840), and we normalize the relative price series to its value in 1950.

$$\min_{\{\theta_{u,j,t}\}_{j=1}^K} \sum_{j=1}^K \left(\frac{L_{u,j,t}}{L_{u,1,t}} - \zeta_{j,t} \right)^2 \quad (65)$$

subject to

$$\sum_{j=1}^K \Omega_{j,t} \theta_{u,j,t} = \theta_{u,t} \quad (66)$$

and subject to (57), (58), (59), (60), (64)

where $\zeta_{k,t}$ is the empirical ratio of urban population between city k in our dataset and the largest city (indexed by $k = 1$), and where $\Omega_{k,t}$ is the urban population weight of city k in the same dataset. The objective function (65) tries to generate a population distribution across cities that is similar to what we observe in the data, by choosing K values of urban productivity $\theta_{u,k,t}$. This choice is subject to constraint (66) saying that the weighted summarize of city-specific productivities $\theta_{u,k,t}$ needs to replicate the level of productivity which was given to the *average city* in the baseline model.

C.6.3 Multiple City Model: Results

Here we present results for the multi-city extension introduced in Section C.6.1.

For aggregate variables of interest (aggregate sectoral employment, aggregate land use, relative price of rural goods/farmland, ...), the model with multiple regions behaves quantitatively very similarly to the baseline with only one city. Intuitively, the one-city model describes well the dynamics of aggregate variables for a representative ‘average’ city. We illustrate in Figure 56 how the time series of the single baseline city evolves next to the time series of an average over our 20 cities for urban density, relative price of rural good, and the rural employment share.

We focus next on the dispersion of city size and density, which are novel outcomes relative to our baseline. This is shown in Figure 57. The first panel shows how urban population relative to the largest city evolves in city and model. We achieve a perfect fit with our solution. This is a mechanical result as a consequence of how we set up the solution as a constrained optimization problem (we set the population distribution as a constraint, as explained in Section C.6.2).

Panel 2 of Figure 57 shows the dispersion of area (in log) in the model and in the data for dates 1870, 1950, 1975, 1990 and 2015.⁸¹ As visible from this second panel, there are significant cross sectional variations in urban area that the model does not reproduce. While the correlation between model and data is very high, area in the model and in the data do not move one for one—the elasticity being significantly above unity. The model does not generate a large enough area in more populated cities relative to smaller ones, particularly so in a given year. As written in the main text, large cities are too dense in the model’s cross-section although the model performs relatively well in the time-series. Note that we abstract from the use of land of economic activities but also from reallocation of jobs away from central locations due to the monocentric structure. To the extent that large cities reallocate more jobs away from the center, our model under-predicts their area. The cross-sectional variations in area also relates to city-specific land use regulations, which are not considered in our theory.

Panel 3 of Figure 57 plots the log of average urban density in a given city against its data counterpart for 1870, 1950, 1975, 1990 and 2015.⁸² It shows that the model implied cross sections of urban densities provides a good fit to the data. The elasticity is reasonably close to unity. The model predicts that, over time, for a given city, urban density falls as urban population increases—in line with the predictions of our baseline one-city model. In the cross-section, more populated cities are however denser as they feature higher housing prices. At a given date, the reallocation of workers towards a more productive city does not imply the strong general equilibrium effects on rural (good and farmland) relative prices, which lies at the heart of the time series evolution of urban density when cities grow in size. It is important to note that qualitatively, both predictions, over time and in the cross-section, are in line with the data. Quantitatively, the model does notably better in the time-series than in the cross-section. As discussed above, in a given year, more populated cities are not large enough in area relative to smaller ones—they are thus significantly denser in the model than they are in the data.

As last sensitivity analysis, we also consider the model with multiple-cities where, in each city, residential location does not map one for one into commuting distance. Using the same parametric assumptions, we extend Eq. 55 for cities of different areas,

$$d_k(\ell) = d_0 \cdot \phi_k + \left(\frac{1}{1 + d_1 \cdot \phi_k} \right) \cdot \ell,$$

⁸¹We use the model’s predictions for 1970 and 2010 as counterparts for 1975 and 2015 as our model provides solutions on 10-year intervals.

⁸²As for area, we take 1970 and 2010 instead because the model is run in 10-year steps.

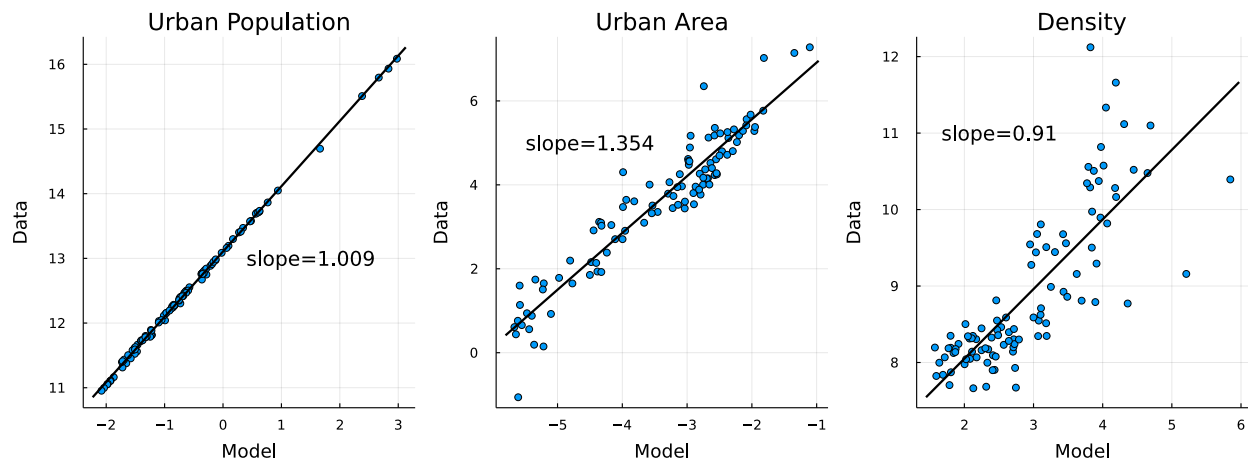


Figure 57: Cross sections of model vs data

Notes: We plot log model vs log data outcomes, combined across dates 1870, 1950, 1975, 1990 and 2015. An ideal model would yield an elasticity of one. The first panel shows the fit of the population distribution across cities and time. Panel two shows how urban area lines up between model and data. Panel three finally shows the urban density cross section.

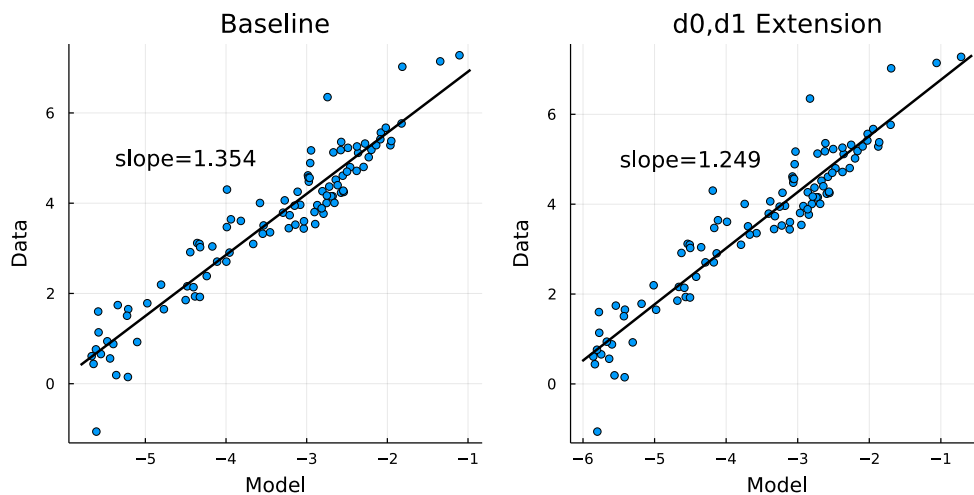


Figure 58: Urban Area Cross Sections. Sensitivity

Notes: Here we illustrate the impact of relaxing monocentricity on the distribution of urban area with the d_0, d_1 extension. We plot the log of model areas vs the log of areas in the data. The corresponding elasticity gets closer to one as we implement the extension, meaning the model is better able to generate larger cities.

where ϕ_k is the equilibrium radius of city k .

The fit between model and data improves under this specification for commuting distance. In line with the data presented in Appendix A.9, commuting distances in the center (resp. at the fringe) are larger (resp. lower) in larger cities in this specification relative to the baseline monocentric model. This, in turn, increases the area of more populated cities in the cross-section at a given date, reducing their average density and bringing the model closer to the data. More populated cities in the model are still noticeably denser than in the data, but less so compared to the baseline monocentric model. The improvement comes from the relative urban area distribution, which fits the data better with this last extension. When looking at areas (in log), the slope between model and data gets closer to unity as illustrated by Figure 58.

References

- Ahlfeldt, Gabriel M, Stephen J Redding, Daniel M Sturm, and Nikolaus Wolf**, “The economics of density: Evidence from the Berlin Wall,” *Econometrica*, 2015, 83 (6), 2127–2189.
- Albouy, David**, “What are cities worth? Land rents, local productivity, and the total value of amenities,” *Review of Economics and Statistics*, 2016, 98 (3), 477–487.
- , **Gabriel Ehrlich, and Minchul Shin**, “Metropolitan land values,” *Review of Economics and Statistics*, 2018, 100 (3), 454–466.
- Alder, Simon, Timo Boppert, and Andreas Müller**, “A theory of structural change that can fit the data,” *American Economic Journal: Macroeconomics*, 2021, *forthcoming*.
- Alonso, William et al.**, “Location and land use. Toward a general theory of land rent.,” *Location and land use. Toward a general theory of land rent.*, 1964.
- Angel, Shlomo, Alejandro M Blei, Daniel L Civco, and Jason Parent**, *Atlas of urban expansion*, Lincoln Institute of Land Policy Cambridge, MA, 2012.
- , **Jason Parent, Daniel L Civco, and Alejandro M Blei**, *Persistent Decline in Urban Densities: Global and Historical Evidence of ‘Sprawl’*, Lincoln Institute of Land Policy., 2010.
- Augé-Laribé, Michel**, “Les statistiques agricoles,” in “Annales de géographie,” Vol. 53 JSTOR 1945, pp. 81–92.
- Bairoch, Paul**, “Les trois révolutions agricoles du monde développé: rendements et productivité de 1800 à 1985,” *Annales*, 1989, pp. 317–353.
- Bastié, Jean**, “La population de l’agglomération parisienne,” in “Annales de géographie,” Vol. 67 JSTOR 1958, pp. 12–38.
- Baum-Snow, Nathaniel and Lu Han**, “The microgeography of housing supply,” *Work in progress, University of Toronto*, 2019.

- Bellefon, Marie-Pierre De, Pierre-Philippe Combes, Gilles Duranton, Laurent Gobillon, and Clément Gorin**, “Delineating urban areas using building density,” *Journal of Urban Economics*, 2019, p. 103226.
- Bertillon, Jacques**, “L’accroissement de la circulation à Londres et à Paris,” *Journal de la société française de statistique*, 1910, *51*, 381–397.
- Bertrand, Pierre and Jean Hallaire**, “Une enquête sur les déplacements journaliers des personnes actives de la région parisienne ou migrations alternantes,” *Journal de la société française de statistique*, 1962, *103*, 186–217.
- Bonnet, Odran, Guillaume Chapelle, Alain Trannoy, Etienne Wasmer et al.**, “Secular trends in Wealth and Heterogeneous Capital: Land is back... and should be taxed,” Technical Report, Sciences Po 2019.
- Boppart, Timo**, “Structural change and the Kaldor facts in a growth model with relative price effects and non-Gorman preferences,” *Econometrica*, 2014, *82* (6), 2167–2196.
- , **Patrick Kiernan, Per Krusell, and Hannes Malmberg**, “The macroeconomics of intensive agriculture,” Technical Report, Mimeo, Stockholm University 2019.
- Brueckner, Jan K**, “Analyzing third world urbanization: A model with empirical evidence,” *Economic Development and Cultural Change*, 1990, *38* (3), 587–610.
- **and Somik V Lall**, “Cities in developing countries: fueled by rural–urban migration, lacking in tenure security, and short of affordable housing,” in “Handbook of regional and urban economics,” Vol. 5, Elsevier, 2015, pp. 1399–1455.
- Brunet, Jean-Paul**, “Le mouvement des migrations journalières dans l’agglomération parisienne au cours de l’entre-deux-guerres,” *Villes en Parallèle*, 1986, *10* (1), 250–269.
- Bustos, Paula, Bruno Caprettini, and Jacopo Ponticelli**, “Agricultural productivity and structural transformation: Evidence from Brazil,” *American Economic Review*, 2016, *106* (6), 1320–65.
- Combes, Pierre-Philippe, Gilles Duranton, and Laurent Gobillon**, “The production function for housing: Evidence from France,” 2017.
- , – , **and –** , “The costs of agglomeration: House and land prices in French cities,” *The Review of Economic Studies*, 2018, *86* (4), 1556–1589.
- , – , – , **and Sébastien Roux**, “Estimating agglomeration economies with history, geology, and worker effects,” in “Agglomeration economics,” University of Chicago Press, 2010, pp. 15–66.
- , **Laurent Gobillon, Gilles Duranton, and Clement Gorin**, “Extracting Land Use from Historical Maps Using Machine Learning: The Emergence and Disappearance of Cities in France

- Extracting Land Use from Historical Maps Using Machine Learning: The Emergence and Disappearance of Cities in France,” *mimeo*, 2021.
- Comin, Diego A, Danial Lashkari, and Martí Mestieri**, “Structural change with long-run income and price effects,” *Econometrica*, 2021, *89* (1), 311–374.
- Corbane, Christina, Aneta Florczyk, Martino Pesaresi, Panagiotis Politis, and Vasileios Syrris**, “GHS built-up grid, derived from Landsat, multitemporal (1975-1990-2000-2014), R2018A. European Commission, Joint Research Centre (JRC) doi:10.2905/jrc-ghsl-10007,” 2018.
- , **Martino Pesaresi, Thomas Kemper, Panagiotis Politis, Aneta J. Florczyk, Vasileios Syrris, Michele Melchiorri, Filip Sabo, and Pierre Soille**, “Automated global delineation of human settlements from 40 years of Landsat satellite data archives,” *Big Earth Data*, 2019, *3* (2), 140–169.
- Davis, Morris A and Jonathan Heathcote**, “The price and quantity of residential land in the United States,” *Journal of Monetary Economics*, 2007, *54* (8), 2595–2620.
- DeSalvo, Joseph S and Mobinul Huq**, “Income, residential location, and mode choice,” *Journal of Urban Economics*, 1996, *40* (1), 84–99.
- Desriers, Maurice**, “L’agriculture française depuis cinquante ans: des petites exploitations familiales aux droits à paiement unique,” *Agreste cahiers*, 2007, *2*, 3–14.
- Duranton, Gilles and Diego Puga**, “The growth of cities,” in “Handbook of economic growth,” Vol. 2, Elsevier, 2014, pp. 781–853.
- **and –**, “Urban land use,” in “Handbook of regional and urban economics,” Vol. 5, Elsevier, 2015, pp. 467–560.
- Eckert, Fabian, Michael Peters et al.**, “Spatial structural change,” *Unpublished Manuscript*, 2018.
- European Union**, “CORINE Land Cover Data: EU Land Monitoring Service 2018, Copernicus , European Environment Agency (EEA).”
- Fléchet, Edmond**, “La statistique agricole décennale de 1892,” *Journal de la société française de statistique*, 1898, *39*, 321–333.
- Florczyk, Aneta J, Christina Corbane, Daniele Ehrlich, Sergio Freire, Thomas Kemper, Luca Maffeni, Michele Melchiorri, Martino Pesaresi, Panagiotis Politis, Marcello Schiavina et al.**, “GHSL data package 2019,” *Publications Office of the European Union, Luxembourg*, doi:10.2760/290498 2019, *29788* (10.2760), 290498.
- Freire, Sergio, Erin Doxsey-Whitfield, Kytt MacManus, Jane Mills, and Martino Pesaresi**, “Development of new open and free multi-temporal global population grids at 250 m resolution,” in “https://agile-online.org/conference_paper/cds/agile_2016/shortpapers/

- [152_Paper_in_PDF.pdf](#)” Association of Geographic Information Laboratories in Europe (AGILE) 2016.
- Glaeser, Edward L and Matthew E Kahn**, “Sprawl and urban growth,” in “Handbook of regional and urban economics,” Vol. 4, Elsevier, 2004, pp. 2481–2527.
- , **Joseph Gyourko, and Raven Saks**, “Why is Manhattan so expensive? Regulation and the rise in housing prices,” *The Journal of Law and Economics*, 2005, 48 (2), 331–369.
- Gollin, Douglas, David Lagakos, and Michael E Waugh**, “Agricultural productivity differences across countries,” *American Economic Review*, 2014, 104 (5), 165–70.
- , **Remi Jedwab, and Dietrich Vollrath**, “Urbanization with and without industrialization,” *Journal of Economic Growth*, 2016, 21 (1), 35–70.
- , **Stephen L Parente, and Richard Rogerson**, “The food problem and the evolution of international income levels,” *Journal of Monetary Economics*, 2007, 54 (4), 1230–1255.
- Grossman, Volker and Thomas Steger**, *Das House-Kapital: A Long Term Housing & Macro Model*, International Monetary Fund, 2017.
- Heblich, Stephan, Stephen J Redding, and Daniel M Sturm**, “The Making of the Modern Metropolis: Evidence from London,” Working Paper 25047, National Bureau of Economic Research September 2018.
- Herrendorf, Berthold, Richard Rogerson, and Ákos Valentinyi**, “Two Perspectives on Preferences and Structural Transformation,” *American Economic Review*, December 2013, 103 (7), 2752–89.
- , – , and – , “Growth and structural transformation,” in “Handbook of economic growth,” Vol. 2, Elsevier, 2014, pp. 855–941.
- Hitier, Henri**, “La statistique agricole de la France,” in “Annales de Géographie,” Vol. 8 JSTOR 1899, pp. 350–357.
- IPCC**, “Sustainable development, poverty eradication and reducing inequalities,” *Roy, Joyashree and Tschakert, Petra and Waisman, Henri and Halim, Sharina Abdul and Antwi-Agyei, Philip and Dasgupta, Purnamita and Hayward, Bronwyn and Kanninen, Markku and Liverman, Diana and Okereke, Chukwumerije and others*, 2018.
- Knoll, Katharina, Moritz Schularick, and Thomas Steger**, “No price like home: Global house prices, 1870-2012,” *American Economic Review*, 2017, 107 (2), 331–53.
- Kongsamut, Piyabha, Sergio Rebelo, and Danyang Xie**, “Beyond balanced growth,” *The Review of Economic Studies*, 2001, 68 (4), 869–882.
- Lagakos, David and Michael E Waugh**, “Selection, agriculture, and cross-country productivity differences,” *American Economic Review*, 2013, 103 (2), 948–80.

- LeRoy, Stephen F and Jon Sonstelie**, “Paradise lost and regained: Transportation innovation, income, and residential location,” *Journal of Urban Economics*, 1983, 13 (1), 67–89.
- Leukhina, Oksana M. and Stephen J. Turnovsky**, “Population Size Effects in the Structural Development of England,” *American Economic Journal: Macroeconomics*, July 2016, 8 (3), 195–229.
- Lewis, W Arthur**, “Economic development with unlimited supplies of labour,” *The manchester school*, 1954, 22 (2), 139–191.
- Marchand, Olivier and Claude Thélot**, “Deux siècles de travail en France: population active et structure sociale, durée et productivité du travail,” 1991.
- Martin, Alfred**, *Étude historique et statistique sur les moyens de transport dans Paris, avec plans, diagrammes et cartogrammes*, Imprimerie nationale, 1894.
- Mauco, Georges**, “Les modes d’exploitation agricole en France,” in “Annales de Géographie,” Vol. 46 JSTOR 1937, pp. 485–493.
- Mauguin, Ch**, “Statistique comparée de l’agriculture française en 1790 et en 1882,” *Journal de la société française de statistique*, 1890, 31, 200–213.
- Mendras, Henri**, *La fin des paysans: changement et innovations dans les sociétés rurales françaises*, Vol. 110, Colin, 1970.
- Merlin, Pierre**, “Les transports en région parisienne,” *Notes et études documentaires (Paris)*, 1997, (5052).
- Michaels, Guy, Ferdinand Rauch, and Stephen J Redding**, “Urbanization and structural transformation,” *The Quarterly Journal of Economics*, 2012, 127 (2), 535–586.
- Miles, David and James Sefton**, “House prices and growth with fixed land supply,” *The Economic Journal*, 2020.
- Mills, Edwin S**, “An aggregative model of resource allocation in a metropolitan area,” *The American Economic Review*, 1967, 57 (2), 197–210.
- Muth, Richard**, “Cities and Housing,” *Chicago: University of Chicago Press*, 1969.
- Nichols, Donald A**, “Land and economic growth,” *The American Economic Review*, 1970, 60 (3), 332–340.
- Orselli, Jean**, “Usages et usagers de la route: pour une histoire de moyenne durée (1860-2008).” PhD dissertation, Paris 1 2008.
- Papon, Francis, Marina Marchal, Sophie Roux, Philippe Marchal, and Jimmy Armoogum**, “Parcours individuels et histoire de la mobilité. Analyse du volet “biographie” de l’Enquête Nationale sur les Transports et les Déplacements 2007-2008,” 2010.

- Piketty, Thomas and Gabriel Zucman**, “Capital is back: Wealth-income ratios in rich countries 1700–2010,” *The Quarterly Journal of Economics*, 2014, 129 (3), 1255–1310.
- Redding, Stephen J**, “Suburbanization in the United States 1970-2010,” Technical Report, National Bureau of Economic Research 2021.
- **and Esteban Rossi-Hansberg**, “Quantitative spatial economics,” *Annual Review of Economics*, 2017, 9, 21–58.
- Restuccia, Diego, Dennis Tao Yang, and Xiaodong Zhu**, “Agriculture and aggregate productivity: A quantitative cross-country analysis,” *Journal of monetary economics*, 2008, 55 (2), 234–250.
- Ricardo, David**, *The Works and Correspondence of David Ricardo, Vol. 1: Principles of Political Economy and Taxation*, Online Library of Liberty, 1817.
- Sauvy, Alfred**, “Variations des prix de 1810 à nos jours,” *Journal de la société française de statistique*, 1952, 93, 88–104.
- Schiavina, Marcello, Sergio Freire, and Kytt MacManus**, “GHS population grid multi-temporal (1975-1990-2000-2015), R2019A. European Commission, Joint Research Centre (JRC) [Dataset] doi:10.2905/0C6B9751- A71F-4062-830B-43C9F432370F,” 2019.
- Schultz, Theodore William**, *The economic organisation of agriculture*, McGraw-Hill, 1953.
- Sicsic, Pierre**, “City-farm wage gaps in late nineteenth-century France,” *Journal of Economic History*, September 1992, 52 (3), 675–695.
- Toutain, Jean-Claude**, *La production agricole de la France de 1810 à 1990: départements et régions: croissance, productivité, structures* number 17, Presses universitaires de Grenoble, 1993.
- **and Jean Marczewski**, “Le produit intérieur brut de la France de 1789 à 1982,” *Economies et sociétés (Paris)*, 1987, 21 (15), 3–237.
- Villa, Pierre**, “Productivité et accumulation du capital en France depuis 1896,” *Revue de l’OFCE*, 1993, 47 (1), 161–200.
- Young, Alwyn**, “Inequality, the urban-rural gap, and migration,” *The Quarterly Journal of Economics*, 2013, 128 (4), 1727–1785.